

Dissertation
zur Erlangung des Doktorgrades der Fakultät für Biologie
der Ludwig-Maximilians-Universität München

**Identification and dissection of novel components involved in
retrograde signaling**



vorgelegt von
Isidora Romani
aus Mailand, Italien

2016

Mit Genehmigung der Fakultät für Biologie
der Ludwig-Maximilians-Universität München

Gutachter: PD Dr. Tatjana Kleine
Gutachter: Prof Dr. Peter Geigenberger

Tag der Einreichung: 10 Februar 2016
Tag der mündlichen Prüfung: 3 Mai 2016

Table of contents

Abstract.....	i
Zusammenfassung	ii
List of tables and figures.....	iii
Abbreviations	v
1. Introduction	1
1.1. Retrograde signaling is a consequence of endosymbiosis	1
1.2. Signaling: Regulatory mechanisms that coordinate the expression of the organeller genomes.....	3
1.3. OGE-dependent retrograde signaling).....	4
1.4. Organelle-gene expression (OGE) translation dependent signaling.....	5
1.5. Retrograde signaling depending on altered reactive oxygen species (ROS) levels in the organelle, they are not able to traverse the cytosol	6
1.6. The mitochondrion Transcription tERmination Factor (mTERF) family.....	8
2. Aim of the work	11
3. Materials and Methods.....	12
3.1 Chemicals and antibodies.....	12
3.2 Crossing of <i>Arabidopsis thaliana</i>	12
3.3 Plant material and growth conditions.....	12
3.4 Chlorophyll analysis.....	14
3.4.1 Chlorophyll a fluorescence measurements.....	14
3.4.2 Chlorophyll concentration measurements	14
3.5 Microscopy	14
3.6 Molecular biology.....	15
3.6.1 Nucleic acids extraction.....	15
3.6.2 Standard PCR and high fidelity PCR	15
3.6.3 First strand cDNA synthesis	16
3.6.4 Real time PCR analysis.....	17

Table of contents

3.6.5 Northern blot analysis	17
3.6.6 Aminoacylation analysis of tRNAs	20
3.6.7 Circular RT-PCR.....	20
3.7 Biochemistry	22
3.7.1 Chloroplast isolation	22
3.7.2 Protein preparation and immuno-blot analysis.....	22
3.7.4 In vivo translation assay	22
3.8 Luminescence screening and detection assay	23
3.8.1 Screening of <i>rls</i> mutants.....	23
4. Results.....	25
4.1 Identification of Mutants for the MTERF6 Locus.....	25
4.1.1 Phenotypic analysis of <i>mterf6</i> mutants	28
4.1.2 Analysis of chloroplast gene expression.....	30
4.1.3 Analysis of the plastid ribosomes in <i>mterf6</i> mutants.....	34
4.1.4 Identification of MTERF6 binding sequences	35
4.1.4 Analysis of rRNA maturation.....	38
4.1.5 Northern blot analysis of the transcript present in the target I (trnV.1), and in the target II trnI.2/trnI.3).....	39
4.1.6 Aminoacylation analysis in <i>mterf6</i> mutants.....	44
4.2 Molecular and physiological screening to identify factors involved in chloroplast-to-nucleus retrograde signaling.....	47
4.2.2 Screening <i>rls</i> mutants.....	47
4.2.3 Internal transcript level of nuclear-encoded photosynthetic genes in the <i>rls</i> mutants.....	49
4.2.4 Effects on protein synthesis in <i>rls</i> mutants that present recovery of the phenotype.....	51
4.2.5 <i>Rls</i> mutants could be involved in plastid gene expression?.....	52
4.2.6 Aminoacylation status in <i>prors1-2</i> plants	54

Table of contents

4.3 Ethanol-induced, transient silencing of PRORS1.....	55
4.3.1 Preliminary hints	55
4.3.2 Investigation of EtOH inducible <i>PRORS1</i> RNAi lines	55
4.3.3 Effects on protein synthesis in plastids.....	56
4.3.4 Photosynthetic parameters of iPRORS1 RNAi plants.....	58
4.3.5 Analysis of gene expression changes.....	59
5. Discussion and conclusions.....	61
5.1 MTERF6 is essential for appropriate photosynthetic functions.	61
5.2 The molecular function of MTERF6	62
5.3 MTERF6 promotes <i>trnL2</i> aminoacylation.	65
5.4 MTERF Proteins might play a role in Retrograde signaling.	65
5.5 RIs (relaxed LHCB suppression) mutants.....	66
5.5.1 EtOH-inducible lines	68
References	71
Acknowledgment	81
Curriculum Vitae	83
Declaration.....	86

Abstract

The evolution of pathways mediating the communication between the cell compartments was very important. Signals originating from the nucleus are called anterograde signals, the signals deriving from the organelles are known as retrograde signals. In this project three approaches were used to determine the molecular aspects of retrograde signaling originating from perturbations in organellar gene expression (OGE). In the first approach we present evidence for the function of the mitochondrial transcription termination factor mTERF6 as a factor involved in aminoacylation of a tRNA for isoleucine in chloroplasts. This is in contrast to the previous known functions of mTERFs. Because metazoan mTERFs were thought to interact with the mitochondrial chromosome and regulate transcription via mechanisms that involve termination and initiation. *Arabidopsis thaliana* MTERF6 is dually targeted to chloroplasts and mitochondria. Knockout of *MTERF6* perturbs plastid development and results in seedling lethality. In the leaky *mterf6-1* mutant, a defect in photosynthesis is associated with reduced levels of photosystem subunits although corresponding mRNA levels are unaffected. Bacterial one-hybrid screening and electrophoretic mobility shift assays revealed a specific interaction between mTERF6 and a DNA and RNA sequence in the chloroplast, the isoleucine tRNA gene proximal of the *rrn16S* gene. In consequence, rRNA maturation is affected in *mterf6-1* mutants, resulting in reduced levels of 16S and 23S rRNAs and consequently in impaired translational capacity. Since introduction of the *genomes uncoupled 1* (*gun1*) mutation into *mterf6-1* plants results in an additive phenotype, we conclude that disturbed chloroplast translation in *mterf6-1* triggers retrograde signaling. In the second approach the *prors1-2* mutant was chosen for our studies of the translation-dependent retrograde signaling pathways due to its impairment of organellar translation, which has been shown to be involved in retrograde signaling processes. A genetic forward screen with mutagenized *prors1* mutants was performed. Luciferase and *LHCB* promoters were chosen as marker for the suppression screen. The mutants plants coming from these screening (relaxed *LHCB* suppression (*rls*)), showed a rescue in the luciferase expression and in the growth performance and were further characterized. In a third approach, OGE defects were provoked in adult *PRORS* RNAi plants by ethanol-dependent repression of *PRORS1* for a short time period (beginning with 32 hours). Indeed, the translational capacity of chloroplasts was reduced, but pigmentation and growth were not influenced, providing a basis for the identification of OGE-dependent direct target genes.

Zusammenfassung

Die Evolution von Kommunikationswegen zwischen Zellkern und Organellen ist sehr wichtig. Die Signale vom Kern zu den Organellen nennt man anterograde Signale, die Signale von den Organellen zum Zellkern retrograde Signale. In diesem Projekt wurden drei Ansätze verfolgt, um die molekularen Aspekte von retrograden Signalen zu verstehen, die durch Störungen in der Organellengenexpression (OGE) hervorgerufen werden. Im ersten Ansatz wurde gezeigt, dass der mitochondriale Transkriptionsterminationsfaktor mTERF6 an der Aminoacylierung der tRNA für Isoleucin in den Chloroplasten beteiligt ist. Dies steht im Kontrast zu den bisherigen bekannten Funktionen der mTERFs. Für die mTERFs aus Mensch und Tier wurde gezeigt, dass sie mit dem mitochondrialen Chromosom interagieren, um die Transkription zu terminieren, aber auch zu initiieren. *Arabidopsis thaliana* MTERF6 ist sowohl in den Chloroplasten als auch in den Mitochondrien lokalisiert. Ein kompletter Verlust von MTERF6 führt zu störender Plastidenentwicklung und Keimlingsletalität. In der *leaky mterf6-1* Mutante sind Proteine für die Photosystem-Untereinheiten reduziert, aber die entsprechenden mRNA Levels sind vergleichbar mit denen des Wildtyps. One-Hybrid-Screening und elektrophoretische Mobilitäts-Shift-Assays, zeigten eine spezifische Wechselwirkung zwischen mTERF6 und einer DNA und RNA-Sequenz in dem Chloroplastengen für eine Isoleucin-tRNA, welches proximal vom *rrn16S* Gen lokalisiert ist. In Konsequenz ist die rRNA Reifung in *mterf6-1* Mutanten beeinträchtigt, was wiederum zu einer Beeinträchtigung der Translationskapazität führt. Da die Einkreuzung der *genomes uncoupled 1 (gun1)* Mutation in *mterf6-1* Pflanzen zu einem additiven Phänotypen führt, vermuten wir, dass gestörte Chloroplastentranslation in *mterf6-1* retrograde Signale hervorruft. Im zweiten Ansatz wurde die *prors1-2* Mutante aufgrund ihrer Beeinträchtigung in der Organellentranslation ausgewählt, um retrograde Signalprozesse aufzuzeigen. Ein genetischer Vorwärts-Screen mit EMS-mutagenisierten *prors1-2* Linien wurde weitergeführt, in dem Luciferase und *LHCB* Promotoren als Marker dienten. Die Mutantpflanzen, die aus diesem Screening (relaxed *LHCB* suppression (*rls*)) hervorgingen, zeigten eine verbesserte Luziferase-Expression und/oder verbessertes Wachstum und wurden weiter charakterisiert.

Im dritten Ansatz wurden OGE-Defekte in adulten *PRORS* RNAi Pflanzen durch Ethanol-abhängige Repression von *PRORS1* für einen kurzen Zeitraum (beginnend mit 32 Stunden) provoziert. Tatsächlich wurden die Translationskapazitäten in den Chloroplasten reduziert, jedoch wurden die Pigmentierung und das Wachstum nicht beeinflusst, was eine wichtige Grundlage für die Identifizierung von OGE-abhängigen Zielgenen ist.

List of tables and figures

Table 1: List of <i>r/s</i> mutants identified in the screen, including the respective parental line	13
Table 2: Sequences of the primers used for the genotyping	16
Table 3: Sequences of the primers used for the real time-PCR analyses	17
Table 4: Sequences of the primers used for the Northern blot analyses	18
Table 5: Sequences of the primers used for the RNA gel blot analyses.....	20
Table 6: Sequences of the primers used for the circular RT-PCR analyses.....	22
Table 7: PAM data for Col.0, <i>mterf6-1</i> and complemented plants (<i>oeMTERF6-1</i>)	30
Table 8: Differential expression of selected early target genes in the PRORS1 RNAi lines treated for 48, 51 or 56 hours with ethanol vapor	60
Figure 1. Schematic representation of circular RT-PCR procedure	21
Figure 2. T-DNA tagging of the <i>MTERF6/AT4G38160</i> locus	25
Figure 3. (A) RT-PCR analysis of wild-type (Col-0), <i>mterf6-1</i> , <i>mterf6-2</i> and <i>mterf6-3</i> mutant plants, and the complemented <i>mterf6-1</i> (35S: <i>MTERF6.1 mterf6-1</i>) plants. (B) Real-time PCR analysis of <i>MTERF6.1</i> mRNA expression of four-week-old <i>mterf6-1</i> plants, and <i>mterf6-1</i> complemented with the first splice variant of the <i>AT4G38160</i> gene (35S: <i>MTERF6.1 mterf6-1</i>).....	26
Figure 4. Phenotypic characterization of <i>mterf6</i> mutants.....	29
Figure 5. (A) Immunoblot analysis of photosynthetic subunit levels in <i>mterf6-1</i> . (B) Northern blot analysis of photosynthetic subunits transcripts in Col-0 and <i>mterf6-1</i>	31
Figure 6. (A). Polysomes analysis. (B) In vivo pulse labeling of thylakoid membrane proteins with [35S] Met in the presence of cycloheximide	34
Figure 7. Immunoblot analysis of plastid ribosome subunits levels in <i>mterf6-1</i>	35
Figure 8. Schematic representation of the chloroplast <i>rrn</i> operon and the <i>MTERF6</i> target site located in the <i>trnI.2</i> gene (target II)	36
Figure 9. Analysis of transcript levels and splice forms of <i>rrn</i> genes and <i>trnA.1</i>	37
Figure 10. Mapping of 16S rRNA 3' ends by circular RT-PCR. The arrows point to the 3' ends detected, and the numbers of clones obtained at the indicated positions are given.....	38
Figure 11. Transcript levels of plastid encoded tRNAs are over accumulating in the <i>mterf6-1</i> mutant compared to wild-type (Col-0) plants.	40
Figure 12. (A) Schematic representation of the chloroplast <i>rrn</i> operon and the <i>MTERF6</i> target site located in the <i>trnI.2</i> gene (target II). (B) Analysis of transcript levels of plastid tRNA genes which are located close to target I.....	41

List of tables and figures

Figure 13. Expression and processing of chloroplast <i>trnL2</i> in wild-type (Col-0) and <i>mterf6</i> plants	42
Figure 14. Analysis of accumulation of the MTERF6 target sequence corresponding to the non-coding RNA in the <i>trnL2</i> intron in wild-type and <i>mterf6-1</i> plants	44
Figure 14. Analysis of <i>trnL2</i> and <i>trnL1</i> and <i>trnThr</i> aminoacylation in soil-grown wild-type (Col-0), <i>mterf6-1</i> and complemented <i>mterf6-1</i> (35S:MTERF6.1 <i>mterf6-1</i>) plants and analysis of plants MS-grown Col-0, <i>mterf6-2</i> and – as a control – <i>rrn1-3</i> seedlings	45
Figure 16. Introduction of <i>gun1</i> mutation into the <i>mterf6-1</i> mutant (<i>mterf6-1/gun1</i>)	46
Figure 17. Phenotypic analysis of <i>rls</i> mutants containing the LHCb1.2 or the LHCb3 promoter-luciferase construct	48
Figure 18. Luminescence screen of the <i>rls</i> mutants	49
Figure 19. LHCb3, LHCb1 and PSbO transcript levels from Col-0, <i>prors1-2</i> , parental lines and <i>rls</i> mutants. Increasing amount (25%, 50%, 75% and 100%) of total RNA extracted from Col-0 and <i>rls</i> mutants	50
Figure 20. LHCb3, LHCb1 and PSbO transcript levels from Col-0, <i>prors1-2</i> , parental lines and <i>rls</i> mutants. Increasing amount (25%, 50%, and 100%) of total RNA extracted from Col-0 and <i>rls</i> mutants	51
Figure 21. In vivo pulse labeling of total proteins with [³⁵ S] Met in the presence of cycloheximide	52
Figure 22. Luminescence screen of the <i>rls</i> mutants seedlings	53
Figure 23. Aminoacylation assay of tRNA prolyl synthase on Col-0, <i>prors1-2</i> and <i>rls</i> mutants selected	54
Figure 24. Col-0, <i>iPRORS1</i> RNAi line <i>i35</i> and <i>prors1-2</i> mutant plants treated with ethanol vapour	56
Figure 25. wild-type (Col-0), Col-0 with the inducible GUS RNAi construct (GUS), <i>prors1-2</i> plants and the inducible <i>iPRORS1</i> RNAi line <i>i35</i> , were grown under long-day (16 h light/8 h dark) conditions and exposed for the indicated lengths of time to ethanol vapour	57
Figure 26. (A) Acetone-extracted chlorophyll was measured photometrically, and chlorophyll concentrations were calculated as described (Lichtenthaler, 1987) and are reported in µg/mg fresh weight. (B) Photosynthetic parameters were derived from measurements on at least three leaves from different plants	58
Figure 27. Photosynthetic parameters were derived from measurements on at least three leaves from different plants	59
Figure 28. Schematic representations of the human mitochondrial and the A. <i>Thaliana</i> plastid genome in the region surrounding the <i>rrn16S</i> gene	64

Abbreviations

Abbreviations

°C	Degree celsius
μE	Microeinstein
μg	Microgram
μl	Microliter
μm	Micrometer
μmol	Micromolar
1-qP	Proportion of closed PSII
bp	Base pair
chl <i>a</i>	Chlorophyll <i>a</i>
chl <i>b</i>	Chlorophyll <i>b</i>
Col-0	Columbia-0
ddH ₂ O	Double distilled water
EMS	E thyl M ethane S ulfonate
<i>flu</i>	Fluorescent in blue light
<i>F_v/F_m</i>	Maximum quantum yield of PSII
GFP	green fluorescent protein
<i>gun</i>	Genome uncoupled mutant
h	Hour
<i>Ler</i>	Landsberg <i>erecta</i>
LUC	Luciferase
M2	Second mutagenized generation
M3	Third mutagenized generation
M4	Fourth mutagenized generation
mg	Milligramm
min	Minute
ml	Milliliter
mM	Millimolar
ms	Millisecond
OGE	Organellar gene expression

Abbreviations

NGE	Nuclear gene expression
NGS	Next generation sequencing
NPQ	Nonphotochemical fluorescence quenching
<i>pam</i>	Photosynthesis altered mutant
PCR	Polymerase chain reaction
PGE	Plastid gene expression
<i>PRORS1</i>	Prolyl-tRNA-synthetase 1
PRPL	Plastidial ribosome protein L
PSII	Photosystem two
<i>rls</i>	Relaxed LHCB suppression
ROS	Reactive oxygen species
NF	Noraflurazon
Linc	Lincomycin
MTERF	M itochondrion T ranscription tER mination F actors
Φ_{II}	Effective quantum yield of PSII
Ci	Curie
DEPC	Diethylpyrocarbonate
DNA	Deoxyribonucleic acid
EDTA	Ethylene diamine tetraacetic acid
HEPES	4-(2-hydroxyethyl)-1-piperazineethanesulfonic acid
mRNA	Messenger RNA
qRT-PCR	Quantitative Real Time PCR
RNA	Ribonucleic acid
rRNA	Ribosomal RNA
RuBisCo	Ribulose-1,5-bisphosphate carboxylase oxygenase
SDS	S odium D odecyl S ulphate
TAE	Tris-acetate-EDTA
T-DNA	Transfer DNA
Tris	Tris(hydroxymethyl)-aminomethane
tRNA	TransferRNA

1. Introduction

1.1. Retrograde signaling is a consequence of endosymbiosis.

Plastids are the largest organelles present in the cells of plants and algae. They are different in size, shape, content and function and include: amyloplasts for the reserves of starch (roots); pigmented chromoplasts for the production of carotenoids (flowers, fruits); the colorless leucoplasts, for the production of monoterpenes and chloroplasts for photosynthesis (green tissues of the plant). All these types of plastids originated from proplastids. In presence of light, proplastids differentiate into chloroplasts which are constituted of characteristic internal space and the stroma, in which they develop a complex system called thylakoid membranes. These membranes, containing pigments, proteins and electron carriers, are responsible for the absorption of sunlight and for storing in the chemical bonds of the molecules NADPH and ATP. These molecules with high energy content are utilized in the stroma, to convert carbon dioxide into sugars during Calvin cycle. (Pesaresi et al., 2006, Margulis L. 1981)

Other important organelles, in both animals and plants, are the mitochondria. Like chloroplast, mitochondria are surrounded by an envelope consisting of two membranes and an internal space, the matrix.

The internal part, located between the two membranes, harboring the mitochondrial electron transport chain and the enzyme ATP synthase, synergies with the matrix to produce mitochondrial ATP during the respiration process.

Chloroplasts are plastids specialized in the process of photosynthesis and are present in all photosynthetic eukaryotes. The size of chloroplasts ranges from 4-6 μm in higher plants to 100 μm in algae. In mesophyll cell, their amount is highly variable ranging from 40 to 50. Chloroplasts are lenticular in higher plants and can acquire different shapes such as stars, ribbons or spirals in the case of algae. These organelles consist of an outer casing formed by a double membrane, which delineates an inter membrane space of about 3 nm. These organelles contain stroma that is rich in enzymes active in the the dark phase of photosynthesis. These

1. Introduction

enzymes are important for the synthesis of fatty acids, DNA, RNA, 70S ribosomes. Moreover, in the chloroplast is present a lamellar system, probably derived by the invagination of the inner membrane, that created vesicles or flattened tanks, called thylakoids, stacked on each other to form the grain (each stack is a granum), connected by stromal lamellae or thylakoids intergrana. (Abdallah F. et al. 2000)

It is well known that chloroplasts and mitochondria originated by the phagocytosis of prokaryotes by primitive eukaryotic cells, as demonstrated on endosymbiotic theory by Margulis L. (1981). During evolution, relation of mutual symbiosis has been established between two organisms. The chloroplasts and mitochondria maintain different characteristics of their prokaryotic ancestors, as for example the presence of ribosome 70S. In addition, as the prokaryotic organisms, chloroplasts divide by fission and are equipped with their own genome. Nowadays, the plastid genome contains a number of genes significantly lower compared to that of the current cyanobacteria. (Abdallah F. et al. 2000).

During the evolutionary process that has transformed the prokaryotic organism in endosymbiont plastid, most of the gene sequences were transferred to the host cell nucleus. In particular, according to recent estimations, about 3000 genes were acquired by the host nucleus, whereas only a small part, approximately 87 genes, was specific to the plastid genome.

As a consequence, most of the proteins present in the chloroplast are encoded by nuclear genes, while a minority is obtained from the plastid genome. Therefore, many protein complexes present in the plastids, such as ribosomes and photosystems, are a mosaic where certain proteins are encoded in the nucleus and others in the organelle. The Rubisco, key enzyme of photosynthesis, is the best example since the small subunit is encoded by the nuclear genome, while the large subunit is encoded by the chloroplast genome (Abdallah F. et al. 2000).

The fact that the proteins localized in chloroplasts and mitochondria are partly encoded by the nuclear genome and part from the genomes of organelles implies the presence of a perfect coordination of gene expression between the different compartments.

Therefore, during the evolution of the eukaryotic cell, it was necessary to develop mechanisms to coordinate the organellar gene expression (OGE) and nuclear gene

1. Introduction

expression (NGE) at multiple levels, with the goal to adapt the nuclear gene expression to the functional state of the organelle.

1.2. Signaling: Regulatory mechanisms that coordinate the expression of the organellar genomes.

The regulatory mechanisms play a pivotal role in coordinating the expression of the organellar genomes and are generally divided into anterograde signaling (from the nucleus to the organelle) and signaling systems retrograde (from the organelle to the nucleus). Organellar gene expression is controlled by nuclear encoded components which can directly influence organellar activity by acting on transcriptional, translational and post translational levels.

Plastid transcription in plastids is mediated by two different polymerases. One is encoded in the nucleus (NEP, nucleus encoded polymerase), while the genes for the core subunits of the second one are located in plastids (PEP, plastid encoded polymerase). However, the transcription of PEP core subunits is performed by NEP, but also under nuclear control (LiereK.et al. 1999). Additional nuclear encoded sigma factors are responsible for promoter specificity and transcript initiation of PEP (Shiina T.et al 2005). This pathway and the principal function of anterograde control has been established. In photosynthetic organisms, this mode of regulation becomes more complex with the cross-talk between mitochondria and chloroplasts (Woodson, J. D. & Chory, J., 2008).

Currently, the best known lines of communication between the chloroplast and nucleus are responsible for conveying the core information on the various activities of the chloroplast. This communication influences the nuclear gene expression and is defined as part of the retrograde signaling pathways. Retrograde signaling is essential during the initial developmental stages of the plastids (biogenic control); the development of organelle biogenesis is a crucial step which needs to be controlled by specific stages and requires subunits and cofactors in correct stoichiometry for an accurate assembly. Retrograde signaling is essential also in the adult stage, in fully developed plants, to react to changes in the environment and it is represented by rapid adjustments in response to environmental constraints with the aim to maintain optimal production and to limit the damages induced by oxidative stress (Pogson, B.J.et al. 2008).

1. Introduction

Several components have been proposed to be involved in plastid retrograde signaling:

- Components of tetrapyrrole biosynthetic pathway intermediates (Benfey, P.N. 1999, Larkin, J.C., et al. 2003, Mochizuki, N. et al. 2001, Strand, A., et al. 2003, Susek, R. et al. 1993).
- Organellar protein synthesis (Koussevitzky S, et al. 2007).
- The redox state of the plastids (Bonardi, V. et al. 2005, Heiber, et al. 2007, Pesaresi P. et al 2007, Piippo, M. et al 2006).
- The levels of reactive oxygen species in plastids (Foyer, C.H. et al 2005, Lee KP, et al. 2007, Wagner, D. et al. 2004).
- Products of secondary metabolism (Estavillo, G.M., et al. 2011, Xiao Y, et al. 2012).
- Oxidation products of carotenoids (Ramel F, et al. 2012).
- Transcription factors (TFs) that can relocate from the chloroplast to the nucleus are implicated in retrograde signaling (Isemer, R., et al. 2012, Sun, L., et al. 2013).

1.3. OGE-dependent retrograde signaling.

The signaling networks of the plastid gene expression (PGE) pathway has been identified for the first time thanks to the use of antibiotics that selectively altered protein synthesis in the organelles. Plants treated with the antibiotics lincomycin or erythromycin suffered a drastic reduction of plastid protein synthesis and simultaneously showed a marked reduction of transcription of nuclear genes encoding chloroplast proteins (Susek et al. 1993). Therefore, it seems evident that the nucleus is able to perceive the alteration of protein synthesis in the plastids and then to rearrange the transcription of different nuclear genes in response to the functional state of the organelles themselves (Pesaresi P, et al. 2007). Susek et al. in 1993 identified a series of mutants in *Arabidopsis thaliana* that were called *gun "genomes uncoupled"*.

The screening was designed to find mutants in which retrograde communication between the chloroplast and nucleus was interrupted. The plants were treated with an herbicide, norflurazone (NF), an inhibitor of carotenoid biosynthesis, in order to generate growth conditions likely to damage the chloroplasts through the

1. Introduction

accumulation of reactive species of oxygen. The *gun* phenotype, in particular, showed no repression of nuclear genes encoding chloroplast proteins when the activity of the chloroplast was inhibited by NF. It is exactly the opposite of what happens in wild type plants subjected to the same treatment. A common thing of these mutants is that they still express nuclear encoded photosynthetic genes like *RBCS* and *LHCB*, even if the chloroplast is disrupted by treatment with NF (Susek, et al. 1993). From the six *gun* mutants, *gun1* affects the PGE pathway suggesting also that plastid translation is necessary for full *LHCB* transcription (Koussevitzky S, et al. 2007, Woodson JD, et al. 2011). The other GUN proteins GENOMES UNCOUPLED 2, 3, 4 and 5 (GUN2, GUN3, GUN4, GUN5), are involved, unlike GUN1, in the biosynthesis of tetrapyrroles. Specifically, GUN2 and GUN3 have a role in the biosynthesis of heme groups, while GUN4 and GUN5 in the biosynthesis pathway of chlorophylls. Although all these proteins play a vital role in the communication between the chloroplast and the nucleus, the intermediate hypothesis proposes that the biosynthesis of tetrapyrroles can act as signaling molecules (Matthew J. et al. 2013). It is known that disruption of the tetrapyrrole pathway induce a transient accumulation of the intermediated Mg-protoporphyrin IX as a related effect on the expression of **Photosynthetic Associated Nuclear Genes** (PhANGs) (Zhang ZW, et al. 2011). Studies on a new *gun* mutant, *gun 6*, have revealed that the heme play also an important role as a signaling molecule during the chloroplast biosynthesis. The mutant presents an over-expression of the gene *FERROCHELATASE1* responsible for synthesizing Heme from Protoporphyrin IX and for circadian clock regulation (Woodson JD, et al. 2011, Salomé PA, et al. 2013).

1.4. Organelle-gene expression (OGE) translation dependent signaling.

It has been shown in previous studies that treatments of leaves with translational inhibitors like lincomycin or chloramphenicol affect dramatically the expression of nuclear photosynthetic genes, showing that the organellar protein synthesis play an important role in retrograde-signaling (Sullivan JA, Gray JC 1999). The effect of the plastid and mitochondrial translation rate on nuclear gene expression have also been

1. Introduction

observed using mutants of *Arabidopsis thaliana*, *mrpl11* and *prpl11*, defective in mitochondrial and plastid ribosomal protein L11 respectively.

In these mutants nuclear photosynthesis gene expression is down-regulated (Pesaresi P, et al. 2006). The down-regulation of photosynthetic nuclear genes is more pronounced in the *mrpl11/prpl11* double mutant. A similar situation is observed in *prors1-1* and *prors1-2* where a dual targeted prolyl-tRNA synthetase is knocked-down. These data support the theory that both chloroplast and mitochondrial translation are important for modulation of nuclear photosynthesis gene expression (Pesaresi P, et al. 2006). The *prors1-1* and *prors1-2* mutants were identified in a screening of *Arabidopsis thaliana* plants mutagenized with T-DNA transposons and the resulting lines were screened selecting plants that exhibit a decreased quantum yield (F_v/F_m) of photosystem II (PSII) (Pesaresi P, et al. 2006).

The mutations identified are localized in the 5' untranslated region of the nuclear gene encoding *PROLYL-tRNA-SYNTHETASE1* (*PRORS1*), itself localized in the chloroplast and in the mitochondria. The function of *PRORS1* is crucial for plants and, the total knockout of the gene is not able to survive over the embryo stage. The *prors1-1* and *prors1-2* are leaky mutants and the *PRORS1* transcript is reduced to 50% and 25%, respectively.

These effects are stronger in *prors1-2* than in *prors1-1*, and they seem to be related to the direct defect in the translation caused by the reduced expression of the *PRORS1* gene, effects that are independent from light or other photooxidative stress (Pesaresi P, et al. 2006).

1.5. Retrograde signaling depending on altered reactive oxygen species (ROS) levels in the organelle.

Plants have developed a complex signaling network involving different endogenous growth regulators that sense and protect them from environmental stresses. One of the common responses to different environmental stresses, both abiotic and biotic, is the accelerated generation of reactive oxygen species (ROS), including superoxide (O_2^-), perhydroxy radical (HO_2^-), hydrogen peroxide (H_2O_2), hydroxyl radical ($\cdot OH$), alkoxy radical (RO), peroxy radical (ROO), singlet oxygen (1O_2), organic hydroperoxide (ROOH) (S. Bhattacharjee 2010, G. Miller, K. Schlauch, R. Tam et

1. Introduction

al. 2009). Accumulation of ROS causes oxidative stress that can fast exacerbate in cellular damages (S. Gill and N. Tuteja, 2010, I. Kovalchuk 2010). ROS are normally produced as product of normal aerobic metabolism, involving largely the membrane-linked electron transport processes, redox-cascades, and metabolisms. This production can be altered under the influence of unfavorable environmental cues. In all aerobic organisms, the ROS-scavenging pathways regulate the concentration of ROS. An imbalance in the metabolism of ROS can leads to a variety of “oxidative stress.” Plant possess the mechanisms that regulate the concentration of ROS according to cell’s need, they possess redox-sensing and signaling pathways, an efficient antioxidative defense that protects the cell from ROS by modifying the production and scavenging mechanisms of ROS. There is ample of work in recent times that suggest the significance of ROS in cell signaling and redox sensing mechanisms, particularly for the survival of the plant under environmental stress (G. Miller, et al 2008, G. Miller, K. Schlauch, R. Tam et al. 2009). Retrograde signaling mediated by autopropagating waves of ROS that travels at a rate of more or less 8.4 cm min^{-1} from the organelles-like chloroplast or mitochondria to nucleus has been proposed for abiotic stress perception and systemic responses (G. Miller, K. Schlauch, R. Tam et al. 2009). Retrograde signaling regulates specific genes involved in the cell protection from photooxidative damage (Foyer, C.H., et al 2005). ROS are also able to act as retrograde signals themselves by increasing antioxidant enzyme production (Lee KP, et al. 2007).

Studies on the *flu* (fluorescent in blue light) mutant conducted by Meskauskiene et al. 2001, amplified the knowledge of ROS pathway. The *flu* mutant presents a strong accumulation of protochlorophyllide, a chlorophyll precursor excitable by light. Shift from dark to light leads to a rapid accumulation of $^1\text{O}_2$ in the chloroplast, with consequent stop of growth and increase of cell death (Meskauskiene R, et al. 2009). It is suggested that $^1\text{O}_2$ is able to travel short distances and even crosses membranes (Skovsen et al. 2005), capable to act outside the chloroplast as well.

The accumulation of ROS has been shown to result in major changes of nuclear gene expression (Lee et al.2007, Galvez-Valdivieso and Mullineaux 2010), for example $^1\text{O}_2$ in the *flu* mutant affects expression of ~1400 nuclear genes. We can assume that the rapid accumulation of $^1\text{O}_2$ changes NGE in order to improve the protection of the cell.

1. Introduction

It has been shown that some mutants which compromise plastid gene expression and disturb plastid protein regulation interfere also with known retrograde signaling pathways. A mutation in the *Arabidopsis* mTERF-related plastid protein SOLDAT10 activates retrograde signaling and suppresses O₂-induced cell death (Koussevitzky S, et al. 2007). In 2009 was performed an experiment to identified SOLDAT10, this protein was identified with a screening second –site mutations that was going to attenuate the fluorescent (*flu*) phenotype. *The soldat10* seedlings suffer from mild photo-oxidative stress, as indicated by the constitutive up-regulation of stress-related genes. The *soldat10/flu* seedlings overaccumulate the photosensitizer protochlorophyllide in the dark and activate the expression of ¹O₂ responsive genes after a dark-to-light shift they do not show a ¹O₂ dependent cell death response. The results of this study reveal the complexity of what is commonly referred to as 'plastid signaling' (Meskauskiene R, et al. 2009).

1.6. The mitochondrion Transcription tERmination Factor (mTERF) family.

The mitochondrion Transcription tERmination Factor (mTERF) family is a large protein family identified in metazoa and plants (Daga A et al 1993, Linden et al. 2005). In metazoan, it is consisted of 4 subfamilies named MTERF1-4, localized in mitochondria and having a modular architecture based on repetitions of a 30 amino acid module. These proteins participate in attenuating transcription from the mitochondrial genome; this attenuation allows higher levels of expression of 16S ribosomal RNA relative to the tRNA gene downstream. The product of this gene has three leucine zipper motifs bracketed by two basic domains that are all required for DNA binding. There is evidence that, for this protein, the zippers participate in intramolecular interactions which establish the three-dimensional structure required for DNA binding. MTERF proteins play different roles, not restricted to transcription termination, such as transcription initiation and the control of mtDNA replication (Jiménez-Menéndez N, et al. 2010).

The role of the mTERFs in plants has still to be deeply investigated. Sequencing the *Arabidopsis thaliana* and *Oryza sativa* nuclear genomes helped to identify novel plant gene families. The numbers of *MTERF* genes identified in *Arabidopsis* and *Oryza* (Babiychuk E, et al. 2011) are much higher than those of animal genomes, 35

1. Introduction

in *Arabidopsis* and 48 in *Oryza sativa*. The main part of annotated *Arabidopsis* MTERFs is targeted to mitochondria or chloroplasts or both. (Tatjana K. 2012) The better characterized *MTERF* genes, from photosynthetic organisms are *MOC1* (*MTERF*-like gene of *Chlamydomonas* 1) from *Chlamydomonas reinhardtii* (Schönfeld, C. et al. 2004), *SOLDAT10* (*SINGLET OXYGEN-LINKED DEATH ACTIVATOR10*; (Meskauskiene R, et al. 2009), and *BELAYA SMERT/RUGOSA2* (*BSM/RUG2*) (Babiychuk E, et al 2011) Quesada V, et al. 2011), and the *Arabidopsis MTERF15* that acts as a splicing factor for *nad2* intron 3 splicing in mitochondria. *MOC1* (*MTERF*-like protein of *Chlamydomonas* 1), is targeted to mitochondria, alteration of the gene causes sensitivity to high light and disrupts transcription of genes for subunits of mitochondrial respiratory complexes (Schönfeld, C et al. 2004).

The leaky mutant *soldat10*, is affected by photooxidative stress, and the total knockout of the gene *SOLDAT10* (*AT2G03050*) is lethal (Meskauskiene et al., 2009). The protein *SOLDAT10* is localized in chloroplasts, and mutation in this gene seems affect levels of 16S and 23S rRNAs. The *A.thaliana* *MTERF* protein (*AT4G02990*), variously named *BELAYA SMERT* or *RUGOSA2* (*BSM*; Babiychuk E, et al. 2011); *RUG2*; (Quesada V, et al. 2011), is essential for the plant development. The *bsm* mutation compromises seedling growth, leading to arrested of embryo development. The *BSM* protein binds chloroplast DNA. The study of mosaic plants reveals that loss of *BSM* during the embryo development perturbs chloroplast and leaf morphology.

MTERFs in plants are required for a proper organelle gene expression. In fact *soldat10*, *bsm*, and *rug2-1* mutations modify the levels of transcripts and proteins of plastid genes. Genes encoding the 16S, 23S and 4.5S rRNAs are downregulated both in *rug2* and *bsm* mutants. Another *MTERF* was identified located in the gene *AT5G55580*. The mutants in this gene is *twirt1* (*twr-1*; *AT5G55580*), shows reduced root growth and present a delay in activation of the shoot meristem (Mokry, M., et al., 2011). *MTERF* seems to play a crucial role in the ontogenesis of organelles. According to experimental data, there are a large number of evidences demonstrating their fundamental role in embryo development and general ontogenesis, albino phenotypes, morphogenetic alterations and lethality. Hsu *et al.* (2015) investigated splicing events in mitochondria from *MTERF15* plants. They

1. Introduction

suggest that *Arabidopsis* MTERF15 acts as a splicing factor for nad2 intron 3 splicing in mitochondria, which is essential for normal plant growth and development. The Mitochondria-localized MTERF15 lacks obvious DNA-binding activity but processes mitochondrial nad2 intron 3 splicing through its RNA-binding ability. MTERFs could be required in the organellar communication, and if MTERF perturbation alters the organelles gene expression (OGE), this may be signaled to the nucleus. In *rug2-1*, the nuclear genes *RpoTp/SCA3* and *AOX1a*, targets of chloroplast and mitochondria retrograde signaling, are upregulated as a compensatory mechanism triggered by impaired chloroplast and mitochondria functions (Quesada V, et al. 2011). Also SOLDAT10 seems involved in a possible role in retrograde signaling (Meskauskiene R, et al. 2009). It was found that a mutation in the MTERF protein SOLDAT10 (singlet oxygen-linked death activator) seems to partially suppress the phenotype of the conditional *flu* mutant of *Arabidopsis thaliana*. The *flu* (fluorescent) mutant accumulates in the dark protochlorophyllide, a photosensitizing molecule that generates $^1O^2$ in the presence of light, causing cell death. The $^1O^2$ is one of the most important ROS that are involved in the plastid retrograde signaling. It seems that in *soldat10* mutant function affects the activity of those signaling factors produced in chloroplasts, and that it acts on the nuclear genes interfering with cell death. Also more than 50 stress-related nuclear genes are over expressed in *soldat10* (Meskauskiene R, et al. 2009). If MTERF proteins influence OGE, they could participate in the coordination of nucleus-mediated chloroplast and mitochondria functions. This is especially relevant for BSM/RUG2, dually targeted to chloroplasts and mitochondria which makes BSM/RUG2 a good candidate for the coordination of the expression of both organelle genomes by the nucleus (Quesada V, et al. 2011). The *mterf* mutants could constitute a good experimental model for studying the complex interactions operating among the different genomes within plant cells, and for this reason, they may represent ideal candidates in the coordination of the expression of organelle and nuclear genomes (Kleine, T. 2012).

2. Aim of the work

The aim of this work will be to identify novel candidates involved in organellar signaling and to create the genetic basis to understand the dynamic process present in organellar signaling. For this purpose three different approaches will be chosen. The first project is about the characterization of the PIGMENT DEFECTIVE 191; PDE191 a novel MTERF (MTERF6) in *Arabidopsis thaliana*, and its possible involvement in organellar signaling. Studies to understand the physiological role on MTERF in plant should be done through the characterization of different *mterf6* allelic mutant and the effect of the mutation in photosynthesis and translation efficiency. Molecular function will be performed to confirm the interaction of MTERF6 with putative conserved RNA binding sequence through northern blot analysis and the involvement of MTERF6 protein in the rRNA maturation. Through this work, should be possible to present a possible involvement of MTERF6 in the retrograde signaling. In the second and third project, we will identify components of translation-dependent retrograde signaling pathways. For this purpose, the *prors1-2* mutant will be used, which is a good candidate for the research of translational-dependent retrograde signaling pathways due to its defective plastidial and mitochondrial translation machinery. Two approaches will be used. The first one is a genetic forward screening to identify new mutants that could take part in the regulation and biogenesis of the plant organelles. Luminescence screen, and genetic and physiological characterization of EMS mutagenized plants (relaxed *LHCB* suppression (rls)), should be performed. The results of these experiments will provide new screening to identify new candidate translation-dependent retrograde signaling pathway. The second approach will be a physiological analysis of plants silenced through iRNA in order to identify target genes and transcription factors implicated in translation-dependent retrograde signaling. The silencing should be induced in adult plants by ethanol-dependent repression of *PRORS1*. Physiological characterization and translation activity analysis through in vivo labeling assay will be done in order to test the efficiency of the *PRORS1* repression.

3. Materials and Methods

3.1 Chemicals and antibodies.

The chemicals used were purchased from Roth (Karlsruhe, Germany), Sigma-Aldrich (Steinheim, Germany), Duchefa (Haarlem, Netherlands), Applichem (Darmstadt, Germany) and Serva (Heidelberg, Germany). Radioactive-labelled dCTP and ATP was ordered from Hartmann Analytik (Braunschweig, Germany). Primary antibodies were obtained from Agrisera (Vännäs, Sweden) and the secondary anti-rabbit antibody from Sigma-Aldrich (Steinheim, Germany).

3.2 Crossing of *Arabidopsis thaliana*.

Anthers in pollen recipient plants were emasculated from closed flowers by dissection. Stigmas in emasculated flowers were then pollinated manually (Weigel *et al.*, 2006).

3.3 Plant material and growth conditions.

The *mterf6-1* mutant (GABI_152G06) was identified in the GABI-KAT collection (Rosso *et al.* 2003) based on alterations in Φ_{II} . The mutants *mterf6-2* (SAIL_360_H09), *mterf6-4* (SALK_098509), were identified in the SIGnAL database (Alonso *et al.*, 2003), and *mterf6-3* (SGT1851-3-3) was found in the database described by Parinov *et al.* (1999). The mutants *prps17-1* and *prpl24-1* (Romani *et al.*, 2012) and *nr1-3* (Bollenbach *et al.*, 2005) have been described previously. With the exception of *mterf6-3* (which is a *Landsberg erecta* strain), all the mutants are in *Columbia-0* (Col-0) background.

The *A. thaliana prors1* mutant is a T-DNA insertion line (ecotype Col-0) was previously identified by Pesaresi *et al.* (2006) based on alterations in the effective quantum yield of PSII (Φ_{II}). In two of these mutants, the photosynthesis altered *mutant15* (*pam15*) and *pam18*, the same genetic locus was found to be affected. It was identified as the 5'-untranslated region of the nuclear gene *PROLYL-tRNA SYNTHETASE1* (*PRORS1*), the product of which acts in both plastids and mitochondria (Pesaresi *et al.* 2006). The *prors1-2* (*pam18*) mutant GABI_261E06, which showed the more severe phenotype, was used for this work.

The mutants used in the screening *rls* project were named *rls* (relaxed *LHCB* suppression; Table 1). The lines *LHCB3:LUC* (*prors1-2*) and *LHCB1.2:LUC* (*prors1-2*) were

3. Materials and Methods

mutagenized with EMS for the screening and generation of the so-called parental lines for the *rls* mutants (Table 1).

Table 1: List of *rls* mutants identified in the screen, including the respective parental line

Parental line	LHCB3:LUC (<i>prors1-2</i>)
Name <i>rls</i>	2-13, 145, 148, 134
<hr/>	
Parental line	LHCB1.2:LUC (<i>prors1-2</i>)
Name <i>rls</i>	45, 502, 518, 681, 743, 463, 615, 716, 83, 316, 749, 660, 436, 189, 255, 272, 280, 371

The plants analyzed in this project were grown on soil in greenhouse under controlled conditions (PFD: 70-90 $\mu\text{Em}^{-2}\text{s}^{-1}$, 16h light: 8h dark cycles) or under controlled environmental chamber (phytotrone) conditions at 22 °C/18 °C with a 16 h/8 h light/dark photoperiod.

Wuxal Super fertilizer (8% nitrogen, 8% P_2O_5 , and 6% K_2O ; MANNA) was used according to the manufacturer's instructions. Where indicated, seedlings were grown on agar (Sigma-Aldrich) containing 1.5% (w/v) Suc and 0.3% (w/v) Gelrite (Roth) at 22°C under 100 $\mu\text{mol photons m}^{-2} \text{s}^{-1}$ provided by white fluorescent lamps. For inhibitor experiments, seedlings were grown on MS medium supplemented with either 5 μM NF (Sigma Aldrich) or 220 $\mu\text{g mL}^{-1}$ lincomycin (Sigma-Aldrich).

3.4 Chlorophyll analysis.

3.4.1 Chlorophyll a fluorescence measurements.

Five plants of each genotype were analyzed, and average values and SD were calculated. In vivo chlorophyll a fluorescence of single leaves was measured using the Dual-PAM 100 (Walz). Pulses (0.5 s) of red light ($5,000 \mu\text{mol photons m}^{-2}\text{s}^{-1}$) were used to determine the maximum fluorescence and the ratio $(F_m - F_0)/F_m = F_v/F_m$. A 15-min exposure to red light ($37 \mu\text{mol photons m}^{-2}\text{s}^{-1}$) was used to drive electron transport before measuring Φ_{II} and $1 - qP$.

3.4.2 Chlorophyll concentration measurements.

For chlorophyll extraction, approximately 30 mg of leaf tissue from 4-week old plants was ground in liquid nitrogen in the presence of 80% acetone. After the removal of cell debris by centrifugation, absorption was measured with the Ultrospec 3100 pro spectrophotometer (GE Healthcare). Chlorophyll concentrations were calculated after Lichtenthaler (1987).

3.5 Microscopy.

To analyse defects in seed development, siliques of Col-0 and heterozygous mutants were manually dissected and observed using a Zeiss LUMAR.V12 stereomicroscope (<http://www.zeiss.com/>). Developing seeds were observed using a Zeiss Axiophot D1 microscope equipped with differential interface contrast (DIC) optics. Images were recorded with an Axiocam MRc5 camera (Zeiss) using the Axiovision program (version 4.1). Whole seeds were observed with a Leica TCS-SP5 confocal laser scanning microscope (Leica Microsystems, <http://www.leicamicrosystems.com/>).

3. Materials and Methods

3.6 Molecular biology.

3.6.1 Nucleic acids extraction.

Genomic DNA was isolated from *A. thaliana* leaves or cotyledons. Nucleic acids were extracted with a DNA extraction buffer (200 mM Tris-HCl pH 7.5, 250 mM NaCl, 25 mM EDTA and 0.5% (w/v) SDS) and precipitated with 0.8 volumes of isopropanol at 16,000 g for 20 minutes. The pellet was then washed in 70% ethanol and resuspended in 200 µl of ddH₂O. No RNase treatment step was needed for PCR analysis (Table 2).

The total RNA was extracted from ground tissue using one volume of extraction buffer (300 mM NaCl, 50 mM TRIS-HCl pH 7.5, and 20 mM EDTA, 0.5% SDS) and one volume of Phenol-Chloroform-Isoamylalcohol (PCI) followed by solubilization at 65°C for 5 minutes. After a centrifugation step (10 minutes at 7,000 g), the supernatant was mixed with one volume of 8 M LiCl, incubated for two hours at -20°C and centrifuged for 30 minutes at 4°C at 7,000 g. The pellet was then washed with 75% ethanol and resuspended in 80 µl of DEPC-treated water.

3.6.2 Standard PCR and high fidelity PCR.

For genotyping of plant material, 1 µl of DNA was used as a template for PCR analysis. For this purpose the PCR was performed in a total volume of 20 µl containing 2 µl of 10x PCR-buffer (QIAGEN), 100 µM dNTPs, 200 µM primers (Table 2), 0.5 units of Taq polymerase. The PCR product was then loaded on a 1% agarose gel. The genes of interest were amplified from Col-0 cDNA with the Phusion High-Fidelity DNA polymerase (Finnzymes). Reactions were performed in a total volume of 20 µl each. The reaction contained 200 µM of each primer, 250 µM dNTPs, 4 µl of 5x Phusion HF reaction buffer and 0.4 units Phusion HF DNA Polymerase. The PCR-products were loaded on a 1% agarose TAE (150 mM Tris-HCl, 1.74 M acetic acid, 1 mM EDTA) gel.

3. Materials and Methods

Table 2: Sequences of the primers used for the genotyping analyses

Atg number	Primer sequence (from 5' to 3')
AT4G38160 <i>mterf6-1</i>	RP TGATGCCACATCGCTTTGAGC
<i>mterf6-1</i>	LP GTGGATAAGCTTCTCACTTTCA
<i>mterf6-2</i>	RP ACAGCATCGACACCAAGCTG
<i>mterf6-2</i>	LP CCTCCGAAAAGCCAAACTTC
<i>mterf6-3</i>	RP ACAGCATCGACACCAAGCTG
<i>mterf6-3</i>	LP TGAATACCTGAAAACACAGG
<i>mterf6-4</i>	RP TCAATTGGATAGCCGGAAAG
<i>mterf6-4</i>	LP AAAGAATTCAGGATAAGAAGC
AT5G52520 <i>prors1-2</i>	RP TCCGGAAAGAGGTCTGTTCC
<i>prors1-2</i>	LP CCAAGCATGAGTTTCTCGAG
SALK	LP TAGCATCTGAATTTCATAACCA
GK	LP CCCATTTGGACGTGAATGTA
LB161	LP GGGCTACTACTGAATTGGTAG

3.6.3 First strand cDNA synthesis.

For cDNA synthesis the iScript reverse transcriptase kit (Bio-Rad, www.biorad.com) was used. In a total volume of 5 µl, 1 µg of RNA, 0.5 µl of 10x PCR buffer (Qiagen, www.qiagen.com) + MgCl₂ and 0.5 units DNase were combined. This mix was incubated at room temperature for 30 minutes. Then 2.5 mM EDTA was added and the mix was incubated for 15 minutes at 65°C. To each sample 2 µl of 5x iScript reaction mix buffer and 0.5µl of iScript reverse transcriptase were added. The samples were topped up to 10 µl with DEPC H₂O. The first-strand cDNA synthesis was performed according to the following protocol by using a thermocycler (BioRad): 5 minutes at 25 °C, 40 minutes at 42°C and 5 minutes at 85 °C.

3. Materials and Methods

3.6.4 Real time PCR analysis.

For real-time PCR analysis, the cDNA and specific primers were added to a solution containing iQ™ SYBRR Green Supermix (Bio-Rad), and the thermal cycling consisted of an initial step at 95°C for 3 min, followed by 40 cycles of 10 s at 95°C, 30 s at 55°C and 10 s at 72°C, after which a melting curve was performed. The genes investigated, and the corresponding primers, are listed in Table 3. Whenever possible, primers were designed to flank intron sites to make it possible to discriminate amplification of genomic DNA. RT-PCR was monitored by using the iQ5™ Multi Color Real-Time PCR Detection System (Bio-Rad). The adjustment of base line and threshold was done according to the manufacturer's instructions. Relative transcript abundances were normalized with respect to the level of the constitutively expressed mRNA for an ubiquitin-protein ligase-like protein (*AT4G36800*) and *Actin1* mRNA (*AT2G37620*). The data were analyzed by using LinRegPCR [Ramakers *et al.*, (2003)] and according to [Pfaffl *et al.* (2001)].

Table 3: Sequences of the primers used for the real time-PCR analyses

Atg number	Primer sequence (from 5' to 3')
"Housekeeping" gene (<i>AT4G36800</i>)	RP CTGTTACGGAACCCAATTC
	LP GGAAAAGGTCTGACCGACA
<i>MTERF6.1</i> (<i>AT4G38160.1</i>)	RP GTGGATAAGCTTCTCACTTT
	LP GGATAAGCTTCTCACTTTCA
<i>PRORS1</i> (<i>AT5G52520</i>)	RP GTATCTAGTAACAGTGTCGT
	LP ATCCACAATGTTACTGTCTC

3.6.5 Northern blot analysis.

Northern blotting and hybridization of probes were performed using standard procedures. Aliquots (2.5–10 µg) of total RNA were denatured and fractionated on a 1.2% agarose gel and blotted onto a nylon membrane (Roche). Blots were stained with 0.04% (w/v) methylene blue in 0.5 M sodium acetate (pH 5.2). Probes complementary to *psbA*, *psbB*, *PSBP*, *PSBS*, *psaA*, *LHCA1*, *LHCA2*, *LHCB1*, *LHCB2*, *rbcL*, *ndhC*, *rrn5S*, *rrn16S*, and *rrn23* were amplified from cDNA and labeled with [α -32P] dCTP. Probes for tRNA detection were generated by end labeling corresponding primers with [γ -32P] ATP using

3. Materials and Methods

polynucleotide T4 kinase (Fermentas; Table 4-5). Hybridizations were performed for 16 h at 65°C (detection of photosynthetic and *rrn* transcripts) or at 44°C (detection of *trn* transcripts). After washing, the filters were exposed to a phosphorimager screen and analyzed with the typhoon variable mode imager (GE Healthcare).

Table 4: Sequences of the primers used for the Northern blot analyses.

Atg number	Primer sequence (from 5' to 3')
<i>AT2G37620</i> <i>ACTIN1</i>	RP TTCACCACCACAGCAGAGC LP ACCTCAGGACAACGGAATCG
<i>ATCG00020</i> <i>PSBA</i>	RP GTGCCATTATTCCTACTTCTG LP AGAGATTCCTAGAGGCATACC
<i>ATCG00680</i> <i>psbB</i>	RP CGGGTCTTTGGAGTTACGAA LP TCCAGCAACAACAAAAGCTG
<i>AT1G06680</i> <i>PSBP</i>	RP TTCTCCTGAACAGTTCCTCTC LP ACACTGAAGGACGTAGCAGC
<i>AT1G44575</i> <i>PSBS</i>	RP GACAGGGATACCGATTTACGA LP ACAATGGACCTTGTTCTTTGAG
<i>ATCG00350</i> <i>psaA</i>	RP AACCAATTTCTAAACGCTGG LP TGATGATGTGCTATATCGGT
<i>AT3G54890</i> <i>LHCA1</i>	RP GTCAAGCCACTTACTTGGGA LP GGGATAACAATATCGCCAATG
<i>AT3G61470</i> <i>LHCA2</i>	RP GAGTTCCTAACGAAGATCGG LP AAGATTGTGGCGTGACCAGG
<i>AT5G54270</i> <i>LHCB3</i>	RP GGAGATGGGCAATGTTGGGA

3. Materials and Methods

		LP TAGTTGCGAAAGCCCACGCA
<i>AT2G05070</i>	<i>LHCB2.2</i>	RP GAGACATTCGCTAAGAACCG LP CCAGTAACAATGGCTTGGAC
<i>ATCG00440</i>	<i>NDHC</i>	RP GTTTCTGCTTTACGAATATG LP TCTATAAAAGCAGATACCCC
<i>ATCG00490</i>	<i>RBCL</i>	RP CGTTGGAGAGACCGTTTCTT LP CAAAGCCCAAAGTTGACTCC
<i>AT3G50820</i>	<i>PsbO2</i>	RP AGACGGAAGCGTGAAGTTCA LP CAATCTGACCGTACCAAACC
<i>ATCG00970</i>	<i>rm5S</i>	RP TATTCTGGTGTCTAGGCGT LP ATCCTGGCGTCGAGCTATTTTT
<i>ATCG00920</i>	<i>rm16S</i>	RP AGTCATCATGCCCTTATGC LP CAGTCACTAGCCCTGCCTTC
<i>ATCG00950</i>	<i>rm23S</i>	RP GTTCGAGTACCAGGCGCTAC LP CGGAGACCTGTGTTTTTGGT

3. Materials and Methods

Table 5: Sequences of the primers used for the RNA gel blot analyses.

Atg number	Primer sequence (from 5' to 3')
<i>ATCG00930</i> <i>trnI.2/3</i> , first exon	CTCTACCACTGAGCTAATAGCC
<i>ATCG00930</i> <i>trnI.2/3</i> , second exon	ATTTGAACCAGAGACCTCGC
<i>trnI.2/3</i> , intron / binding site	CCCAGGCACAACGACGCAA
<i>ATCG00940</i> <i>trnA.1</i>	GAGCGGAGCTCTACCAACTG

3.6.6 Aminoacylation analysis of tRNAs.

For RNA isolation, which preserves aminoacylation of tRNAs, frozen tissue was ground in liquid nitrogen. After the addition of 300 μ L of 0.3 M sodium acetate (pH 4.5) and 10 mM Na₂EDTA, RNA was isolated according to Varshney et al. (1991).

tRNA was mixed with 1.5 μ L of sample buffer (0.1 M sodium acetate (pH 5.0), 8 M urea, 0.05% bromphenol blue, and 0.05% xylene cyanol) and fractionated on a 0.4-mm-thick 6.5% polyacrylamide gel containing 8 M urea in 0.1 M sodium acetate buffer (pH 5.0). Electrophoresis at 500 V (-12 V/cm) was performed in a cold room until the bromphenol blue dye reached the bottom of the gel (20-24 h). The portion of the gel between the xylene cyanol and bromphenol blue dyes, which contained the tRNAs of interest, was electroblotted onto a nylon membrane (Roche) using a Electroblot apparatus at 20 V for 90 min with 40 mM Trisacetate, 2 mM Na₂EDTA (pH 8.1) as transfer buffer.

Detection of tRNA were done by Northern Blot probed with [γ -³²P]ATP end-labeled oligonucleotide probes specific for *trnI.2*, *trnI.1*, *trnT* and *trnPro*.

tRNA-Pro-Nth 5'TAGGGATGACAGGATTTGAAC3' ,*trnT* 5'ATGGCGTTACTCTACCACT3'

tRNA-Ile-2nd-exon 5'GCGAGGTCTCTGGTTCAAAT3'

3.6.7 Circular RT-PCR.

For the determination of 16S rRNA end sequences, total RNA (5 μ g) was treated with 40 units of T4 RNA ligase (New England Biolabs) in a total volume of 50 μ L. RNA was precipitated by the addition of 5 μ L of 3 M sodium acetate (pH 5.2) and 100 μ L of 99% ethanol, and the pellet was washed in 70% ethanol. cDNA was then synthesized using SuperScript II RNaseH reverse transcriptase (Invitrogen) and the reverse primer *16S-R1* (Table 6). The region of the circularized 16S rRNAs containing the junction between the

3. Materials and Methods

original 5' and 3' ends was then amplified by RT-PCR using 16S-R2 and 16S-F1 primers. The circular RT-PCR products were cloned using the pGEM-Easy Kit and sequenced.

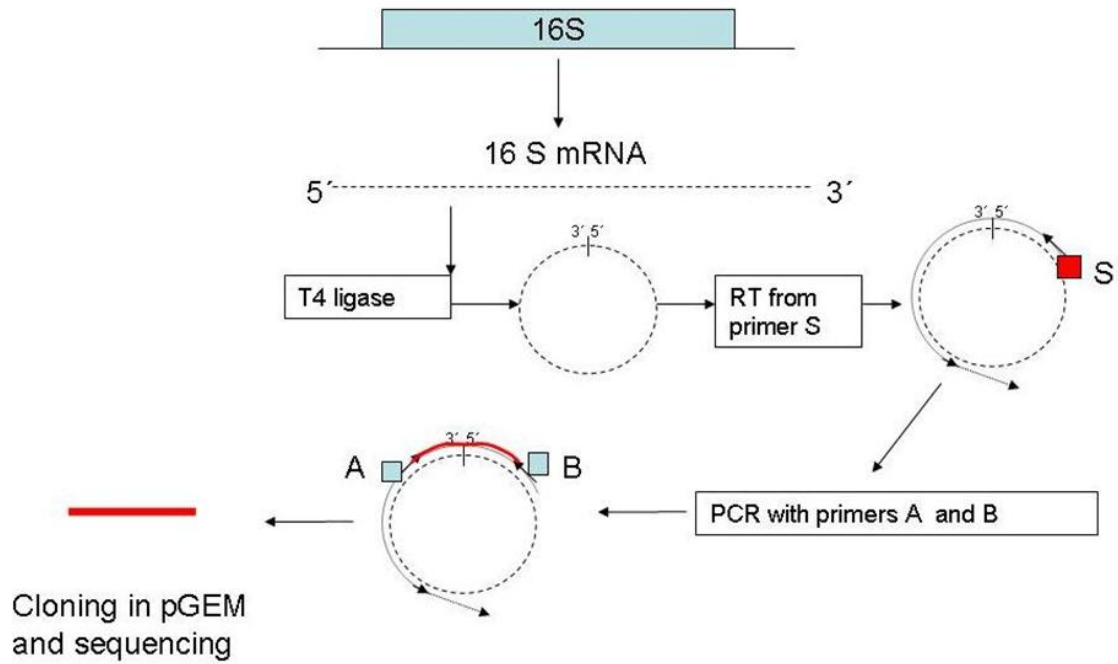


Figure 1: Schematic representation of circular RT-PCR procedure

Table 6 : Sequences of the primers used for the circular RT-PCR analyses.

Atg number		Primer sequence (from 5' to 3')
<i>ATCG00920</i>	16S	R1(S) GTATTAGCAGCCGTTTCCAG
<i>ATCG01210</i>	16S	R2(A) TCCAAGGGCAGGTTCTTAC
	16S	F1(B) TAATCGCCGGTCAGCCATAC

3. Materials and Methods

3.7 Biochemistry.

3.7.1 Chloroplast isolation.

Four weeks old light-adapted plants were homogenized in 0.45 M Sorbitol, 20 mM Tricine-KOH pH 8.4, 10 mM EDTA, 10 mM NaHCO₃ and 0.1% BSA. The material was then filtered through a single-layer of Miracloth (Calbiochem), and the filtrate was centrifuged at 4°C and 700 g for 7 minutes. The pellet was resuspended carefully in resuspension buffer (0.3 M Sorbitol, 20 mM Tricine-KOH pH 8.4, 2.5 mM EDTA and 5 mM MgCl₂). The suspension was centrifuged using a two-step Percoll gradient (40%-80% (v/v) in resuspension buffer) at 4°C and 6,500 g for 20 minutes. Intact chloroplasts were collected at the interface of the percoll gradient and washed once with resuspension buffer.

3.7.2 Protein preparation and immuno-blot analysis.

Frozen plant material was homogenized in 2X Laemmli buffer (200 mM Tris-HCl, pH 6.8, 4% SDS, 20% glycerol, 5% β-mercaptoethanol), and solubilized for 15 minutes at 65°C. After a centrifugation step (16,000 g, 10 min) the supernatant was boiled 5 minutes to denature the sample. Stroma and thylakoid samples were treated in the same way. The total protein extraction was then loaded on a Tris-glycine 12% SDS-PAGE (Schägger and von Jagow, 1987), afterwards, proteins were transferred to PVDF membranes (Ihnatowicz *et al.*, 2004) and immuno-decorated with antibodies.

3.7.4 In vivo translation assay.

The in vivo labeling assay was performed basically as described by Pesaresi, 2011. To this end, 6 mm leaf discs were incubated in 1 mM K₂HPO₄-KH₂PO₄ pH 6.3, and 0.1% (w/v) Tween-20 and 20 µg/ml cycloheximide to block cytosolic translation. [35S] methionine was added to the buffer in a final concentration of 0.1 mCi/ml and vacuum-infiltrated into the leaf tissue. The material was then exposed to light (20 µmol photon m⁻² s⁻¹) and four leaf discs were collected at each time point (5, 15 and 30 min). Total proteins were extracted as described above and fractionated by Tris-glycine SDS-PAGE (12% PA).

3.8 Luminescence screening and detection assay.

For luminescence screening of the plants from the M2 and the M3 generation, one leaf per plant was cut off, brushed with luciferin (Promega, USA) and incubated for 10 min in the dark. For the M2 generation from the first mutagenesis, the leaves were scanned with the Typhoon Variable Mode Imager (GE Healthcare) using ImageQuant 5.2 (GE Healthcare). For the M3 generation of the first and for both generations of the second EMS mutagenesis, the signals were detected by Fusion FX7 chemiluminescence and fluorescence imager (Pleq, Germany). For quantification of the firefly luciferase, the Luciferase Assay Kit (Promega, USA) was used according to the manufacturer's instructions. The firefly luciferase generates light from luciferin in a multistep process. First, D-luciferin is adenylated by MgATP to form luciferyl adenylate and pyrophosphate. After activation by ATP, luciferyl adenylate is oxidized by molecular oxygen to generate a dioxetanone ring. A decarboxylation reaction leads to an excited state of oxyluciferin.

3.8.1 Screening of *rls* mutants.

The *PRORS1* gene encodes for the chloroplast-localized prolyl-tRNA synthetase. The knock-down mutant (*prors1-2*) presents a down regulation of nuclear-encoded photosynthetic genes. Therefore, *prors1-2* mutant represent an appropriate candidate for a genetic forward screening to indentify new mutants suitable for the dissection of translational-dependent retrograde signaling pathways. This project was focused on the characterization of *relaxed LHCB suppression (rls)* mutants, previously screened by a genetic forward luminescence screen and determination of the expression level of nuclear-encoded photosynthetic genes [dissertation of Lukas Mittermayr 2013].

These new mutants were generated by EMS mutagenesis, and identified through a genetic forward screen. Analysis of the *LHCB* expression, monitored by luciferase, and the observation of the phenotype of the mutagenized plants were used as screening method [Dissertation of Lukas Mittermayr LMU 2013].

Before this work started, a promoter-luciferase construct was transferred into a Col-0 *Arabidopsis thaliana* plant (pro:*LUC* Col-0). In addition, *LHCB1.2* and *LHCB3* were chosen as promoters, and were cloned upstream of the luciferase gene. These promoters were used, because the *LHCB1.2* and *LHCB3* transcripts are normally down-regulated in the *prors1-2* mutant however the expression remained strong enough to ensure signal detection in the luminescence screen. The pro:*LUC* Col-0 plants were crossed with *prors1-2* and the third generation was mutagenized with EMS. The Fourth generation of the

3. Materials and Methods

mutagenized plants (M4) was screened in this project for a rescue of the phenotype (leaf size and leaves pigmentation) and a rescue of the *LHCB1.2* or *LHCB3* through Northern blot analyses.

4. Results

Part of the results presented in this chapter have been recently published in *Plant Physiology*, "MTERF6, a Member of the Arabidopsis Mitochondrial Transcription Termination Factor Family, Is Required for Maturation of Chloroplast tRNA^{Ala} (GAU)" (Romani *et al.* 2015).

4.1 Identification of Mutants for the MTERF6 Locus.

All the experiments were performed on *Arabidopsis thaliana* plants, ecotype Columbia (Col-0). Three T-DNA insertion lines were analyzed to investigate the effect of the alteration of the *MTERF6* Gene *At4g38160*, (also known as *PIGMENT DEFECTIVE 191*; *PDE191* or *MTERF6*). The Isolation of the genomic sequence flanking the left side of the T-DNA allowed the identification of insertion lines. The first line named *mterf6-1* is a knock-down homozygous mutant with an insertion site in the 5'-untranslated region (UTR) of the gene *AT4G38160* at position -115 to the start codon. The second line, termed *mterf6-2*, is a homozygous knock-out line, where the T-DNA insertion falls into an exonic region of the gene *AT4G38160*, at +706 bp from the start codon. The third line, named *mterf6-3*, has a T-DNA insertion at 511 bp from the start codon. According to the TAIR, The Arabidopsis Information Resource, *AT4G38160* is a single-copy gene with three predicted isoforms transcript splice forms *AT4G38160.1*, *AT4G38160.2* and *AT4G38160.3*, which harbor the same 5' end but different 3' ends (Figure 2).

4. Results

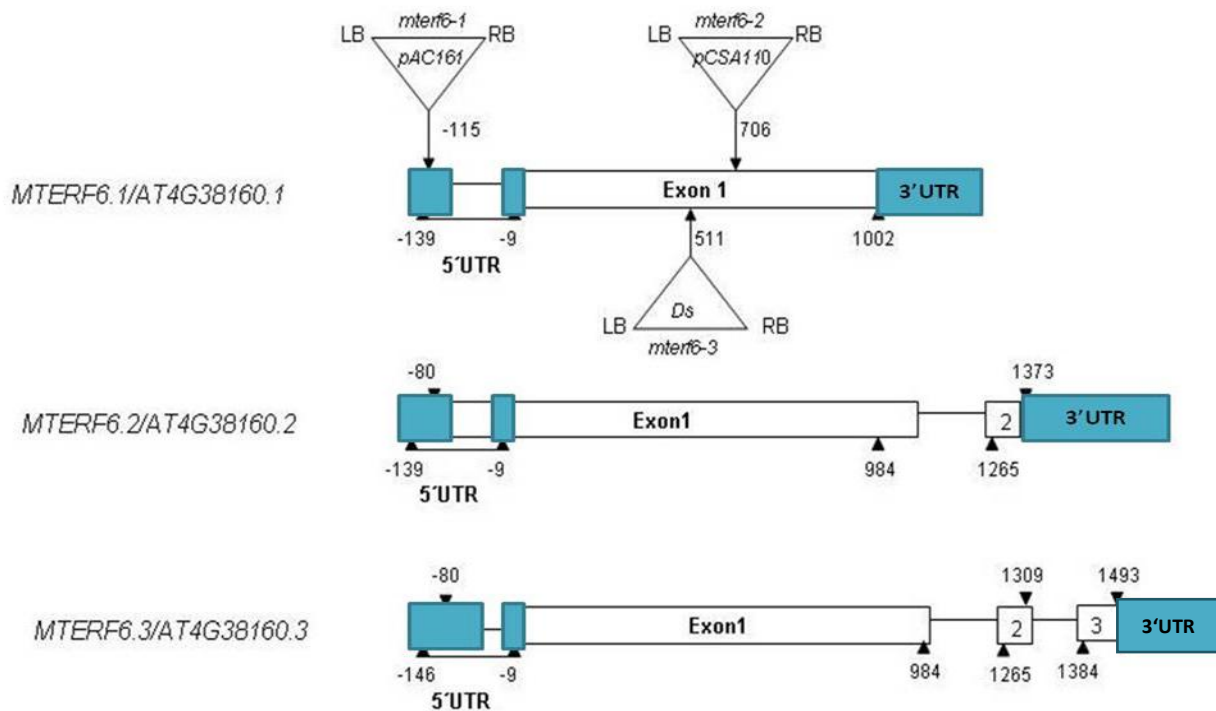


Figure 2. T-DNA tagging of the *MTERF6/AT4G38160* locus

Three different splice forms (*AT4G38160.1*, *AT4G38160.2*, *AT4G38160.3*) according to TAIR are shown: exons are indicated as numbered white boxes, introns as black lines and 5'UTR and 3'UTR (blue boxes) Arrowheads indicate the positions of translation initiation and stop codons. Sites, designations and orientations of T-DNA and Ds insertions are indicated (RB, right border; LB, left border). The *mterf6-1* allele was identified in the GABI-KAT collection (Rosso et al., 2003) as line GABI_152G06; *mterf6-2* corresponds to the SAIL_360_H09 line donated from Syngenta to the SALK collection (Alonso et al., 2003). In the *mterf6-3* allele, a copy of the Ds transposon (Parinov et al., 1999) is inserted in the first exon. The insertions are not drawn to scale

In order to determine the effects of the T-DNA insertions on *AT4G38160* gene expression, mRNA levels derived from Col-0 and the mutants were evaluated by RT-PCR.

Total RNA was retro transcribed with Reverse Transcriptase enzyme and on the resulting complementary DNA (cDNA); gene-specific primers were used to quantify transcription levels (RT-PCR). Real-time PCR (and semi-quantitative RT-PCR (Figure 3A-B) showed that the T-DNA insertion in *mterf6-1* induces a strong decrease of *AT4G38160* levels, whereas the insertion in *mterf6-2* and in *mterf6-3* causes the complete loss of transcript. The RT-PCR data suggest that the *mterf6-1* phenotype might be caused by knockdown of the *AT4G38160* gene.

4. Results

To confirm the mutation, the line *mterf6-1* was genetically complemented with the full-length first splice variant (*AT4G38160.1*) fused upstream to the enhanced green fluorescence protein (eGFP) reporter gene under the control of the Cauliflower mosaic virus (CaMV) 35S promoter (Romani et al. 2015). This complemented line was also used as a control during the RT-PCR experiment.

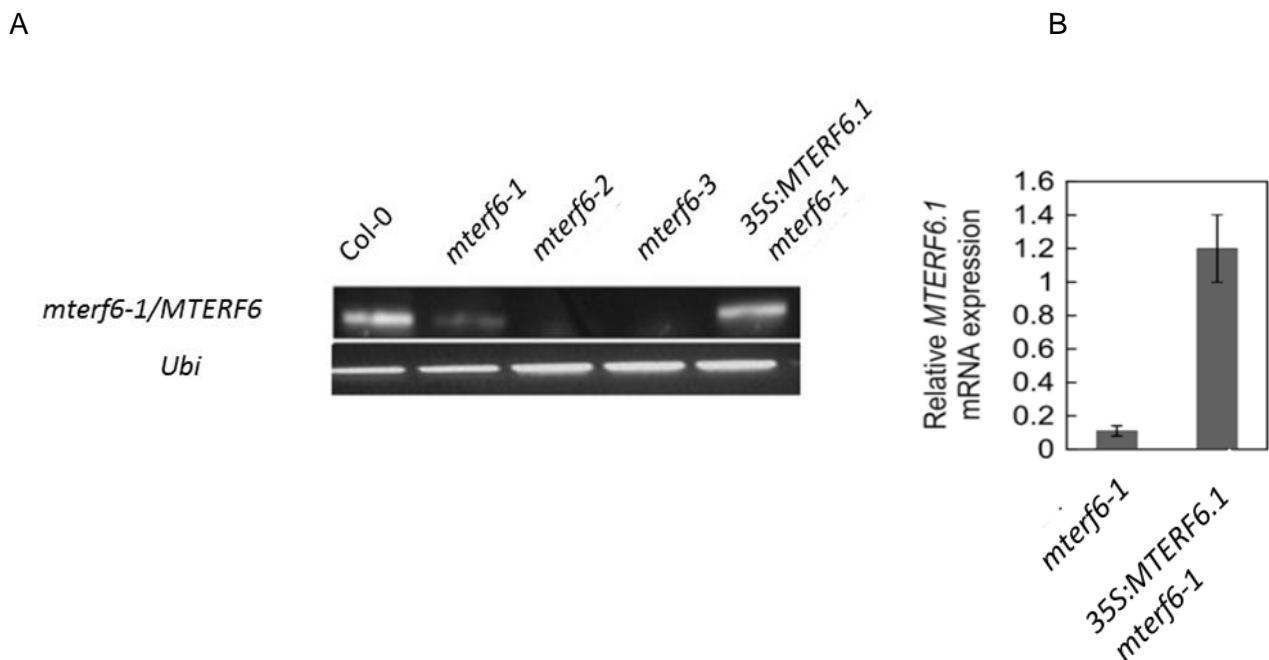


Figure 3. (A) RT-PCR analysis of wild-type (Col-0), *mterf6-1*, *mterf6-2* and *mterf6-3* mutant plants, and the complemented *mterf6-1* (*35S:MTERF6.1 mterf6-1*) plants. RT-PCR was performed with primers specific for *AT4G38160* splice form 1 (*MTERF6.1*) and Ubiquitine primer as a control. (B) Real-time PCR analysis of *MTERF6.1* mRNA expression of four-week-old *mterf6-1* plants, and *mterf6-1* complemented with the first splice variant of the *AT4G38160* gene (*35S:MTERF6.1 mterf6-1*). *MTERF6.1* mRNA levels are expressed relative to those in the Col-0 control which was set to 1. The results were normalized to the expression level of *AT4G36800*. Bars indicate standard deviations.

4. Results

4.1.1 Phenotypic analysis of *mterf6* mutants.

The *mterf6-1* mutant is characterized by a photosynthetic phenotype, pale, and small size in comparison to the Col.0, and it is able to complete the growth cycle (Figure 4).

In the *mterf6-2* (SAIL_360_H09) and *mterf6-3*, DS insertion SGT1851-3-3 position 706 and 511 to the start codon, was not possible to identify homozygous plants, suggesting a possible defect in the early stages of seed development. To identify the homozygous plants, silique analysis were performed on *mterf6-2*/MTERF6 and *mterf6-3*/MTERF6 plants. The analysis allowed the identification of approximately 25% white ovules (122 out of 523 ovules for *mterf6-2*/MTERF6 and 70 out of 276 ovules for *mterf6-3*/MTERF6; Chi quadrat test) (Figure 4). Homozygous *mterf6-2* mutant seeds were able to grow exclusively in presence of medium containing sucrose. The seedlings mutant *mterf6-2* displayed an albinotic phenotype with growth inhibition after two weeks while the *mterf6-1* seedlings showed a phenotype similar to the Col-0 under these conditions (Figure 4).

4. Results

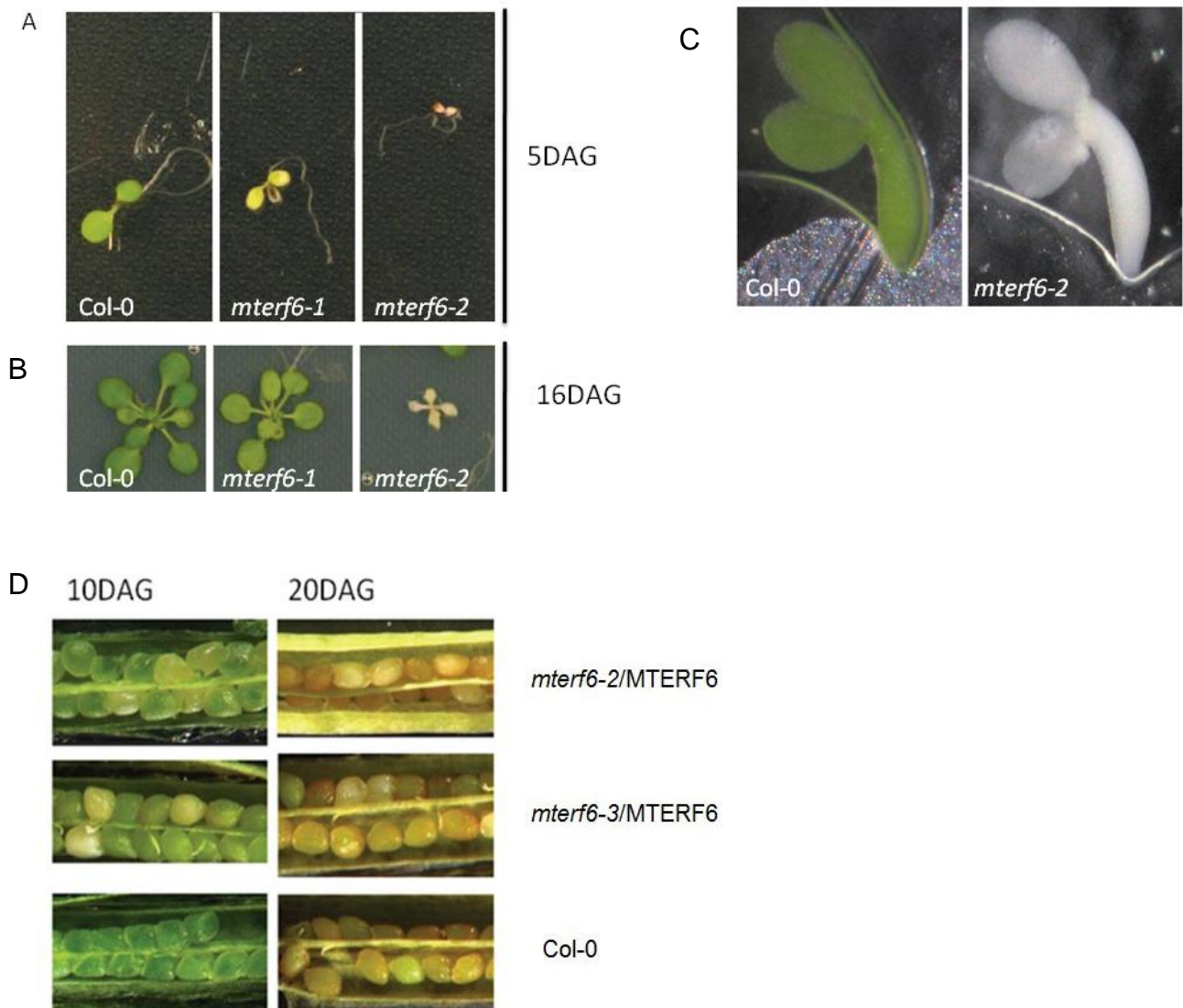


Figure 4. Phenotypic characterization of *mterf6* mutants:

(A) Phenotypes of 5 DAG (days after germination) wild-type (Col-0), *mterf6-1* and *mterf6-2* plants.

(B) Phenotypes of 16 DAG (days after germination) wild-type (Col-0), *mterf6-1* and *mterf6-2* plants.

(C) Images of isolated fully mature embryos (bent cotyledon stage) from Col-0 and *mterf6-2/MTERF6* seeds.

(D) In siliques of *mterf6-2/MTERF6* and *mterf6-3/MTERF6* white ovules are found intermixed with normal green ovules. White ovules 25% (122/523 for *mterf6-2/MTERF6* and 70/276 for *mterf6-3/MTERF6* second allele) of all ovules analyzed.

4. Results

Fluorimetric analysis were carried out using a **P**ulse **A**mplitude **M**odulated chlorophyll fluorometer (PAM) to confirm the photosynthetic phenotype of *mterf6-1* plants. The mutant *mterf6-1* (GABI_152G06) showed alterations in the effective quantum yield of photosystem II (PSII), designated Φ_{II} , was significantly reduced compared to the wild type (Table 7). Furthermore, the maximum quantum yield of PSII (Fv/Fm) was drastically reduced (Col-0, 0.81 ± 0.01 ; *mterf6-1*, 0.54 ± 0.03), implying a defect in energy transfer within PSII. An increment in the excitation pressure of PSII, estimated by the parameter 1-qP, was observed (Table 7).

Table 7: PAM data for Col.0, *mterf6-1* and complemented plants (oeMTERF6-1).

	Fv/Fm av.	Yield av.	NPQ av	1-qp
Col.0	0.81 (+/- 0.01)	0.70 (+/- 0.03)	0.14(+/- 0.03)	0.11(+/- 0.03)
<i>mterf6-1</i>	0.54 (+/- 0.03)	0.43(+/-0.02)	0.11 (+/-0.04)	0.57(+/- 0.04)
oe <i>MTERF6-1</i>	0.82(+/- 0.01)	0.69(+/-0.04)	0.16 (+/- 0.02)	0.14(+/- 0.03)

4.1.2 Analysis of chloroplast gene expression.

To study the effects of decreased MTERF6 activity, the leaky *mterf6-1* mutant was employed. Immunoblot analysis was performed on total protein extracts from Col-0 and *mterf6-1* leaves to investigate whether the defect in photosynthetic activity recognized in the *mterf6-1* mutant was a consequence of reduced amounts of photosynthetic proteins. In the *mterf6-1* mutant, chloroplast-encoded subunits of PSII and PSI, the cytochrome b6f complex, and the chloroplast ATP synthase, accumulated to lower levels compared to the Col-0 (Figure 5A). On the contrary, the accumulation of nuclear encoded proteins like PsbP (a subunit of the oxygen-evolving complex), NdhL (a subunit of the chloroplast NAD(P)H dehydrogenase complex), and Lhca2 and Lhcb1 (subunits of LHCI and LHCII, respectively), was comparable to the Col-0 levels. The reduced accumulation of plastid-encoded thylakoid proteins in the *mterf6-1* mutant could be caused by a translational defect or might be the consequence of impaired accumulation of their transcripts. From the immunoblot detection analysis revealed that *mterf6-1* might have a defect in translational levels of photosynthetic subunits encoded by the chloroplast genome. Therefore, two possibilities may explain this scenario; the first possibility is that the defect is located more up-stream, and that the transcription of the genes for the plastidial subunits is somehow affected, the second possibility is that the defect could be the result of a direct impairment

4. Results

of translational or post-translational process (e.g. protein stability, processing etc...) in the chloroplast.

To explore a possible role of MTERF6 in the transcription, northern blot analysis of transcript levels of wild-type and *mterf6-1* plants were performed, investigating photosynthetic subunits from all complexes. The analysis showed no notable changes in transcript levels for all of the genes investigated (Figure 5B). Controversy, immunoblot analysis displayed specific reduction of levels of chloroplast encoded proteins in *mterf6-1* mutants (Figure 5A). Taken together, the findings suggest that the reduced amounts of chloroplast-encoded photosynthetic proteins detected in the *mterf6-1* mutant are not associated with lower levels of transcripts of the corresponding chloroplast genes.

4. Results

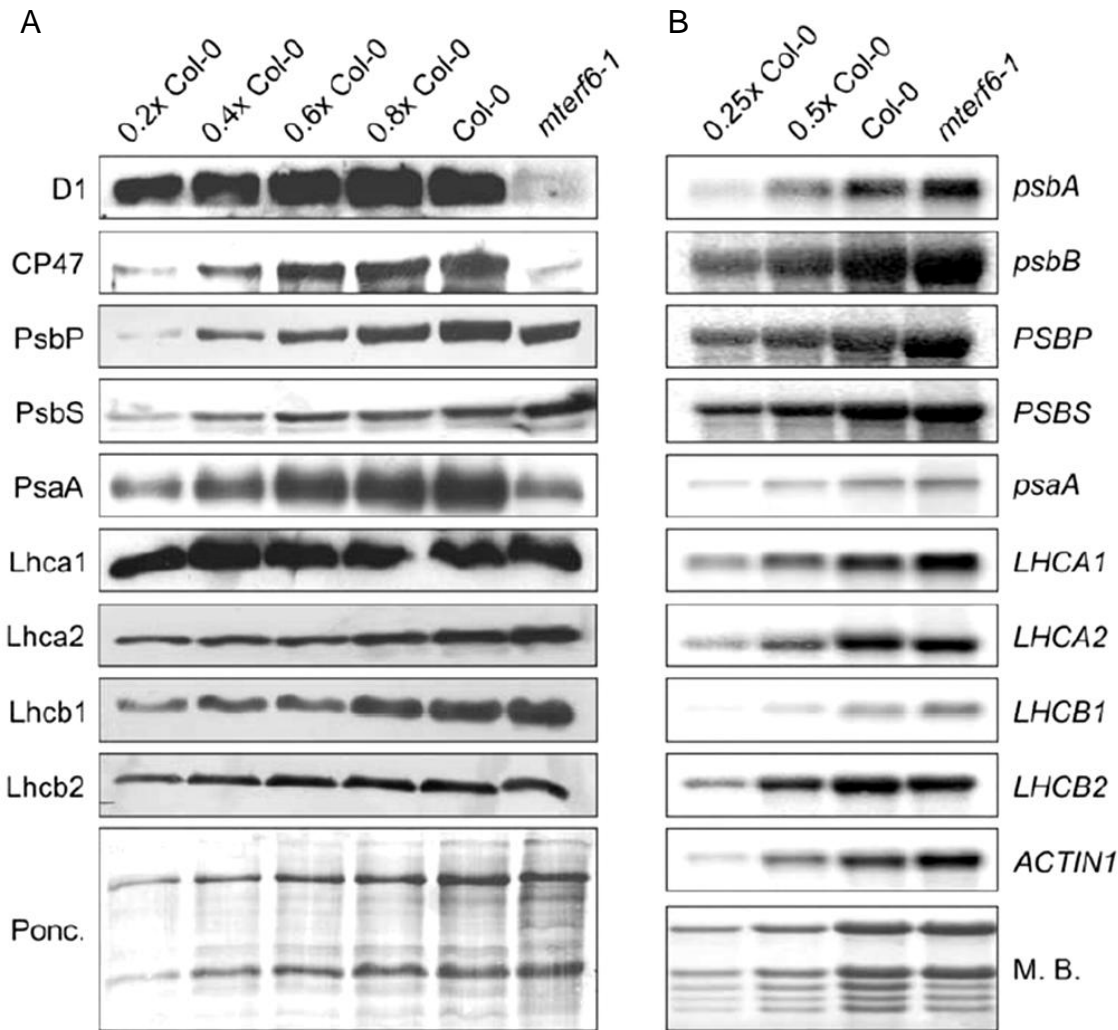


Figure 5. (A) Immunoblot analysis of photosynthetic subunit levels in *mterf6-1*.

Increasing amount of Col-0 total protein extract (0.2, 0.4, 0.6, 0.8 and 1x) and 1x *mterf6-1* were loaded. Total leaf protein extract from Col-0 and *mterf6-1* were fractionated by SDS –PAGE. After blot transfer, different antibodies were used to quantify protein contents. A ponceau staining of membranes were used as loading controls (bottom panel).

(B) Northern blot analysis of photosynthetic subunits transcripts in Col-0 and *mterf6-1*.

Increasing amount (0.25, 0.5x and 1x) of total RNA extracted from Col-0 and *mterf6-1* (1x) were loaded on denaturing formaldehyde gels. After blot transfer, the resulting membranes were hybridized with different ³²P labelled DNA probes and transcripts visualized by autoradiography. Methylene blue staining of membranes (bottom panel) served a loading reference. (Arianna Morosetti dissertation LMU 2012, Romani et al. 2015)

To investigate the possibility that the defect could be the result of a direct impairment of translational or post-translational process in the chloroplast, the synthesis of plastid-

4. Results

encoded thylakoid membrane proteins was studied by pulse labeling of Col-0 and *mterf6-1* mutant leaves in the presence of cycloheximide, which inhibits the translation of nucleus-encoded proteins.

Four leaves discs were collected after 10 and 30 minutes of incubation with [³⁵S] methionine in the presence of light. After pulse labeling for 20 min, the synthesis of the D1 protein was reduced in *mterf6-1* when compared to the Col-0 (Figure 6B) and labeled proteins of the α - and β - subunits of ATP synthase (CF1 α/β) were absent in *mterf6-1*. Subsequent chases of 15 and 60 min with unlabeled methionine showed that the turnover rate of D1 was unaffected in the mutant (Figure 6B).

The effects of the *mterf6-1* mutation on the translation of chloroplast transcripts were also examined by analyzing the association of *psaB* and *psbB* mRNA with polysomes. Plant extracts were fractionated in sucrose gradients under conditions that preserve polysome integrity and mRNAs were identified by hybridization with specific probes. In general, efficiently translated RNAs are almost all associated with ribosomes and migrate deep into the gradient. In fact, rRNAs in Col-0 and *mterf6-1* polysome gradients showed not an equal, but a similar distribution, as determined by ethidium bromide staining. However, *psaB* and *psbB* mRNA association was shifted in the non-polysomal fractions in *mterf6-1* as compared to Col-0. This data suggest that the majority of mRNA in *mterf6-1* chloroplasts is not engaged in translation, thus leading to a reduction in synthesis of chloroplast proteins (Figure 6A).

4. Results

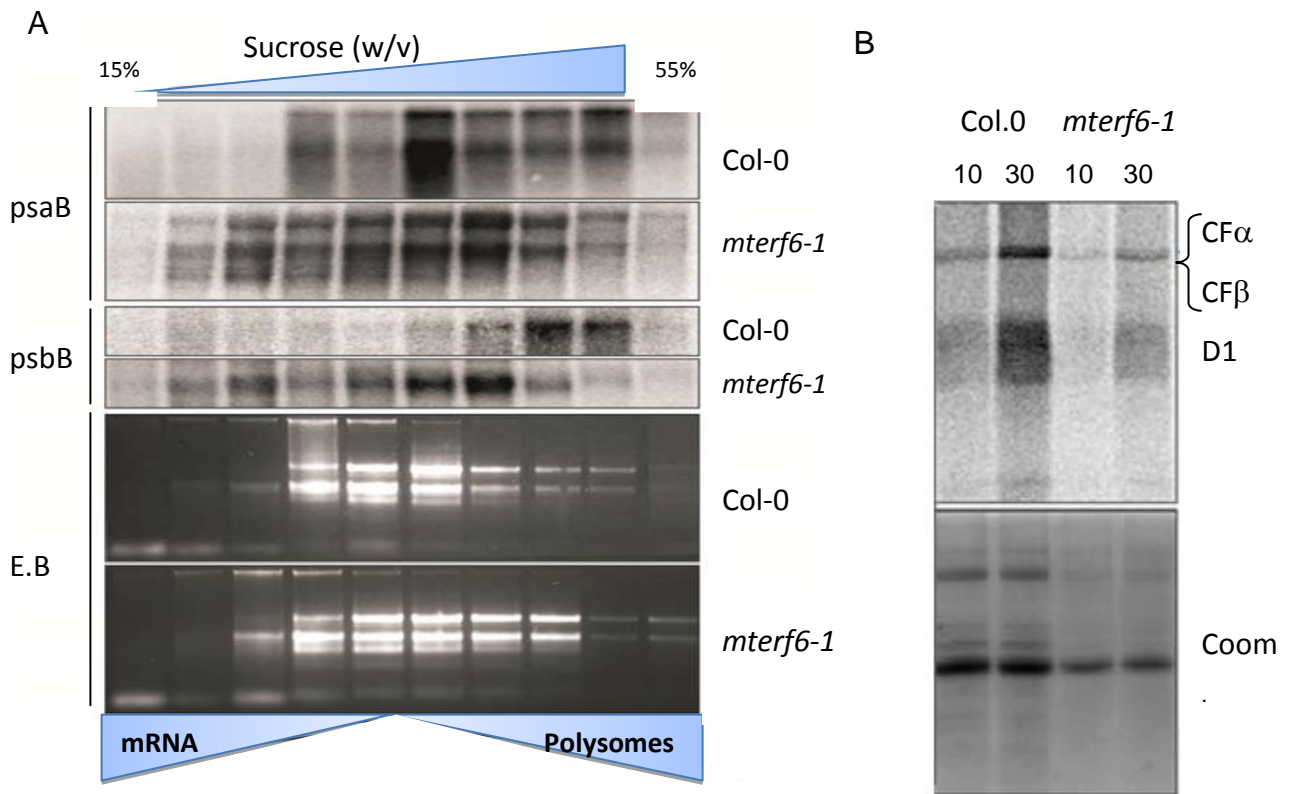


Figure 6. (A). Polysomes analysis: Whole-cells extracts from Col-0 and *mterf6-1* plants were fractionated in linear 0.44 to 1.6 M (15 to 55%) sucrose gradients by ultracentrifugation. Gradients were divided into 10 fractions, and RNA was isolated from equal volumes. RNA blots were hybridized with [α - 32 P]-dCTP labeled cDNA fragments specific for *psaB* and *cp47*. Ribosomal RNAs were stained with ethidium bromide (E. B.).(Romani *et al.* 2015)

(B) In vivo pulse labeling of thylakoid membrane proteins with [35 S] Met in the presence of cycloheximide. Proteins were resolved by SDS-PAGE after pulse labeling for 10 and 30 min and visualized by autoradiography.

Coom: Coomassie Blue served as loading reference (Romani *et al.* 2015)

4.1.3 Analysis of the plastid ribosomes in *mterf6* mutants.

Total RNA preparations of Col.0 and *mterf6-1* and *mterf6-2* and the *rnr1-3* mutant [40] and the chloroplast ribosomal mutants *prps17-1* and *prpl24-1*, (Romani, I. et al. 2012), served as controls for altered rRNA accumulation, were analyzed. In *mterf6-2* and *rnr1-3*, already Bioanalyzer profiles revealed the reduction of both the 16S-18S rRNA and the 23S-18S rRNA ratios, indicating a reduced accumulation of the small and the large plastid ribosomal subunits. (Romani *et al.* 2015). This finding was supported by immunoblot analysis of total protein extracts from wild-type, *mterf6-1*, *mterf6-2*, and *rnr1-3* seedlings. In the *mterf6-1*

4. Results

mutant, representative proteins of the small (chloroplast-encoded Rps7 and nucleus-encoded RPS5) and large (nucleus-encoded RPL4) plastid ribosomal subunits accumulated to lower levels, as in the wild type (Figure. 7). This reduction was more pronounced in *mterf6-2* and *rnr1-3* seedlings (Figure 7). This data indicates that the accumulation of ribosomal subunits is reduced.

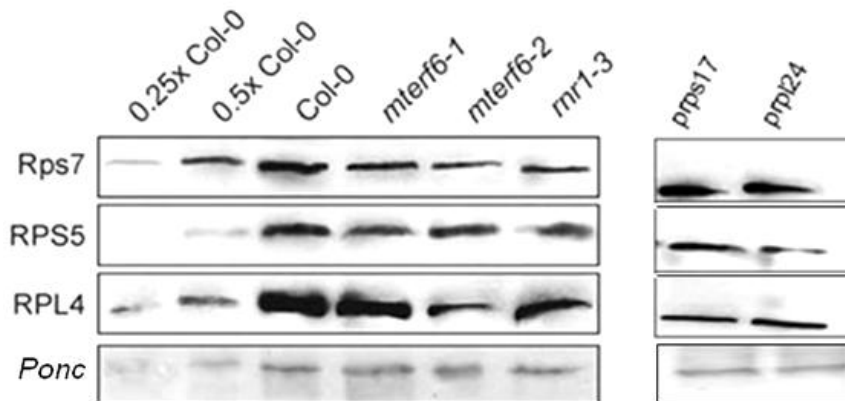


Figure 7. Immunoblot analysis of plastid ribosome subunits levels in *mterf6-1*.

Increasing amount of Col-0 total protein extract (0.25, 0.5, and 1x) and 1x *mterf6-1*, *mterf6-2* and *rnr1-3*, *prps17* and *prpl24*, were loaded. Total leaf protein extract from Col-0 and *mterf6-1* and *mterf6-2* and *rnr1-3*, *prps17* and *prpl24* seedlings were fractionated by SDS –PAGE and blot transfer, different antibodies were used to quantify protein contents of plastid encoded Rps7 and the nucleus encoded RPS5 and RPL4 proteins. Loading was adjusted to fresh weights of seedlings. A ponceau staining of membranes were used as loading controls (bottom panel)

4.1.4 Identification of MTERF6 binding sequences.

Studies conducted on animal models have shown that MTERFs are able to bind DNA and regulate transcription of mitochondrial genes, in particular organellar rRNA operons (Terzioglu M, et al 2013). Therefore, the question to answer was whether MTERF6 might similarly interact with plant organellar DNAs. MTERF6 harbors seven MTERF domains and its predicted structure match with the human MTERF1, suggesting the possibility of a similar molecular function shared by the two proteins. To investigate this hypothesis, bacterial one-hybrid screening, electrophoretic mobility shift assays, and coimmunoprecipitation were already accomplished before this thesis started (Romani et al. 2015). The B1H and EMSA results demonstrated that MTERF6 is able to bind a 15bp sequence downstream the 16SrRNA sequence, found within the two chloroplast rRNA

4. Results

operons (Figure 8), and a significant amount of sequences were found in or adjacent to six chloroplast genes, referred to as target I (*trnV.1*), target II (*trnI.2/trnI.3*). In the light of the results published for metazoan MTERFs and the results here presented, northern blot analysis was carried out to detect alterations in the rRNA operon transcription. A series of probes was designed to trace the maturation of 16S, 23S and 5S rRNA, total RNA was analyzed by northern blot analysis (Figure. 9). The *rnr1-3* mutant, showing plastid ribosome deficiency similar to the one noticed in the *mterf6-2* mutant, was included as a control. Results indicated that in *mterf6* mutants, but not in the *rnr1-3* mutant, levels of the mature *trnA.1* and 5S rRNA transcripts were increased (Figure 9). In contrast, the levels of mature 23S rRNA were decreased in *mterf6-1* and decreased to approximately 50% of the wild-type levels in *mterf6-2* and *rnr1-3* seedlings, and was possible to detect an over accumulation of unprocessed precursor (Figure. 9).

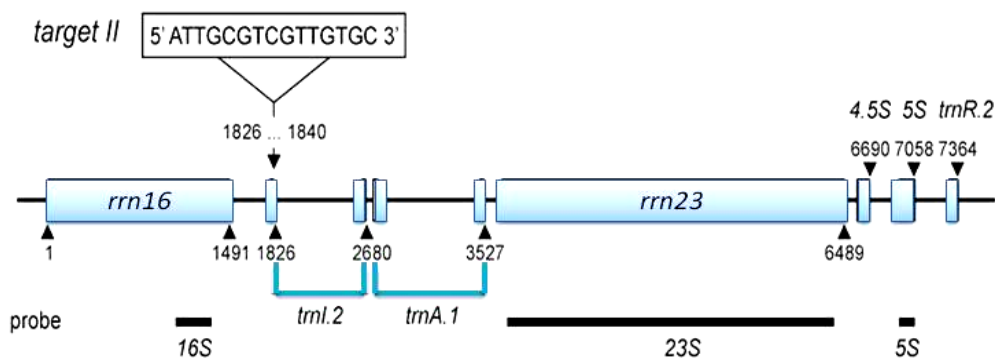


Figure 8. Schematic representation of the chloroplast *rrn* operon and the MTERF6 target site located in the *trnI.2* gene (target II). blue boxes indicate genes encoding rRNA and tRNA, respectively; introns are depicted as solid lines. The positions of the probes used in northern-blot analysis are marked by black rectangles under the operon. (Romani *et al.* 2015)

4. Results

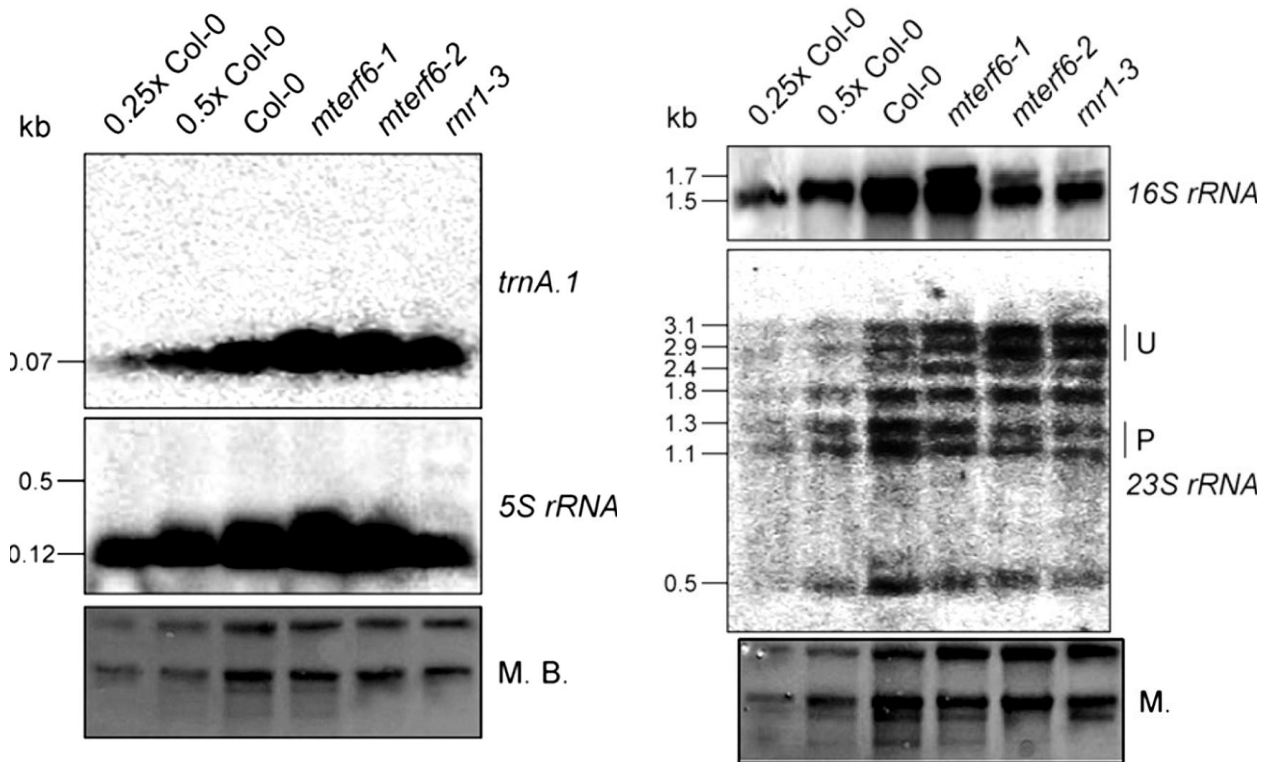


Figure 9. Analysis of transcript levels and splice forms of *rrn* genes and *trnA.1*. Total RNA was isolated as, resolved on a denaturing gel, transferred onto a nitrocellulose membrane, and probed with [α - 32 P]dCTP-labeled cDNA fragments specific for *rrn16*, *rrn23*, and *rrn5* and and [γ - 32 P]ATP end-labeled oligonucleotide probe specific for *trnA.1*. rRNA was visualized by staining the membrane with Methylene Blue (M. B.) as a loading control. (Romani *et al.* 2015)

Previous studies on rRNA maturation in plants showed that in higher-plant chloroplasts, a precursor rRNA transcript containing the 16S, 23S, 4.5S and 5S rRNA is produced from the *rrn* operon (Bellaoui M, *et al.* 2003). This primary transcript is, consequently, processed into the 23S-4.5S rRNA precursor, the 16S and the 5S rRNA. The 23S-4.5S rRNA precursor is subsequently cleaved into the 23S and 4.5S rRNAs. Alteration in the maturation pathway can induce an over accumulation of 16S and 23S rRNAs, as found, for example, in the *rnr1-3* mutant (Bollenbach TJ, *et al.* 2005) as well as in differentiation and *greening-like1* (*dal1*; Bisanz C, *et al.* 2003) and several other *Arabidopsis* mutants defective in plastid ribosomal proteins (Tiller N, Bock R 2014). From the results presented it is deducible that MTERF6 influences the mechanisms involved in the rRNA correct maturation in the chloroplast.

4. Results

4.1.4 Analysis of rRNA maturation.

Previous analysis showed was found that genes encoding proteins involved in plastid rRNA processing as for example *RNR1* are coexpressed with *MTERF6*. *RNR1* is one of the few proteins which play a direct role in rRNA processing and its activity is essential for rRNA maturation (Bollenbach Tj et al. 2005).

In this part of project, we tested whether a relative lack of *MTERF6* extrovert similar effects on rRNA maturation to the *rnr1* mutation by mapping the 5' and 3'ends of 16S rRNA in *mterf6-1* and wild-type plants by circular RT-PCR (Figure.10). All clones analyzed carried mature 5' ends in wild-type and *mterf6-1* plants. Furthermore, all wild-type derived clones and seven out of nine *mterf6-1* derived clones presented a mature 3' ends. The remaining two *mterf6-1* derived clones contained only one nucleotide 3' extension (Figure.10). Consequently, *mterf6-1* plants did not exhibit the same molecular phenotype as *rnr1* plants, in which no mature 16S rRNA 3'ends are detected. Bollenbach *et al.* (2005) found that 10 of their 11 clones contained five-nucleotide 3' extensions. Overall, it is not clear if the altered rRNA maturation in *mterf6* mutants is due to a direct effect resulting from a lack of binding of *MTERF6* at the *rnr* operon or results from a partial loss of translation and therefore represents a secondary effect of the reduction of *MTERF6* levels.

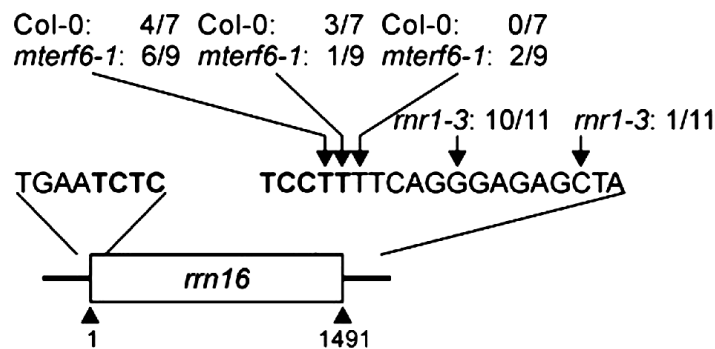


Figure 10. Mapping of 16S rRNA 3' ends by circular RT-PCR. The arrows point to the 3' ends detected, and the numbers of clones obtained at the indicated positions are given. The *rnr1-3* data are taken from Bollenbach *et al.* (2005). The 5' and 3' ends of the mature 16S rRNA sequence are depicted in boldface. (Romani *et al.* 2015)

4. Results

4.1.5 Northern blot analysis of the transcript present in the target I (*trnV.1*), and in the target II *trnI.2/trnI.3*).

To confirm whether binding of MTERF6 to target I detected in vitro (downstream of the *trnV.1* gene encoding *tRNA^{Val}*) influences *trnV.1* expression, Northern blot analysis was performed (Figure 11). The analysis showed that the accumulation level of *trnV.1* accumulated were higher in *mterf6-1* compared to the Col-0. Transcripts of *trnM* encoding *tRNA^{Met}*, which is located 5' of *trnV.1*, but transcribed in the opposite direction (Figure 12A), were also more abundant in *mterf6-1*. Instead *ndhC*, which is located in 3' of the putative MTERF6 binding site, presented an identical amounts accumulated in *mterf6-1* and Col-0 plants (Figure 11). Interestingly, transcripts of trn genes distantly located with respect to the MTERF6 target I (*trnV.1*) target site, such as *trnG.2* and *trnE* encoding *tRNA^{Gly}* and *tRNA^{Glu}*, were also elevated in *mterf6-1* compared to the Col-0 (Figure 11).

4. Results

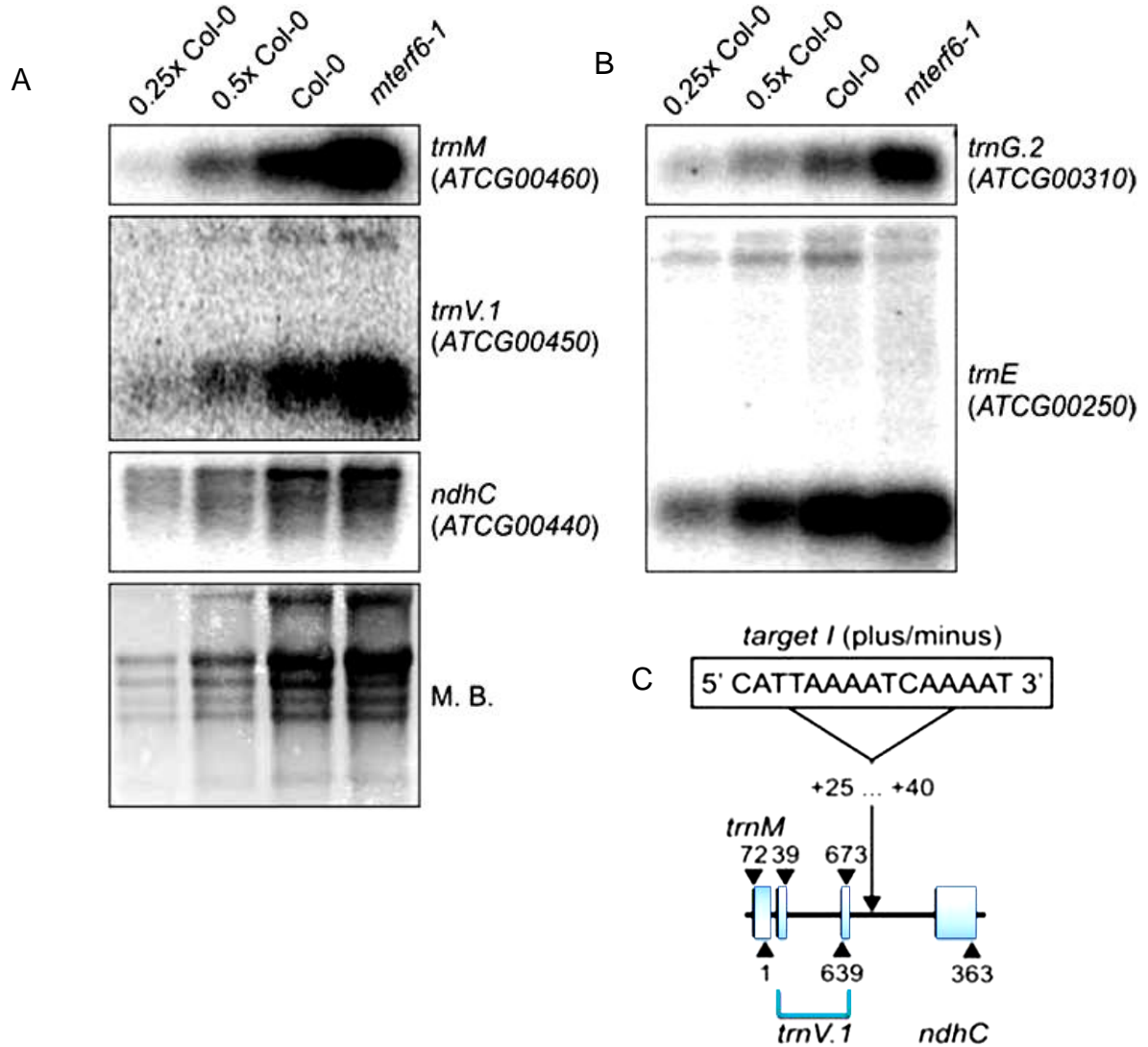


Figure 11. Transcript levels of plastid encoded tRNAs are over accumulating in the *mterf6-1* mutant compared to wild-type (Col-0) plants.

(A) Analysis of transcript levels of genes located adjacent to target I in wild-type and *mterf6-1* plants. Total RNA was isolated as in Figure 2C, resolved in a formaldehyde denaturing gel, transferred onto a nitrocellulose membrane and probed with [γ - 32 P]-ATP end-labeled oligonucleotide probes specific for *trnM* and *trnV.1* or a [α - 32 P]-dCTP labeled cDNA fragment (in the case of *ndhC*).

(B) Analysis of transcript levels of plastid tRNA genes which are not located adjacent to target I. Northern analysis was conducted as in (B) with [γ - 32 P]-ATP end-labeled oligonucleotide probes specific for *trnG.2* and *trnE*. rRNA was visualized by staining the membrane with methylene blue (M. B.) and served as loading control.

(C) Schematic representation of the MTERF6 binding site downstream of the *trnV.1* gene (target I). Exons and introns are depicted as blue boxes and black lines, respectively.

4. Results

This allows to speculate that the over accumulation of *trnG.2* and *trnE* transcripts might be due to a lack of binding of MTERF6 to a specific binding sites, or a compensatory consequence of upregulation of *trnV.1* transcripts and therefore a secondary effect of the reduction of MTERF6 level.

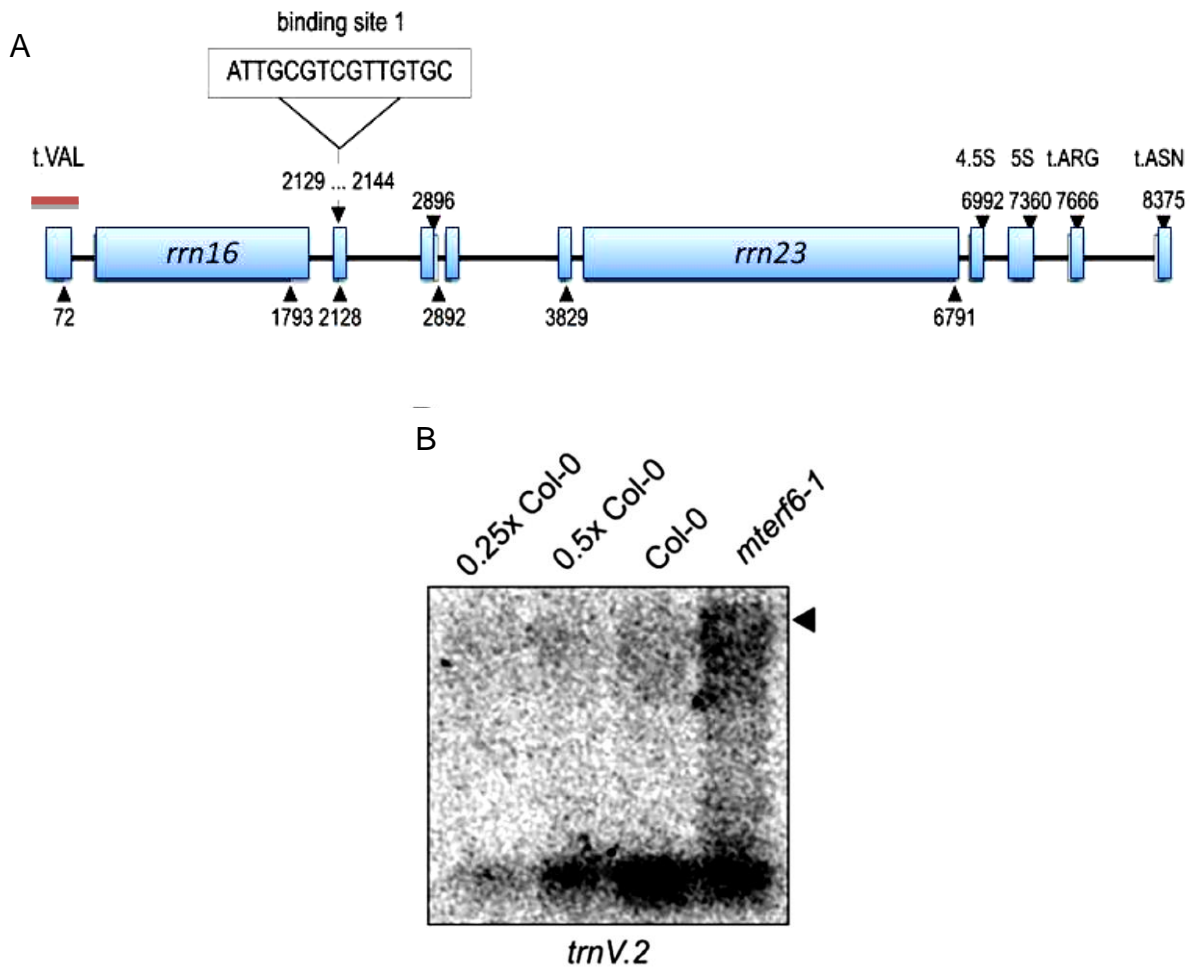


Figure 12. (A) Schematic representation of the chloroplast *rrn* operon and the MTERF6 target site located in the *trnI.2* gene (target II). Blue white boxes indicate genes encoding rRNA and tRNA, respectively; introns are depicted as solid lines. The positions of the probes used in northern-blot analysis are marked by red rectangles.

(B) Analysis of transcript levels of plastid tRNA genes which are located close to target I. Northern analysis was conducted with [γ - 32 P]-ATP end-labeled oligonucleotide probes specific for *trnV.2* (Romani *et al.* 2015)

In order to investigate at what extent MTERF6 influences the expression and maturation of the target II, in particular *trnV.2* and *trnI.2*, RNA gel blot hybridizations were executed using probes targeting the *trnI.2* exons, as well as its intron (Figure 12 B). The results

4. Results

indicated that in *mterf6-1* mature *trnV.2* transcript levels were decreased compared to Col-0, but an unprocessed precursor was accumulated.

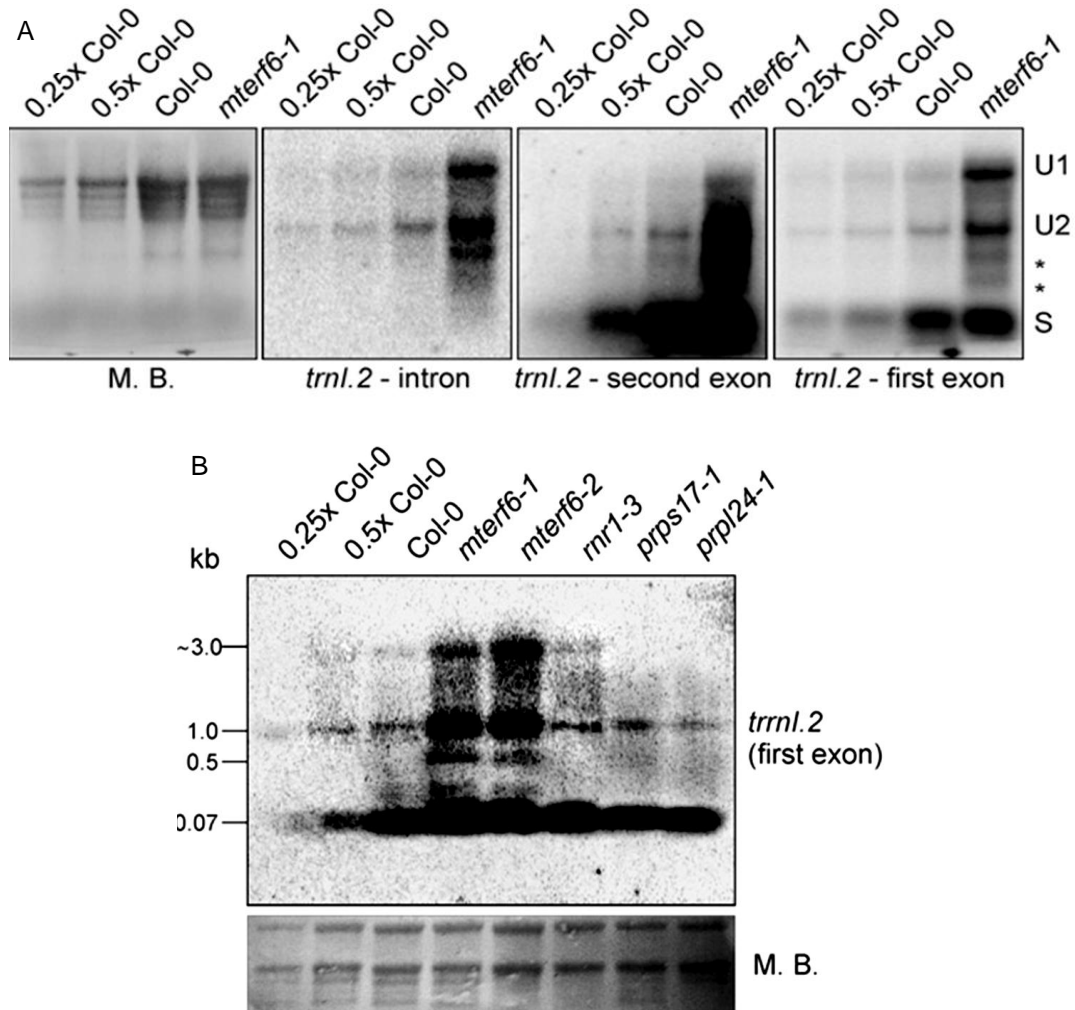


Figure 13. Expression and processing of chloroplast *trnL.2* in wild-type (Col-0) and *mterf6* plants. (A), Analysis of the levels and splicing patterns of the *trnL.2/trnL.3* (*trnL.2*) transcript in wild-type (Col-0) and *mterf6-1* soil-grown plants. Total RNAs were isolated as in Figure 2B, resolved on a denaturing gel, transferred onto a nylon membrane, and probed with [γ - 32 P] ATP end-labeled oligonucleotide probes specific for the intron and first and second exons. rRNA was visualized by staining the membrane with Methylene Blue (M. B.) as a loading control. (B), Analysis of the levels and processing patterns of the *trnL.2/trnL.3* (*trnL.2*) transcript in wild-type (Col-0), *mterf6-1*, and *mterf6-2* seedlings and, as controls, *rnr1-3*, *prps17-1*, and *prpl24-1* seedlings grown on MS medium. Total RNA was treated as in (A) and probed with [γ - 32 P] ATP end-labeled oligonucleotide probes specific for the first exon of *trnL.2*. rRNA was visualized by staining the membrane with Methylene Blue as a loading control. (Romani *et al.* 2015)

S, Spliced; U1, unprocessed 1; U2, unprocessed 2.

4. Results

From the RNA blot on *trnI*, it was visible that both unspliced and mature *trnI.2* RNAs accumulated at higher levels in *mterf6-1* compared to Col-0 (Figure 13). Moreover, additional unspliced forms of a weaker intensity were found in *mterf6-1* mutant plants (asterisk in Figure 14); however, it is likely that they also exist in Col-0 plants as indicated by the weak bands obtained by probing with *trnI.2* second exon antisense primers (Figure 14). In conclusion, MTERF6 seems not to play a role in *trnI.2* splicing.

Previous researchers discovered that the MTERF6 target II (*trnI.2*) binding sequence corresponds to a recently identified 19-bp short non-coding RNA in the *trnI.2* intron (Ruwe H1 et al. 2012, Schmitz-Linneweber et al. 2012). However, it is still not clear the function of these chloroplast ncRNAs.

Recent studies showed the possibility that the biogenesis of chloroplast short RNAs could be implicated in a mechanism of protection from RNA degradation. Thus, to investigate a possible role of MTERF6 in a RNA protection mechanism, total RNA from Col-0 and *mterf6-1* plants was resolved in a high percentage (17%) urea polyacrylamide gel, transferred on a nitrocellulose membrane and probed with a [γ -³²P]-ATP end-labeled oligonucleotide probe specific for the MTERF6 binding sequence. The results indicate that non-coding *trnI.2* RNA, not present in Col-0 is accumulated in *mterf6-1* plants (Figure 14). The presence of small RNA suggests that the *mterf6-1* phenotype is not caused by the absence of the non-coding *trnI.2* RNA.

4. Results

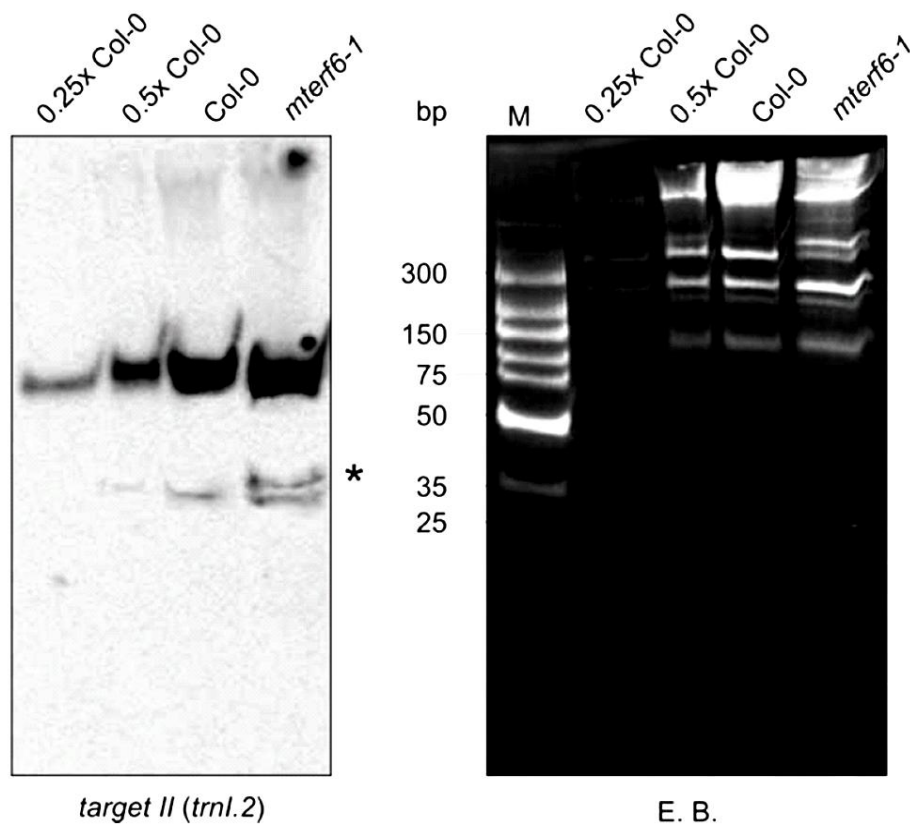


Figure 14. Analysis of accumulation of the MTERF6 target sequence corresponding to the non-coding RNA in the *trnI.2* intron in wild-type and *mterf6-1* plants.

Increasing amount (0.25, 0,5x and 1x) of total RNA extracted from Col-0 and *mterf6-1* (1x) were loaded on denaturing polyacrylamide urea gel 17%. After blot transfer, the resulting membranes were hybridized with with [γ - 32 P]-ATP end-labeled oligonucleotide probe specific or the MTERF6 binding sequence. RNAs were stained with ethidium bromide (E. B.) and served as a loading control. (Romani et al. 2015)

4.1.6 Aminoacylation analysis in *mterf6* mutants.

Previous studies on human describe that an A-to-G transition in the middle of the MTERF1-protected DNA region drastically reduces the affinity of MTERF1 for its target sequence (Kleine T, Leister D 2015) resulting in the MELAS syndrome (mitochondrial myopathy, encephalopathy lactic acidosis, and stroke-like episodes). Another mutation in the tRNA^{Leu}(UUR) gene causes aminoacylation deficiency of tRNA^{Leu}(UUR) and also reduced association of mRNA with ribosomes (Chomyn A, Enriquez JA 2000). Based on these previous results, it was opportune to investigate the aminoacylation status of *trnI.2* in *mterf6* mutants. The proportion of tRNA that is charged with its amino acid in vivo was

4. Results

determined for plastid *trnL.2* [coding for tRNA^{Ile}(GAU)] and as controls for *trnL.1* [coding for tRNA^{Ile}(CAU)] and *trnT.1* [coding for tRNA^{Thr}(GGU)] using acid conditions for RNA extraction and gel electrophoresis. Results indicate a marked reduction in the efficiency of charging of *trnL.2* with its amino acid Ile in *mterf6-1* plants (Figure 15); this defect was rescued in complemented *mterf6-1* plants. Charging of *trnL.2* was not abolished in *rnr1-3* seedlings but was reduced in *mterf6-2* seedlings (Figure. 15). In contrast, *trnL.1* and *trnT.1* were charged at normal levels in both *mterf6* mutants and the *rnr1-3* mutant. These data suggest that MTERF6 is required for the maturation of *trnL.2*.

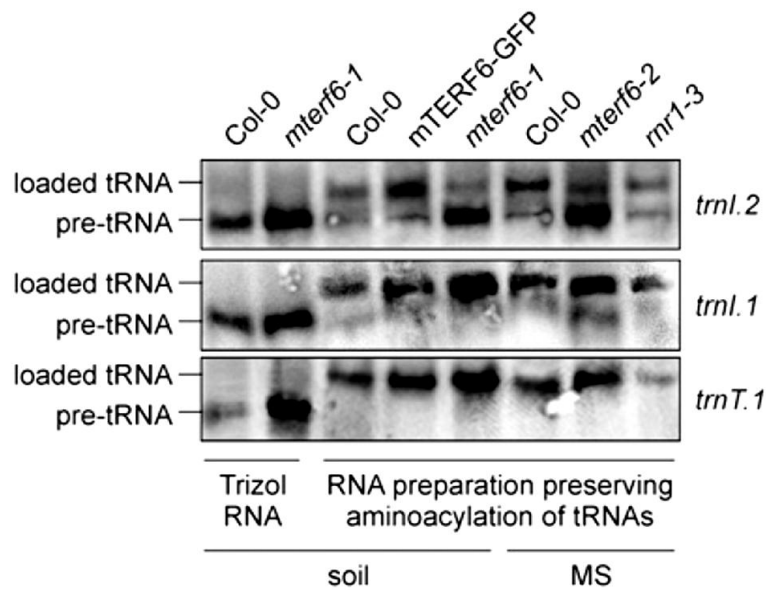


Figure 15. Analysis of *trnL.2* and *trnL.1* and *trnT.1* aminoacylation in soil-grown wild-type (Col-0), *mterf6-1* and complemented *mterf6-1* (35S:MTERF6.1 *mterf6-1*) plants and analysis of plants MS-grown Col-0, *mterf6-2* and – as a control – *rnr1-3* seedlings. Total RNA was isolated with the Trizol method and isolated under conditions that preserve aminoacylation of tRNAs. Samples of 5 µg of RNA were separated by electrophoresis, blotted and probed with [γ -³²P] ATP end-labeled oligonucleotide probes specific for *trnL.2* and *trnL.1*. In the gel system used here (see Methods), the aminoacylated tRNA, migrates slower than its corresponding deacylated pre-tRNA. To see the difference in the electrophoretic mobility, aliquots of Trizol-prepared WT and MTERF6-1 RNA were included on the gel. (Romani *et al.* 2015).

4.1.7 Norflurazon test on *mterf6-1* plants

The first mutant screen designed to identify components of plastid signaling was performed in *Arabidopsis thaliana* (Susek, R. E.; Ausubel, F. M. & Chory, J., 1993). That screen was based on the assumption that the light-dependent induction of nuclear photosynthesis-related genes, such as *LHCB1.2*, is prevented in seedlings grown in the

4. Results

presence of norflurazon (NF), a carotenoid biosynthesis inhibitor [Oelmüller, R., and Mohr, H. (1986)]. Five different *gun* (genomes uncoupled) mutants were isolated, which displayed *LHCB1.2* expression despite their photodamaged plastids as a result of NF treatment, (Susek, R. E.; Ausubel, F. M. & Chory, J., 1993) (Mochizuki, N., et al. 2001). Except for GUN1, a nucleic-acid binding chloroplast protein that is defective in OGE, all GUN proteins were found to be involved in tetrapyrrole biosynthesis (Mochizuki, N., et al. 2001)(Larkin, J.C., et al. 2003).

To elucidate whether MTERF6 and GUN1 could genetically interact, a *gun1* mutation was introduced by crossing into the *mterf6-1* mutant and a double mutant *mterf6-1gun1* was generated. This double mutant presented a more severe phenotype than *mterf6-1* mutant plants (Figure 16).



Figure 16. Introduction of *gun1* mutation into the *mterf6-1* mutant (*mterf6-1/gun1*) results in an additive phenotype. Phenotypes of one-week (MS) and 25-day old (soil) wild-type (Col-0), *mterf6-1*, *gun1* and *mterf6-1/gun1* plants are shown.

4.2 Molecular and physiological screening to identify factors involved in chloroplast-to-nucleus retrograde signaling.

This chapter will focus on the characterization of *relaxed LHCB suppression (rls)* mutants, previously screened by a genetic forward luminescence screen (dissertation of Lukas Mittermayr, 2014).

The mutants used here, were generated by EMS mutagenesis. Analysis of the *LHCB* expression, monitored by luciferase, and the observation of the phenotype of the mutagenized plants were used as screening method.

4.2.2 Screening rls mutants.

Before this thesis started, 13377 plants were screened, from which 654 were selected by detection of the luminescence performed with the Fusion FX7 chemiluminescence and fluorescence imager (Peqlab). Plants which rescued the phenotype, and present a luminescence signal were propagated to the next generation. A third screen, as previously described, was performed, reducing the candidate number from 654 to 24 potential candidates. Both parental lines, *LHCB1.2pro: LUC prors1-2* and *LHCB3pro:LUC prors1-2*, presented a similar phenotype, including a smaller size and a pale leaf color. The phenotype of the selected mutants varied from pale green similar to the parental lines to a darker green resembling the wildtype phenotype (Figures 17). The leaf size of the rls mutants selected reached nearly the size of the wild type and displayed luminescence activity (Figure 18).

4. Results

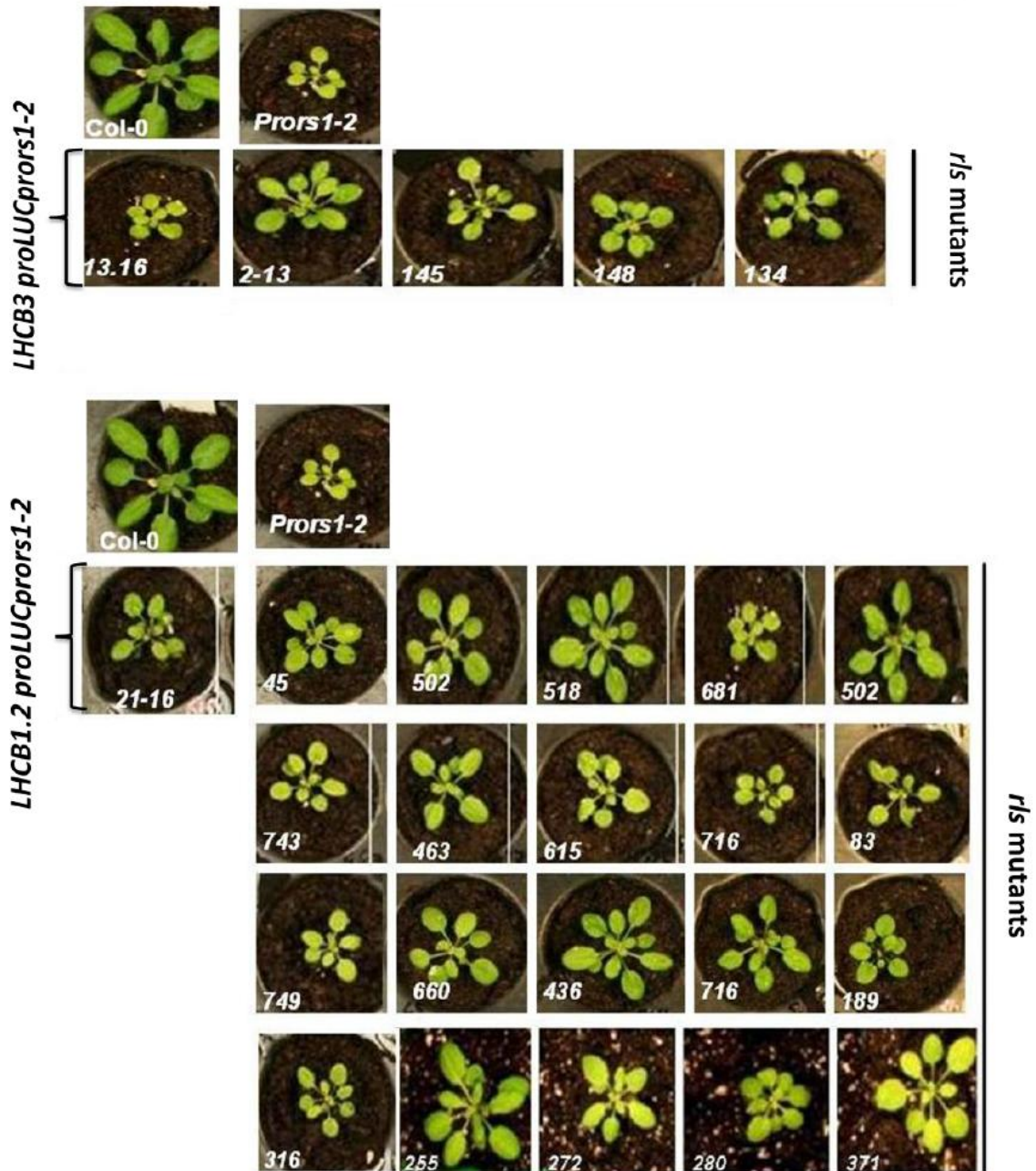


Figure 17. Phenotypic analysis of *rls* mutants containing the *LHCB1.2* or the *LHCB3* promoter-luciferase construct. The picture was taken on day 28 and includes the wild type (Col-0), the parental line *LHCB1.2pro:LUC prors1-2* or 21-16 and *LHCB3pro:LUC prors1-2* or 13-16 and the *rls* mutants, that present the *LHCB3* and *LHCB1.2* promoter-luciferase construct

4. Results

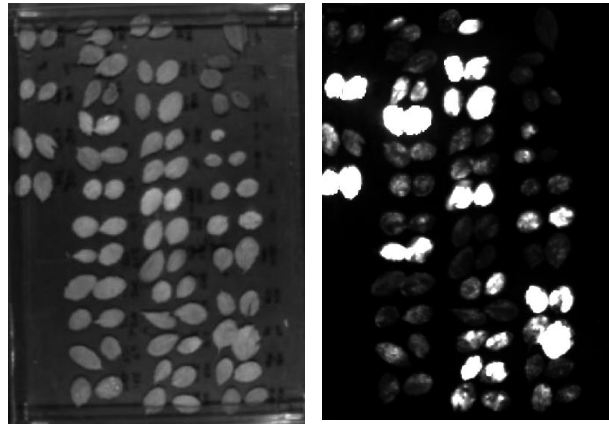


Figure 18. Luminescence screen of the *rls* mutants. One leaf per plant (25 days after germination) was brushed with luciferin and incubated for 10 min in the dark before detection of the luminescence signals. Scanning of leaves with: Fusion FX7 chemiluminescence and fluorescence imager (Peqlab)

4.2.3 Internal transcript level of nuclear-encoded photosynthetic genes in the *rls* mutants.

The *rls* mutants obtained were utilized to investigate whether the rescue effects are not due to up-regulation of *PRORS1* gene expression. Previous studies showed that in the knock-down mutant (*prors1-2*) the RNA expression of the *PRORS1* gene, are reduced to 25% compared to Col-0 (Pesaresi P, *et al.* 2001) and present a down regulation of nuclear-encoded photosynthetic genes responsible for the light reactions of photosynthesis.

The expression of the *PRORS1* transcript in the *rls* mutants and in their parental lines (*LHCB3pro:LUC prors1-2* and *LHCB1.2pro:LUC prors1-2*) was determined by real-time PCR (dissertation of Lukas Mittermayr 2014).

The originating *rls* mutants showed a similar mRNA levels of the *PRORS1* transcript displayed in the parental lines (*LHCB3pro:LUC prors1-2* and *LHCB1.2pro:LUC prors1-2*), indicating that the rescue phenotypes observed before are not caused by a difference in the accumulation of *PRORS1* transcript

The next step was to analyze the levels of *PSBO* (*AT3G50820*), *LHCB1.2* (*AT1G29910*) and *LHCB3* transcript (*AT5G54270*) via Northern blot analysis. *LHCB3pro:LUC prors1-2* showed a reduction of *LHCB3* transcript level compared to Col-0 and *prors1-2* with concomitant increment of the other three transcripts compared to *prors1-2*. In addition, *rls148* and *rls145* and *rls2-13* displayed an increase of the *LHCB* transcripts compared to

4. Results

*LHCB3*pro:*LUC prors1-2*. All four transcript amounts were found to be elevated in *rls255*, *rls83*, *rls255* and *rls681*. (Figure 19-20)

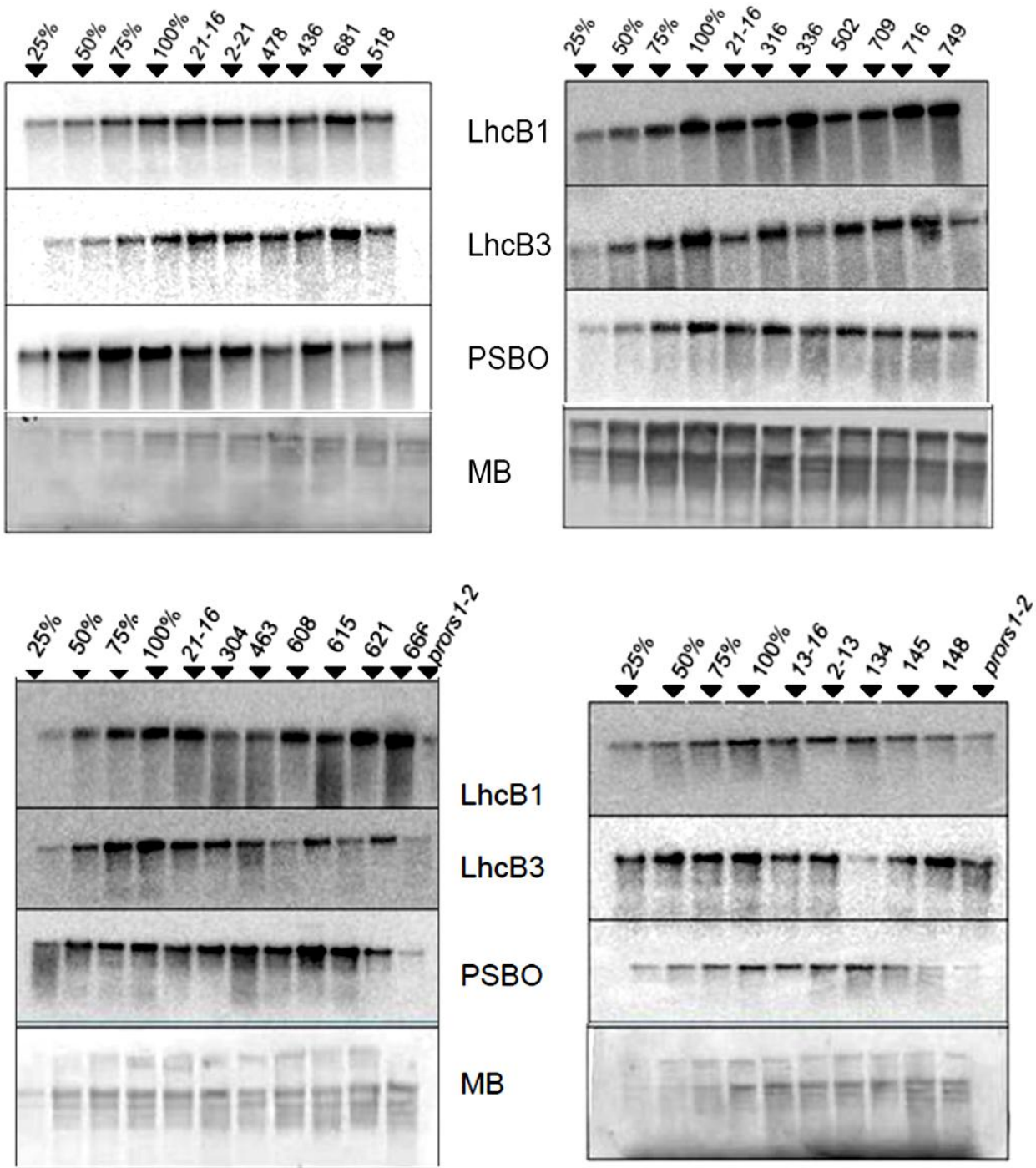


Figure 19. *LHCB3*, *LHCB1* and *PSBO* transcript levels from Col-0, *prors1-2*, parental lines and *rls* mutants. Increasing amount (25%, 50%, 75% and 100%) of total RNA extracted from Col-0 and *rls* mutants. As loading control, the methyl blue stained nylon membrane (M.B.) was used.

4. Results

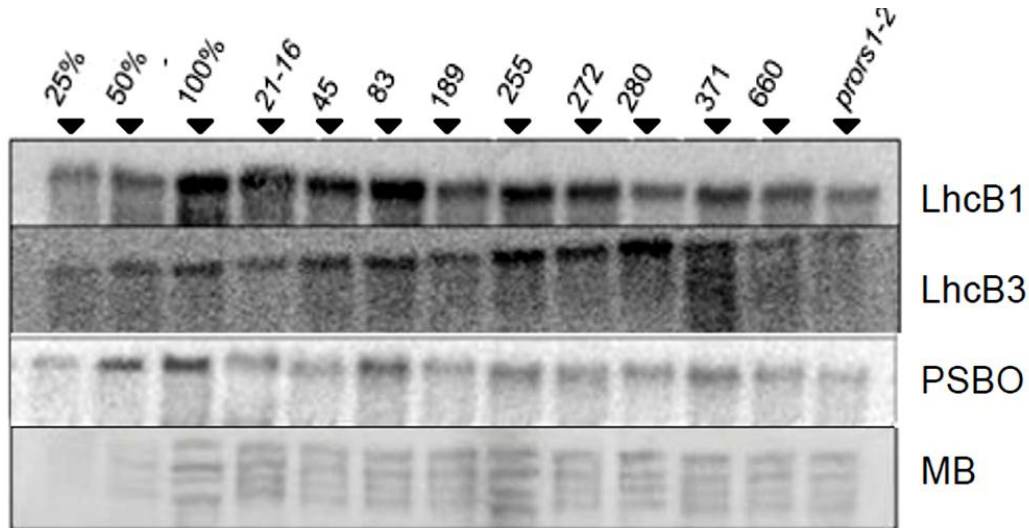


Figure 20. *LHCB3*, *LHCB1* and *PSBO* transcript levels from Col-0, *prors1-2*, parental lines and *rls* mutants. Increasing amount (25%, 50%, and 100%) of total RNA extracted from Col-0 and *rls* mutants. As loading control, the methyl blue stained nylon membrane (M.B.) was used.

4.2.4 Effects on protein synthesis in *rls* mutants that present recovery of the phenotype.

To investigate whether rescue of phenotype lead to direct restoration of translational process (e.g. protein stability, processing.) in the chloroplast, the synthesis of plastid-encoded chloroplast proteins was studied. A pulse labeling was carried out for Col-0, the parental lines *LHCB3**pro:LUC prors1-2(13-16)*, *LHCB1.2**pro:LUC prors1-2(21-16)* and *rls* mutants leaves (*rls83*, *rls255*, *rls148*, *rls145*) and *gun1* and *gun5* in presence of cycloheximide, which inhibits the translation of nucleus-encoded proteins. Leaf discs were collected after 10 and 30 minutes of incubation with (³⁵S) methionine in the presence of light. After pulse labeling for 20 min, the synthesis of the D1 protein was strongly recovered in *rls 145* and *255 rls* and slightly recovered in *rls148* and *rls83*, when compared with the parental line (Figure 21). The *gun1* and *gun5* were used as a control to detect a possible involvement of the *rls* mutant with the retrograde signaling.

4. Results

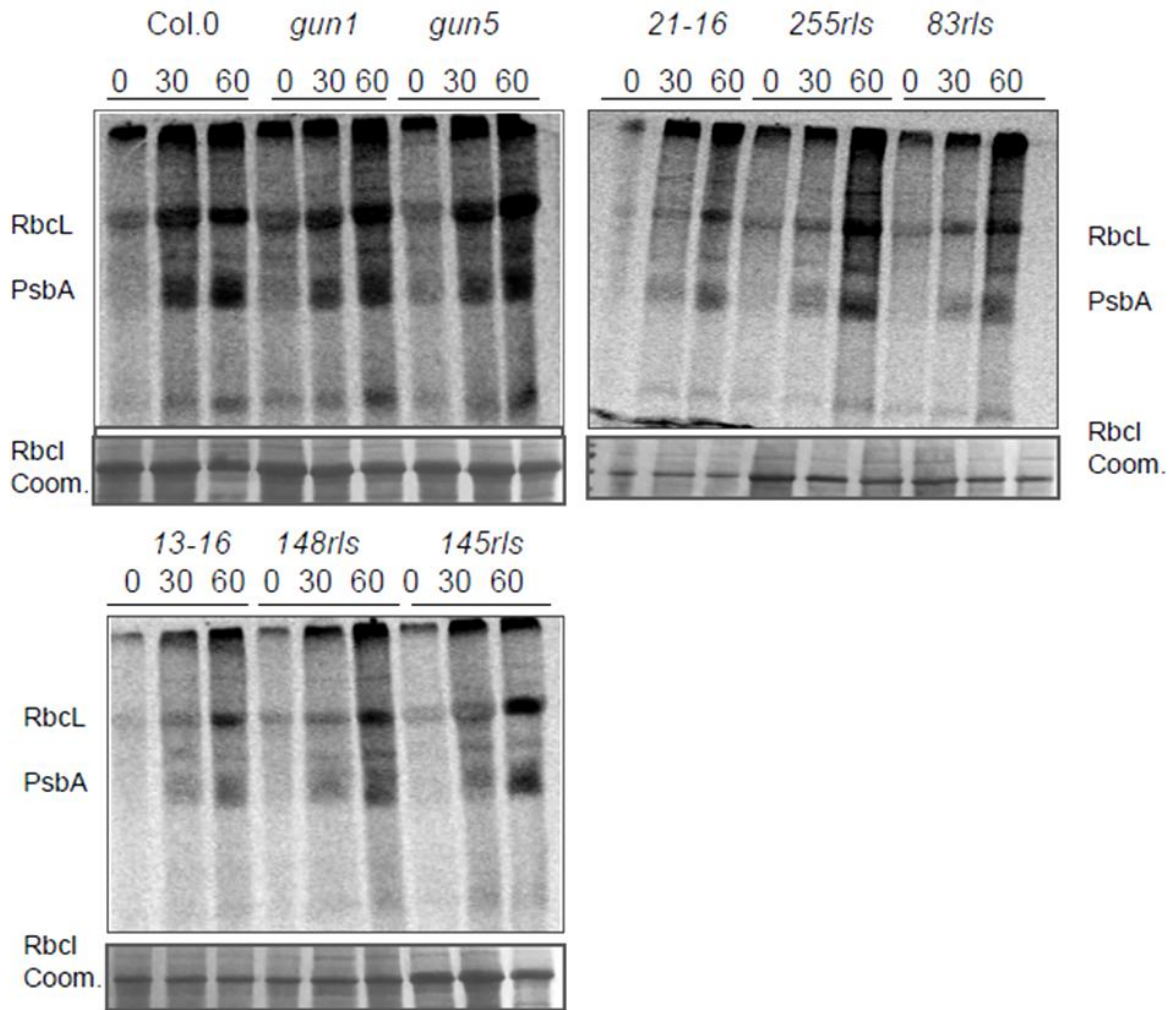


Figure 21. In vivo pulse labeling of total proteins with $[^{35}\text{S}]$ Met in the presence of cycloheximide. Proteins were resolved by SDS-PAGE after pulse labeling for 0, 30, 60 min and visualized by autoradiography. Coom, Coomassie Blue served as loading reference.

The *rls* 255, 83, 148, 145 were chosen because they displayed a better rescue in the previous northern blot.

4.2.5 Rls mutants could be involved in plastid gene expression?

Analyses on NF (noraflurazon) and on Linc (lincomycine) were performed in order to investigate a possible involvement of Rls mutants in plastid gene expression.

Col-0 seedlings and parental lines and *rls* mutants were grown under $100 \mu\text{mol photons m}^{-2} \text{ s}^{-1}$ white light on MS supplemented with only $50 \mu\text{M}$ NF and Linc. After 10 days the phenotypes were analyzed and cotyledons of all seedlings. Subsequently, luminescence test was performed to measure the Luciferase activity. The analyses were done on the pool of *rls* mutants that presented a better rescue of the phenotype. The *rls*681, *rls*83,

4. Results

rls255, *rls463*, *rls436*) on NF and Linc after luciferine treatment didn't display luciferase activity (data not shown). This might be provoked by the presence of norflurazon (NF) and Lincomycine, which are known to interfere with the expression of the light-dependent induction of nuclear photosynthesis-related genes, *LHCB1.2* as *LHCB3*. (as the promoters that induce the activity of the Luciferase).

Nevertheless, it was possible to detect Luciferase activity in NF and Linc plates with *rls 145* and *rls 148* seedlings indicating that *LHCB1.2* as *LHCB3* were still induced during the NF and Linc treatment. These data suggested the possibility that *rls 148* and *rls 145* could be a novel *gun* mutant. However, further experimental approaches are needed to dissect the effect of *rls* mutations that induce the *prors1-2* phenotype rescue and the localization in the genome through sequencing. This might reveal potential novel candidates involved in the coordination of the expression of organellar and nuclear genomes. (Figure 22)

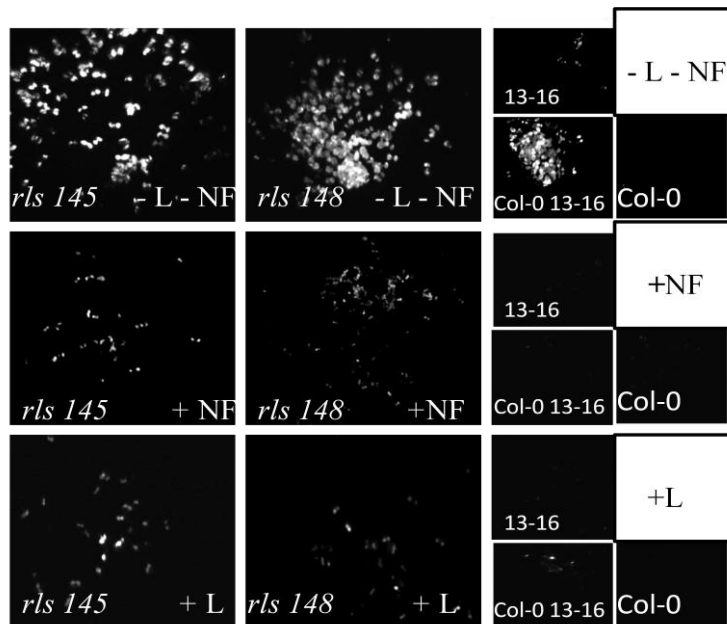


Figure 22. Luminescence screen of the *rls mutants* seedlings. Col-0 *LHCB3pro:LUC/Col(13-16)* (control with constitutiveactivation of LUC and expression of LHCB), *LHCB3pro:LUC/prors1-2(13-16)* and *rls 145*, *rls 148* seedlings were grown for 10 days in continuous low light conditions (5 $\mu\text{mol photons m}^{-2} \text{s}^{-1}$ white light) on MS medium supplemented with 50 nM NF/Lync.

Luciferin was applied by spry and incubated for 10 min in the dark before detection of the luminescence signals. Scanning of leaves with: Fusion FX7 chemiluminescence and fluorescence imager (Peqlab)

NF: norflurazone

L: Lincomycine

4. Results

4.2.6 Aminoacylation status in *prors1-2* plants.

The *PRORS1* gene codify for the *PROLYL-tRNA-SYNTHETASE1* (*PRORS1*), itself localized in the chloroplast and in the mitochondria.

Aminoacyl-tRNA synthetases are essential enzymes that help to ensure the fidelity of protein translation by accurately aminoacylating (or “charging”) specific tRNA substrates with cognate amino acids [Splan KE et al. (2008)]

The aminoacylation assay was used to observe levels of aminoacylation of the mutant *prors1* and of the *rls* mutant. Results from this experiment could clarify if the rescue in the *rls* mutants is induced by a rescue of the aminoacylation activity of *PRORS1* or by some other process not yet clear.

The aminoacylation status of Col-0, *prors1-2* and of certain *rls* mutants were extracted in acid conditions and loaded in a gel electrophoresis. Results indicated a marked reduction in the efficiency of charging of prolyl-tRNA with its amino acid prolyl in *prors1-2* and *rls681*, *rls45* plants (Figure.26); this defect could be rescued in complemented *rls148*, *rls255*, *rls2-13*.

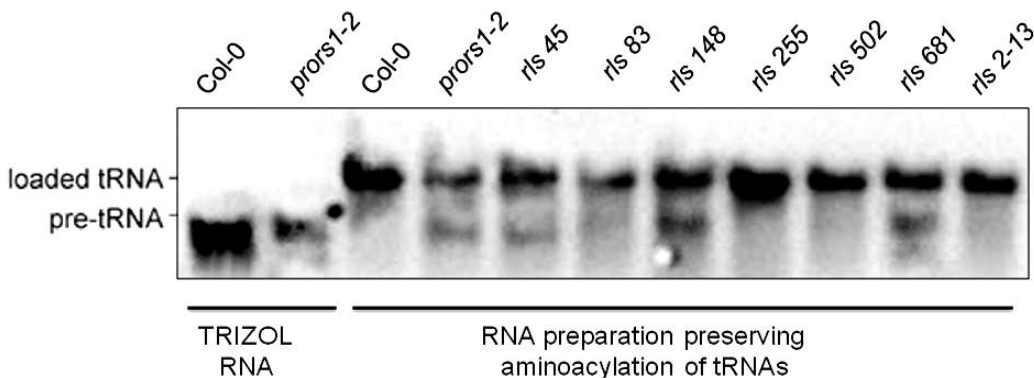


Figure 23. Aminoacylation assay of tRNA prolyl synthase on Col.0, *prors1-2* and *rls* mutants selected.

4.3 Ethanol-induced, transient silencing of *PRORS1*.

4.3.1 Preliminary hints.

The data collected in this part served as the basis for experiment in which whole-genome transcriptomes expressed during down-regulation of *PRORS1* were analyzed with the aim to identify OGE-target genes. The results presented in this chapter have been published in 2014 “Identification of target genes and transcription factors implicated in translationdependent retrograde signaling in Arabidopsis” (Dario Leister, Isidora Romani *et al.* Mol.plant. DOI: 10.1093/mp/ssu066).

Through this EtOH inducible experiment, we tried to identify the earliest effects of altered OGE on nuclear transcript accumulation. *PRORS1* gene was silenced by ethanol-inducible expression system.

4.3.2 Investigation of EtOH inducible *PRORS1* RNAi lines.

The aim of this part was to analyze previously generated ethanol-inducible *PRORS1* RNAi lines. As shown before this thesis started, *PRORS1* transcript levels were diminished in a range of 55 and 80% of wild-type after 32 h, and declined to a minimum rate between 15 and 40% of wild-type levels after 48 h. The knockdown was stable up to 51-56 h of treatment. Exposure of wildtype and *prors1-2* plants to ethanol vapor didn't result in a phenotypic change. However, *iPRORS1* RNAi lines appeared slightly paler than wild-type plants after 48 and 56 h of ethanol treatment. (Figure 24)

4. Results

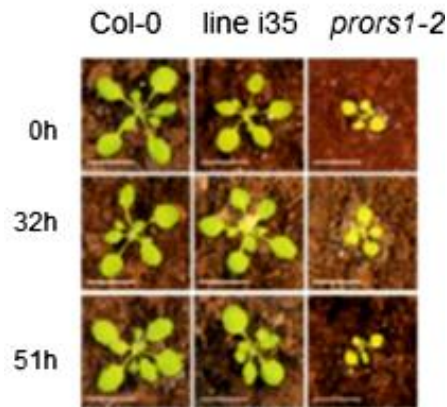


Figure 24. Col-0, *iPRORS1* RNAi line i35 and *prors1-2* mutant plants treated for the indicated lengths of time with ethanol vapour. (Leister, Romani et al. 2014)

4.3.3 Effects on protein synthesis in plastids.

Pesaresi et al, 2006 demonstrated that plastid translation is impaired in *prors1-2* chloroplast. In the light of that, the effect on the translation rate was measured in *iPRORS1* RNAi plants treated with ethanol vapor for 0, 32 and 51 h (Figure 24). This experiment aimed also to clarify whether ethanol explicates an effect on the plastid translation rate *per se*. The pattern of synthesis of plastid-encoded proteins was studied by pulse-chase labeling. Leaf discs were collected after 10 and 30 minutes of incubation with [³⁵S] methionine in the presence of light.

The samples analyzed were the ethanol-treated (for 0, 32 and 51 h) *iPRORS1* RNAi lines and, as controls, wildtype containing either an ethanol-inducible *GUS* RNAi construct (*GUS*) or not (*Col-0*), and *prors1-2*. From the *in vivo* labeling appeared that the ethanol treatment has no direct influence on the plastid translation rate, as observed in the controls (Figure 25). The accumulation of labeled and non-labeled RbcL was reduced in *prors1-2* leaves compared to *Col-0* whereas in the *iPRORS1* RNAi line the accumulation of labeled and non-labeled RbcL decreased upon ethanol treatment, displaying a significant reduction after 32 h of ethanol treatment, and decrement after 51 h (Figure 25).

4. Results

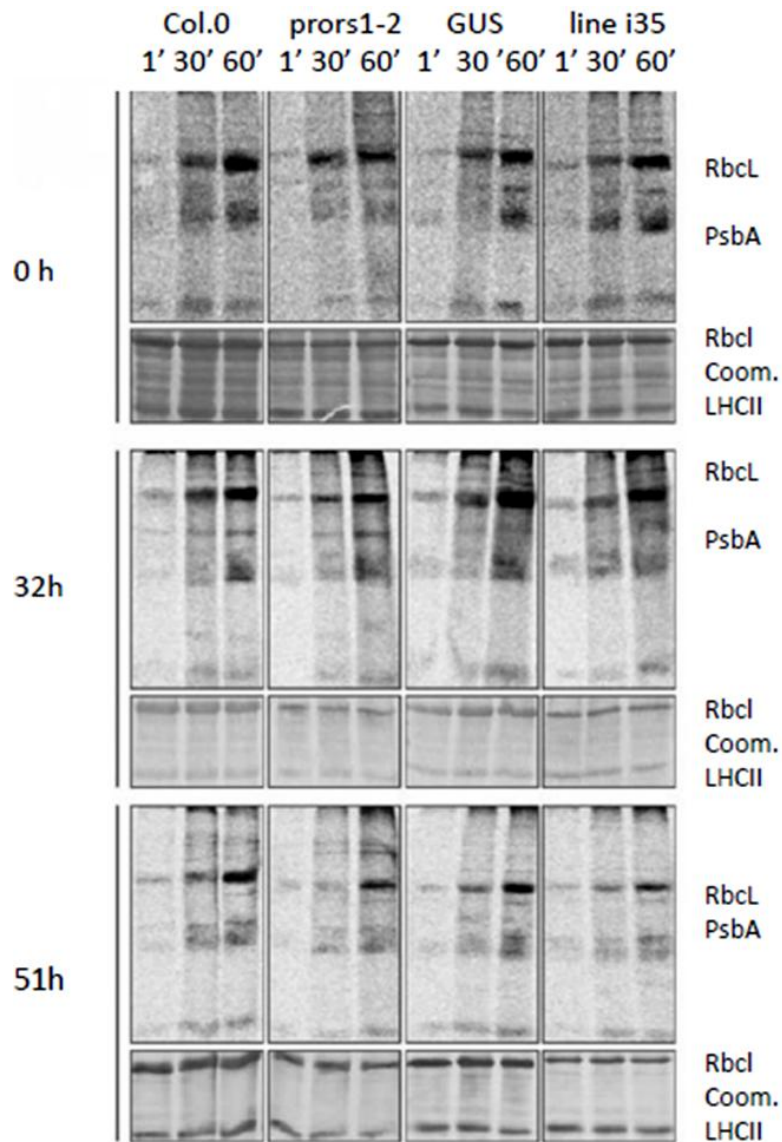


Figure 25. wild-type (Col-0), Col-0 with the inducible GUS RNAi construct (GUS), *prors1-2* plants and the inducible *iPRORS1* RNAi line i35, were grown under long-day (16 h light/8 h dark) conditions and exposed for the indicated lengths of time to ethanol vapour.

(A) Analysis of plastid protein synthesis. Thylakoid membrane and stromal proteins were isolated from leaves. Pulse-labelling with [³⁵S] Met for 1, 30 and 60 min, and subsequent fractionation by SDS-PAGE, is shown. The portion of the Coomassie (Coom.) served as a loading reference. (Leister, Romani et al. 2014)

4. Results

4.3.4 Photosynthetic parameters of iPRORS1 RNAi plants.

The previous data showed that iPRORS1 RNAi plants seemed paler after ethanol induction; therefore it was crucial to analyze the amounts of chlorophyll present in ethanol-treated wild-type, *prors1-2* and iPRORS1 RNAi mutants leaves. In order to accomplish this experiment, an acetone-extracted chlorophyll was performed and measured photometrically with subsequent calculation of chlorophyll concentrations as described previously (Lichtenthaler H.K. 1987). The chlorophyll content, the Chl *a/b* ratio, were reduced in the *prors1-2* mutant, as reported before (Pesaresi P, *et al.* 2001) and this reduction was not affected by ethanol treatment. In addition, ethanol had no impact on chlorophyll content in wild-type leaves (Figure 26B). The iPRORS1 RNAi plants presented a slightly, but significant ($p < 0.05$), lower chlorophyll content after 32 and 51 h of induction, although the Chl *a/b* ratio remained unchanged (Figure 26A).

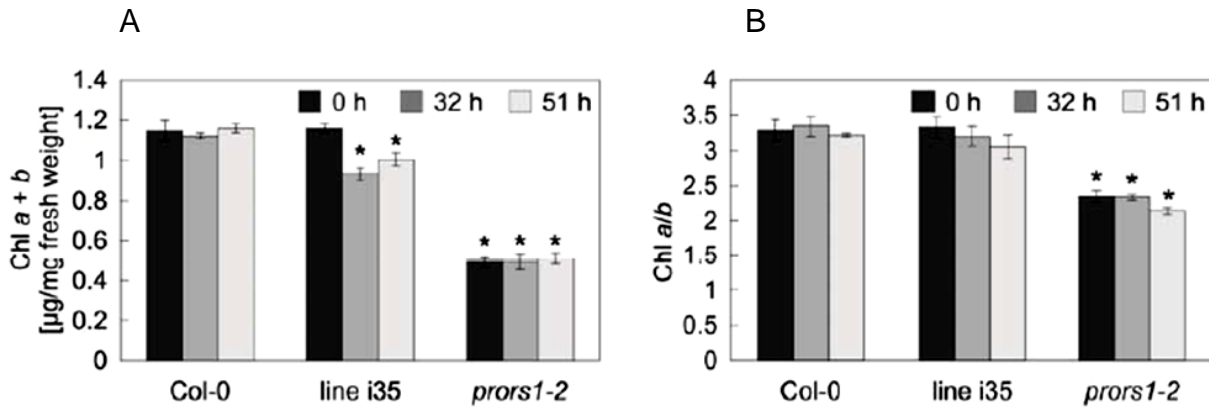


Figure 26. (A) Acetone-extracted chlorophyll was measured photometrically, and chlorophyll concentrations were calculated as described (Lichtenthaler, 1987) and are reported in $\mu\text{g}/\text{mg}$ fresh weight.

(B) Photosynthetic parameters were derived from measurements on at least three leaves from different plants. Actinic light intensity was $95 \mu\text{mol photons m}^{-2} \text{sec}^{-1}$. The data are shown as mean values \pm SD. Statistically significant differences (t-test; $p < 0.05$) between wild-type (time point 0 h) and mutant samples are indicated by an asterisk. F_v/F_m , maximum quantum yield of PSII; Φ_{II} , effective quantum yield of PSII; Chl, chlorophyll.

Photosynthetic parameters were analyzed through dual pam and were derived from measurements on at least three leaves with a different plant origin. Actinic light intensity was $95 \mu\text{mol photons m}^{-2} \text{sec}^{-1}$. The photosynthetic parameters, such as maximum (F_v/F_m) and effective (Φ_{II}) quantum yields of PSII are reduced in the *prors1-2* mutant

4. Results

(Pesaresi *et al.*, 2006; Figure 27A) but were virtually unchanged in induced *iPRORS1* RNAi mutant plants compared to Col-0 (Figure 27B).

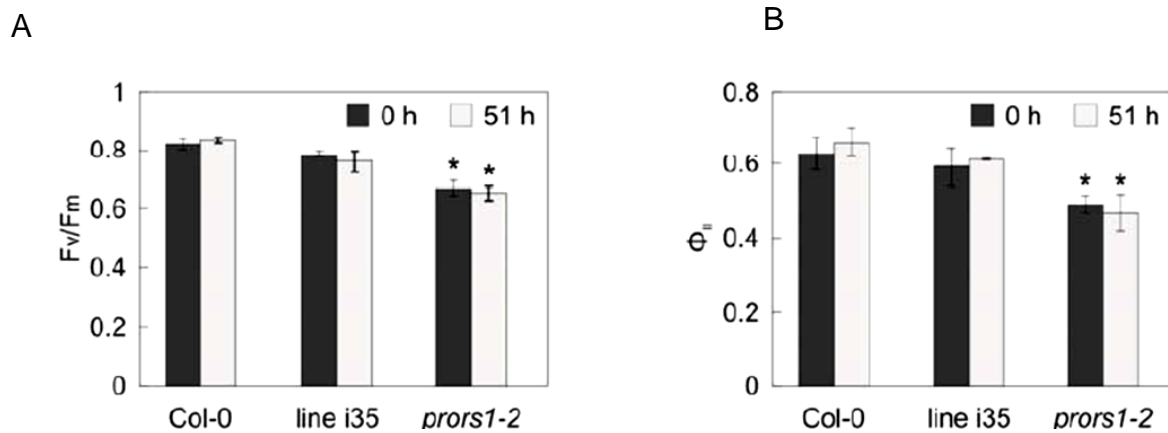


Figure 27. Photosynthetic parameters were derived from measurements on at least three leaves from different plants. Actinic light intensity was $95 \mu\text{mol photons m}^{-2} \text{sec}^{-1}$. The data are shown as mean values \pm SD. Statistically significant differences (t-test; $p < 0.05$) between wild-type (time point 0 h) and mutant samples are indicated by an asterisk. Fv/Fm, maximum quantum yield of PSII; Φ_{II} , effective quantum yield of PSII; Chl, chlorophyll (Leister, Romani et al 2014)

4.3.5 Analysis of gene expression changes.

Was shown that after 32 h of *PRORS1* repression, the translational capacity of chloroplasts was reduced, and this effect subsequently intensified, while basic photosynthetic parameters were still unchanged at 51 h. These physiological data served as the basis for a time-series experiment in which whole-genome transcriptomes expressed during down-regulation of *PRORS1* were analyzed. This approach led to the identification of OGE-target genes and co-regulated gene sets. Analysis of changes in whole-genome transcriptomes during exposure to ethanol were done by Leister in 2015 (Leister, Romani et al. 2014) and reveal that induced *PRORS1* silencing affects the expression of 1020 genes in all. Some of these encode photosynthesis-related proteins, including several down-regulated light-harvesting chlorophyll *a/b* binding (LHC) proteins.

4. Results

Table 8. Differential expression of selected early target genes in the *PRORS1* RNAi lines treated for 48, 51 or 56 hours with ethanol vapour.

AGI_Code	Gene title	Gene symbol	48h	51h	56h
<i>AT2G34430</i>	PSII light-harvesting chlorophyll a/b binding protein subunit B1	<i>LHCB1.4</i>	0.28	0.64	0.90
<i>AT1G19150</i>	PSI light-harvesting chlorophyll a/b binding protein 2	<i>LHCA6</i>	0.65	0.49	0.23
<i>AT4G14690</i>	Early light inducible protein 2	<i>ELIP2</i>	0.60	0.43	0.33
<i>AT5G38430</i>	Rubisco small chain 1B	<i>RBCS1B</i>	1.11	0.26	0.13
<i>AT5G38420</i>	Rubisco small chain 2B	<i>RBCS2B</i>	0.77	0.46	0.18
<i>AT1G03630</i>	Protochlorophyllide reductase C	<i>POR C</i>	0.48	0.52	0.55
<i>AT1G77490</i>	L-ascorbate peroxidase	<i>TAPX</i>	0.82	0.44	0.40
<i>AT3G05625</i>	TPR protein		0.65	0.26	0.36
<i>AT3G48250</i>	PPR	<i>BIR6</i>	0.98	1.06	2,38
<i>AT5G27110</i>	PPR		0.91	1.06	2.07
<i>AT3G15590</i>	PPR		1.61	1.77	3.65

5. Discussion and conclusions

In this work, the molecular aspects of retrograde signaling were elucidated employing three approaches. The first approach clarified the function of MTERF6. In the second approach the *prors1-2* mutant was chosen to study the translation-dependent retrograde signaling pathways, due to its impairment of organellar translation, which has been shown to be involved in retrograde signaling. The EtOH inducible approach was used to identify the earliest effects of altered OGE. Indeed, the analyses of OGE-dependent retrograde signaling are normally based on analyses of mutants with altered OGE. This kind of analyses are difficult to lead for compensatory responses that cover the primary signaling defect and by secondary effects that influence other retrograde signaling pathway.

5.1 MTERF6 is essential for appropriate photosynthetic functions.

The knock-down line mutant *mterf6-1* phenotype displayed a reduction of the efficiency of PSII suggesting impairment in photosynthesis (Figure 4 and Table 7).

The *mterf6-1* plants presented chlorotic and smaller leaves in comparison to wild-type plants. Moreover, the mutant plants showed a slower development, although they were able to complete their life cycle producing viable seeds. Contrariwise, in mutants *mterf6-2*, carrying knockout of *MTERF6*, the phenotype appeared more severe. In fact, the plant was not able to grow on soil but exclusively on media supplemented with sugar showing albino cotyledons (Figure 4). Albino plants rarely grow further than the 4th leaf stage. Protein analysis (Figure 5) demonstrated a specific de-regulation of different photosystems proteins that are encoded by the chloroplast genome, such as PETB, ATPB, D1, CP43, CP47, PSAA, and PSAB. Taken together these data, including the reduction in levels of proteins belonging to photosynthetic complexes, the poor photosynthesis performance revealed through the fluorimetric analysis, the chlorotic phenotype in the leaky line and the albino leaves in the knock-out mutant, strongly indicates a linkage between mutation of the gene *MTERF6* and alteration in plastid development and photosynthesis activity.

The immuno blot data and northern blot (Figure 5) suggest that levels of nucleus-encoded photosynthetic proteins are not diminished in the *mterf6-1* mutant. Moreover, the reduced amount of chloroplast-encoded photosynthetic proteins observed in the *mterf6-1* mutant seems not to be associated with lower levels of transcripts of the corresponding

5. Discussion and conclusions

chloroplast genes. In vivo labeling, the synthesis of the D1 protein and the α - and β -subunits of the ATP synthase (CF1 α/β) were found to be reduced in *mterf6-1* (Figure 6B). In the analysis of the association of *psbA* and *rbcL* mRNA with polysome, rRNAs in Col-0 and *mterf6-1* polysome gradients showed similar, but not identical distributions (Figure 6A). These findings suggest that the majority of these mRNAs in *mterf6-1* chloroplasts are not engaged in translation, which accounts for the reduction in synthesis of chloroplast proteins.

From the analysis of the Plastid Ribosomes through rRNA quantification, performed by Romani et al. (2015) and immunoblot analysis of the representative plastid ribosome subunit (Figure 7) seems that the ribosome assembly is not affected in *mterf6* mutants, but the accumulation of ribosomal subunits is reduced.

5.2 The molecular function of MTERF6

In the work previously published, it was defined a specific interaction between MTERF6 and a RNA sequence in the chloroplast a downstream the 16SrRNA region and isoleucine tRNA gene (*trnI.2*). This function shares analogies with other human MTERFs (Kruse et al., 1989). In contrast to the chloroplast genome, the human mitochondrial genome is intron-less and its 37 genes are tightly packed. Therefore, the mature RNAs contain no or only short 5' or 3' flanking sequences. The two mitochondrial DNA strands have different buoyant densities in a cesium chloride gradient, and are referred to as the heavy (H) and the light (L) strand (Kip E. Guja et al. 2012).

The two rRNAs, 14 tRNAs and 12 mRNAs are all encoded by the H strand. Transcription in human mitochondria starts at three different initiation points: one L-strand (LSP) and two H-strand (HSP1 and HSP2) promoters. Transcription initiated at the HSP1 promoter is terminated at a specific site in the gene for *tRNA^{Leu}* located 3' of the *rrn16* gene. The Human MTERF1 binds this specific region in 16SrRNA site (David A. Clayton et al. 2000). Surprisingly, in the chloroplast genome MTERF6 binds to a sequence located in the *trnI.2* intron (target II), which also lies 3' of the *rrn16* gene (Figure 8).

5. Discussion and conclusions

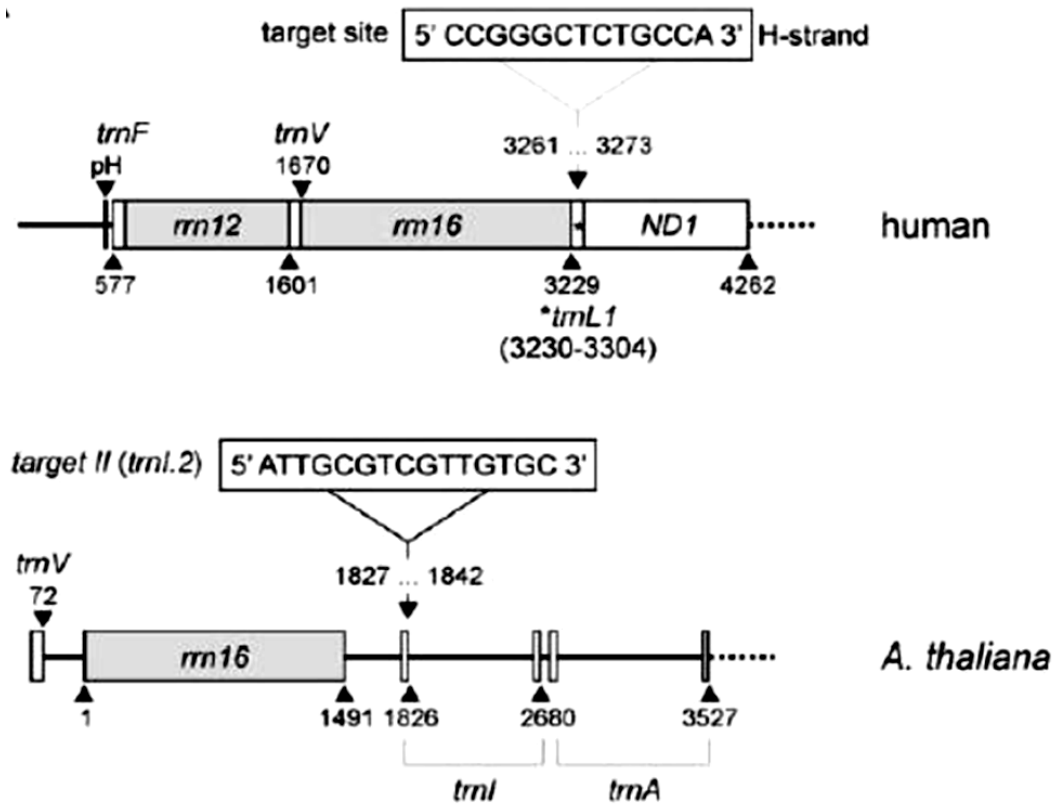


Figure 28. Schematic representations of the human mitochondrial and the *A. thaliana* plastid genome in the region surrounding the *rrn16S* gene. The human MTERF1 target site at the gene coding for tRNA^{Leu} is essential for termination as determined by Christianson and Clayton (1988). The gray and white boxes indicate genes encoding rRNA and tRNA and NADH dehydrogenase subunit 1 (ND1), respectively; introns are depicted as solid lines. PH: heavy strand promoter (Romani *et al.* 2015)

In plants, the genes for chloroplast rRNAs (23S, 16S, 5S, and 4.5S) are located in the large inverted repeat region of chloroplast genomes, where they form part of the *rrn* operon. This operon, which includes three tRNA genes (*t.Val*, *t.Ile*, *t.Ala*), is transcribed as a large polycistronic RNA that is processed by endoribonucleases and exoribonucleases to yield the mature rRNA and tRNA species (Bollenbach Tj *et al.* 2005). The primary precursor is initially processed by excision of the tRNAs and by additional endonucleolytic cleavages to generate 16S and 5S rRNA precursors, and a dicistronic 23S–4.5S processing intermediate. Subsequent endonucleolytic processing of the 23S–4.5S rRNA to generate monocistronic 23S and 4.5S rRNAs appears to occur on the ribosome and prior 3' end maturation of 4.5S rRNA. The 16S, 23S and 5S rRNA precursors generated by endonucleolytic cleavage require further processing to establish mature 5' and 3' ends

5. Discussion and conclusions

(Bollenbach Tj et al.2005). The molecular players that mediate plastid rRNA processing are poorly understood, but they include two 3' to 5' exoribonucleases. One is a polynucleotide phosphorylase (PNPase) that is involved in 23S rRNA processing and in the metabolism of tRNAs and mRNAs (Walter M, Kilian J, Kudla J 2002, Güeto, P Botella-Pavía, et al. 2006), and the other is a homolog of E. coli RNase R (*RNR1*) that is involved in the maturation of 23S, 16S, and 5S rRNAs (Kishine M, et al. 2004, Bollenbach TJ, et al. 2005). In order to investigate more in details the maturation of 16SrRNA and other two rRNAs – 5S and 23S and *trnA.1* and their interaction northern hybridization was utilized. The knock-down and knock-out mutants seemed to accumulate 16SrRNA precursor, and also a mature and unprocessed rRNA species. These results indicated that in *mterf6* mutants but not in the *rnr1-3* mutant, there is an increase of levels of mature *trnA.1* and 5S rRNA transcripts. The levels of mature 23S rRNA were decreased circa 50% of the Col-0 levels in *mterf6* and *rnr1-3* seedlings, and there was an over accumulation of an unprocessed precursor (Figure 9). This overaccumulation of 16S and 23S rRNAs has already been found before in the *rnr1-3* mutant (Bollenbach TJ, et al. 2005) as well as *dal1* which accumulates 16S and 23S precursor rRNAs (Bisanz C, et al. 2003) and tomato *dcl*, in which 4.5S rRNA processing is defective (Bellaoui M, et al. 2003). Mutants who accumulate 16SrRNA precursors are also: *hcf7*, maize high chlorophyll fluorescence7 (Barkan, A., et al. 1994), maize *rnc1* (Watkins, K.P., et al. 2007), *wco*, *Arabidopsis* white cotyledon (Yamamoto, T. et al. 2000) and *suv1*, suppressor of variegation1 (Yu H, Chen X, et al. 2008). In the mutants cited, defect in the normal 16SrRNA maturation is accompanied to normal or above-normal levels of chloroplast mRNAs. However, upon decreased rates of chloroplast protein synthesis and reduced accumulation of chloroplast proteins, mutants with defects in the correct maturation of the *rrn* operon are often showing white cotyledons (*wco*) and white leaves (*hcf7*, *rnc1*); in some cases are incapable of autotrophic growth (*rnr1*), or they have defects in embryo development and general morphogenesis (*rnr1*, *dal*) as seen in *mterf6* mutants (*mterf6-2* knock out line).

In relation with the MTERF6 interaction with *tRNA ile* region, seems that the lack of MTERF6 leads to an over accumulation of *tRNA^{Ile}* (*GAU*) (*trnI.2*) RNAs. In fact, both unspliced and mature *trnI.2* RNAs accumulated abundant levels in *mterf6-1* compared to Col-0 (Figure 13-14). However, the over accumulation of *trnI.2* transcripts could be caused by an accelerated *trnI.2* transcription rate in *mterf6* mutants. Nevertheless, the run-on analysis performed by Romani *et al.*, (2015) showed that the transcription rates of *trnI.2*,

5. Discussion and conclusions

rrn16 (5' of the target II binding site), *trnA.1* and *rrn23* (both 3' of the target II binding site) were similar in *mterf6-1* and Col-0 plants.

5.3 MTERF6 promotes *trnL2* aminoacylation.

In *mterf6-1* and more in *mterf6-2* the level of aminoacylated *trnL2* was reduced (Figure 15). The plastid isoleucyl-tRNA synthetase was identified as OVULE ABORTION 2 (OVA2) (Berg M, et al. 2005). However, the knock-out *mterf6-2* mutant did not display an aborted ovule phenotype, but was able to survive on sugar-supplemented MS medium up to the seedling stage (Figure 4). Likely, this difference in survival of OVA2 and MTERF6 knock-out lines is due to the fact that OVA2 aminoacylates the two plastid tRNAs for Ile, *trnL1* and *trnL2*, but in the *mterf6* mutants *trnL1* is charged to wild-type levels and only aminoacylation of *trnL2* is strongly reduced in *mterf6-2* seedlings (Figure 15).

During the transcription, tRNAs are modified by nuclear-encoded tRNA-modifying enzymes. These posttranscriptional modifications are critical for all core aspects of tRNA function, such as folding, stability, and decoding (Basma El et al. 2012). Thus, MTERF6 might be involved in introducing a critical tRNA modification to *trnL2* with consequent no load of incorrect modified pre-*trnL2* with its amino acid isoleucine in MTERF6 mutants. This would result in an elongation defect and explain the reduced translation rate in *mterf6-1* mutants, as observed for *A. thaliana* mutants *tada* defective for the chloroplast tRNA adenosine deaminase arginine (Delannoy E, et al. 2009). Future studies to delineate which tRNA modification is explicated by MTERF6 are needed.

5.4 MTERF Proteins might play a role in retrograde signaling.

The findings obtained in this study suggest that MTERF6 and GUN1 genetically interact and *mterf6-1/gun1* mutants displayed a more severe phenotype than *mterf6-1* mutant plants (Figure 16).

Future studies are needed to prove whether other MTERF mutants will extend the gun mutant list, and this will contribute to elucidate how OGE is involved in the phenomenon of uncoupling genomes in the presence of norflurazon or lincomycin.

Moreover, sub-classification of MTERF proteins (Kleine, T. 2012) implies that several plant MTERF proteins might operate in the nucleus and/or the cytosol in addition to the organelles, or might be localized both to mitochondria and the nucleus. Consequently, further experimental approaches are necessary to dissect the functions of MTERF proteins, to reveal their role in the coordination of the expression of organellar and nuclear

5. Discussion and conclusions

genomes, and to explain the selective pressures that led to the expansion of the MTERF family in higher plant genomes.

5.5 RIs (relaxed LHCB suppression) mutants

In this project were screened *prors1-2* plants in order to identify novel mutants suitable for the dissection of translational-dependent retrograde signaling pathways. To accomplish this aim was applied the general method of **E**thyl **M**ethane**S**ulfonate (**EMS**) mutagenesis. The *prors1-2* mutant was chosen for this study due to its reduced organelle translation in chloroplasts and mitochondria. *PRORS1* gene (in *Arabidopsis thaliana*), encodes for the chloroplast-localized prolyl-tRNA synthetase (Pesaresi P. *et al.* 2001). Here, it was shown that the knock-down mutant (*prors1-2*) presents a down regulation of nuclear-encoded photosynthetic genes. This mutant is potentially an appropriate candidate for a genetic forward screening. In a former approach, the promotor of a regulated gene *LHCB* was fused to a reporter gene firefly luciferase (LUC) and EMS mutagenesis was applied.

EMS mutagenesis is suitable for both forward and reverse genetic studies. Recent advances in next-generation sequencing have greatly invigorated the process of identifying EMS-induced mutations (Koornneef, M., *et al.* 1982) EMS induces C-to-T changes resulting in C/G to T/A substitutions (Hoffman, G.R 1980). At a low frequency, EMS generates G/C to C/G or G/C to T/A transversions by 7-ethylguanine hydrolysis or A/T to G/C transition by 3-ethyladenine pairing errors (E.A. Codomo C.A. Taylor.N.E *et al* 2003). Based on codon usage in *Arabidopsis*, the frequency of EMS-induced stop codon and missense mutations has been calculated to be ~5% and ~65%, respectively (McCallum CM, Comai Let *al.* 2000).

EMS mutagenesis generates randomly distributed mutations throughout the genome in *Arabidopsis*. (YongSig Kim, *et al.* 2005).

From a genetic and phenotypic screen of EMS mutagenized *prors1-2* mutants performed, 24 *rls* (relaxed LHCB suppression) mutants were selected for physiological characterization (Table1). The *rls83*, *rls255*, *rls145*, *rls148* mutants, showing the most interesting phenotypes, were analyzed through northern blot and *in vivo* labeling, presented a rescue in the amount of antenna complex LHCB. In the mutant lines *rls145*, *rls148* and *rls 255* the synthesis of the D1 protein was strongly restored when compared with the parental line (Figure 19-20-21)

These *rls* mutants were select not for the rescue of the chloroplast activity and photosynthesis efficiency but as good candidate that presented NGE rescue as already

5. Discussion and conclusions

observed in the northern blot results. Further studies on Noraflurazon (NF) and Lincomycin (Linc) were performed to investigate in depth *rls* mutant lines, in particular *rls 148* and *rls 145*. The main aim was to examine the *rls* mutant lines to discover potential novel gun mutant. The *rls* mutants on NF and Linc, after luciferine treatment did not display luciferase activity because the expression of *LHCB* gene was inhibited by noraflurazon (Figure 22). However, luciferase activity in NF and Linc plates in *rls 145* and *rls 148* seedlings was detectable meaning that *LHCB* gene expression was not impaired and the *LHCB1.2* as *LHCB3* were still induced during the NF and Linc treatment. The data obtained accompanied to further experiments suggested that *rls145* and *rls148* might be novel gun mutants.

Nonetheless, further experimental approaches are needed to dissect the effect of *rls* mutations that induce the *prors1-2* phenotype recovery and the localization in the genome of the EMS mutation to reveal potential novel candidates involved in the coordination of the expression of organellar and nuclear genomes

Mapping the location of causal mutations using genetic crosses has traditionally been a complex, multistep procedure, but next-generation sequencing now allows the rapid identification of causal mutations at single-nucleotide resolution even in complex genetic backgrounds (Page and Grossniklaus 2002). Next-generation sequencing produces a wealth of high-resolution genetic data, provides enhanced delimitation of the genomic location of mutations. In the next-generation sequencing (NGS) technologies whole-genome sequencing data are derived from pooled F2 segregants and are analyzed for single nucleotide polymorphisms (SNP) (Uchida N, et al. 2014). The next step will be the isolation of genomic DNA from the idoneus population of *rls* and then analyzed by next generation sequencing. Next generation sequencing technology is required to perform the mapping. The mapping can be performed utilizing the information obtained from the SNPs (**S**ingle **N**ucleotide **P**olymorphisms) detected in the respective DNA sequence obtained from each analyzed *rls* candidates. Subsequently, the SNPs originating from the EMS mutagenesis will be separated from the SNPs derived from other sources such as sequencing errors. Only SNPs including changes from guanine (G) to adenine (A) or cytosine (C) to thymine (T) will be take in consideration. The last step will include filtering the selection of SNPs and the localization of the SNPs, determined with regard to their appearance in a locus of interest by the TAIR SeqViewer (<http://www.arabidopsis.org/servlets>).

5. Discussion and conclusions

In vitro and in vivo analyses of mutant tRNAs by aminoacyl-tRNA synthetases assay are very useful to identify elements important to study the tRNAs activity. In this thesis was described the use of gel electrophoretic method for measuring the levels of aminoacylation of mutant *prors1-2* (*PROLYL-tRNA-SYNTHEASE1*) and the *rls* mutants. Our finding that aminoacyl-tRNA migrates differently from tRNA has proved useful for determining the effect of mutations *prors1-2* on aminoacylation activity of the tRNA and the rescue of it in some of the *rls* mutants analyzed. Interesting for further studies is the mutant *rls 255*, not only present a strong recovery of the aminoacylation of the tRNA (Figure 23) but also the protein synthesis (Figure 21) and the internal transcript level of nuclear-encoded photosynthetic genes is restored, further experimental approaches are necessary. (Figure 19-20).

5.5.1 EtOH-inducible lines

In order to focus on the initial response to perturbation of OGE, was applied an acute OGE-specific stimulus by down-regulating PRORS1 in adult Col-0 plants.

The reason is that so far the analysis of OGE-dependent retrograde signaling based on analyses of mutants with altered OGE are difficult to lead.

The concept of retrograde signaling is that the organelles communicate their developmental and metabolic state to the nucleus, thus enabling NGE to be appropriately modified. Although many signals have been delineated, the signals that pass between the cellular compartments, the cytosolic pathways, and the receivers in the nucleus are largely unknown. Nevertheless retrograde signaling was discovered over 30 years ago, it is still not clear how many different signaling pathways actually exist, how they interact with each other, and whether or how they can be distinguished from each other. Most of our knowledge about retrograde signaling refers to artificial metabolic states evoked by treatment with inhibitors (Woodson, J. D. & Chory, J., 2008). The ability to exploit natural stimuli for signaling is crucial for further progress. To avoid secondary effects, such as downregulation of photosynthetic capacity, we have used inducible RNAi to produce a shorter-term impairment in OGE.

In vivo labeling experiment (Figure 25) demonstrated that after 32 and 52 hours EtOH treatment, the translational capacity of chloroplasts was reduced in the RNAi line35. Additionally, it was also observed a reduction of leaves pigmentation and decrease of growth and photosynthesis efficiency, suggesting a possible reproduction of the physiological condition of *prors1-2* mutant. The data collected in this project served as the

5. Discussion and conclusions

basis for a series experiment in which whole-genome transcriptomes expressed during down-regulation of *PRORS1* were analyzed. It was possible to identify the OGE-target genes and co-regulated gene sets candidate cis-acting elements that seems to be involved in the transcriptional co-regulation of gene sets were found and were also identified responding TFs. [Leister, Romani *et al.* (2014)] Time series of microarray experiments provide a robust basis for the experimental identification of primary target genes of OGE-dependent signaling. Analysis of whole-genome transcriptomes at various times after application of the stimulus identified 1020 genes as candidates for loci that sense defects in the translational capacity of chloroplasts and/or mitochondria in adult plants. These genes were named OGERepression Target (ORT) genes. Intriguingly, although the *prors1-2* phenotype itself represents the end result of a chronic disturbance of OGE and is presumably influenced by strong secondary effects only 387 genes show changes in transcription level in the mutant. Genes related to photosynthesis were prominent among the repressed ORT genes together with genes encoding plastid ribosomal proteins, a TPR and two PPR proteins (Table 8). The PPR family has approximately 450 members, and the PPR and TPR motifs are closely related (Small and Peeters, 2000). The majority of PPR and TPR proteins in *A. thaliana* are targeted to mitochondria and/or chloroplasts, and are thought to participate in OGE functions like processing, editing, stabilization, and translation of RNA molecules (Schmitz-Linneweber and Small, 2008). Co-regulation of nuclear gene sets impinging on cp OGE, especially the cp ribosomes, and photosynthesis has been shown before (Biehl *et al.*, 2005; Leister *et al.*, 2011) and was interpreted as an instance of nuclear transcriptional control of plastid ribosome abundance, which helps to ensure coordinated expression of cp- and nucleus-encoded components of the photosynthetic machinery (Biehl *et al.*, 2005). However, many more PPR genes are found among the up-regulated ORT set and, interestingly, most of these encode proteins predicted to localize to mitochondria (Leister D., Romani I. *et al.* 2014).

These genes analyses can help to define overlaps and synergies with other retrograde signaling pathways, for instance the target genes of state transition/long-term response signaling (Bräutigam *et al.*, 2009). Indeed, it was recognized overlaps between earlier OGE-dependent signaling, cold-acclimation, and light signaling pathways. Some of these genes encode photosynthesis-related proteins, including several down-regulated light-harvesting chlorophyll a/b binding (LHC) proteins. Interestingly, genes for presumptive

5. Discussion and conclusions

endoplasmic reticulum proteins are transiently up-regulated. Further analyses investigate several NAC-domain-containing proteins that are among the transcription factors regulated. Possible cis-acting elements may coordinate the transcriptional co-regulation of genes sets include both G-box variants and sequence motifs with no similarity to known plant cis-elements (Leister, Romani *et al.* 2014).

Furthermore, both the transient up-regulation of presumptive ER proteins and the identification of a cis-element, which might be bound by an ER-derived TF, indicate a signal routing via the ER (Leister, Romani *et al.* 2014.)

Eventually, Leister et al (2014) provide a comprehensive list of responding TFs and conserved motifs in the promoter regions of co-regulated gene sets which confers a point of departure for further work designed to identify TFs on which OGE-dependent retrograde signals act. (Leister, Romani *et al.* 2014).

6. References

References

Abdallah F, Salamini F, Leister D (2000) A prediction of the size and evolutionary origin of the proteome of chloroplasts of Arabidopsis. *Trends Plant Sci* 5: 141-142.

Babiychuk E, Vandepoele K, Wissing J, Garcia-Diaz M, De Rycke R, Akbari H, Joubès J, Beeckman T, Jänsch L, Frentzen M, et al (2011) Plastid gene expression and plant development require a plastidic protein of the mitochondrial transcription termination factor family. *Proc Natl Acad Sci USA* 108: 6674–6679

Barkan, A., Walker, M., Nolasco, M., and Johnson, D. (1994). A nuclear mutation in maize blocks the processing and translation of several chloroplast mRNAs and provides evidence for the differential translation of alternative mRNA forms. *EMBO J.* 13, 3170–3181

Basma El.Yacoubi, Marc Bailly, and Valérie de Crécy-Lagard (2012) Biosynthesis and Function of Posttranscriptional Modifications of Transfer RNAs *Annual Review of Genetics* DOI: 10.1146/annurev-genet-110711-155641

Bellaoui M, et al. (2003) Elg1 forms an alternative RFC complex important for DNA replication and genome integrity. *EMBO J* 22(16):4304-13

Benfey P.N, (1999) Is the shoot a root with a view? *Curr.Opin. Plant Biol.* 2, 39

Berg M., Rogers R, Muralla R, Meinke D (2005) Requirement of aminoacyl tRNA synthetases for gametogenesis and embryo development in Arabidopsis. *Plant J* 44: 866–878

Bisanz C.Bégot L, Carol P, Perez P, Bligny M, Pesey H, Gallois JL, Lerbs- Mache S, Mache R (2003) The Arabidopsis nuclear DAL gene encodes a chloroplast protein which is required for the maturation of the plastid ribosomal RNAs and is essential for chloroplast differentiation. *Plant Mol Biol* 51: 651–663

6. References

Bonardi, V., Pesaresi, P., Becker, T., Schleiff, E., Wagner, R., Pfannschmidt, T., Jahns, P., and Leister, D. (2005). Photosystem II core phosphorylation and photosynthetic acclimation require two different protein kinases. *Nature* 437: 1179–1182

Bollenbach TJ, Lange H, Gutierrez R, Erhardt M, Stern DB, Gagliardi D (2005) RNR1, a 39-59 exoribonuclease belonging to the RNR superfamily, catalyzes 39 maturation of chloroplast ribosomal RNAs in *Arabidopsis thaliana*. *Nucleic Acids Res* 33: 2751–2763

Chomyn A, Enriquez JA, Micol V, Fernandez-Silva P, Attardi G (2000) The mitochondrial myopathy, encephalopathy, lactic acidosis, and stroke-like episode syndrome-associated human mitochondrial tRNA^{Leu} (UUR) mutation causes aminoacylation deficiency and concomitant reduced association of mRNA with ribosomes. *J Biol Chem* 275: 19198–19209

David a. Clayton (1988) Nuclear gadgets in mitochondrial DNA replication and transcription Department of Development Biology, Beckman Center, Stanford University School of Medicine, Stanford, CA 94305-5427, USA DOI: [http://dx.doi.org/10.1016/0968-0004\(91\)90043-U](http://dx.doi.org/10.1016/0968-0004(91)90043-U)

Dellanov E, Le Ret M, Faivre-Nitschke E, Estavillo GM, Bergdoll M, Taylor NL, Pogson BJ, Small I, Imbault P, Gualberto JM (2009) *Arabidopsis* tRNA adenosine deaminase arginine edits the wobble nucleotide of chloroplast tRNA^{Arg}(ACG) and is essential for efficient chloroplast translation. *Plant Cell* 21: 2058–2071

Estavillo G.M., et al. (2011). Evidence for a SAL1- PAP chloroplast retrograde pathway that functions in drought and high light signaling in *Arabidopsis*. *Plant Cell* 23: 3992–4012

Foyer, C.H., and Noctor, G. (2005). Redox homeostasis and antioxidant signaling: A metabolic interface between stress perception and physiological responses. *Plant Cell* 17, 1866-1875

6. References

- Gill S. and N. Tuteja, (2010) "Reactive oxygen species and antioxidant machinery in abiotic stress tolerance in crop plants," *Plant Physiology and Biochemistry*, vol. 48, no. 12, pp. 909–930
- Heiber, I., Ströher, E., Raatz, B., Busse, I., Kahmann, U., Bevan, M. W., et al. (2007). The redox imbalanced mutants of *Arabidopsis* differentiate signaling pathways for redox regulation of chloroplast antioxidant enzymes. *Plant Physiol.* 143, 1774–1788. doi: 10.1104/pp.106.093328
- Hsu YW, Wang HJ, Hsieh MH, Hsieh HL, Jauh GY (2014) *Arabidopsis* MTERF15 is required for mitochondrial nad2 intron 3 splicing and functional complex I activity. *PLoS ONE* 9: e112360
- Isemer, R., Mulisch, M., Schafer, A., Kirchner, S., Koop, H. U., and Krupinska, K. (2012b). Recombinant Whirly1 translocates from transplastomic chloroplasts to the nucleus. *FEBS Lett.* 586, 85–88.
- Kleine T, Leister D (2015) Emerging functions of mammalian and plant MTERFs. *Biochim Biophys Acta* 1847: 786–797
- Kleine, T. (2012). *Arabidopsis thaliana* MTERF proteins: evolution and functional classification. *Front. Plant Sci.* 3:233. doi: 10.3389/fpls.2012.00233
- Kishine M, Takabayashi A, Munekage Y, Shikanai T, Endo T, Sato F (2004) Ribosomal RNA processing and an RNase R family member in chloroplasts of *Arabidopsis*. *Plant Mol Biol* 55: 595–606
- Kip E. Guja and Miguel Garcia-Diaz (2012) Hitting the Brakes: Termination of Mitochondrial Transcription *Biochim Biophys Acta.*; 1819(9-10): 939–947. doi:10.1016/j.bbagr.2011.11.004.

6. References

- Kruse B, Narasimhan N, Attardi G (1989) Termination of transcription in human mitochondria: identification and purification of a DNA binding protein factor that promotes termination. *Cell* 58: 391–397
- Koussevitzky S, Nott A, Mockler TC, Hong F, Sachetto-Martins G, et al. (2007) Signals from chloroplasts converge to regulate nuclear gene expression. *Science* 316: 715-719.
- Kovalchuk I., “Multiple roles of radicles in plants,” in *Reactive Oxygen Species and Antioxidants in Higher Plants*, S. Dutta (2010) Gupta, Ed., pp. 31–44, CRC Press, New York, NY, USA
- Larkin J., Brown, M.L., and Schiefelbein, J. (2003). How cells know what they want to be when they grow up? Lessons from epidermal patterning in *Arabidopsis* *Annu. Rev. Plant Biol.* 54, 403–430
- Lee KP, Kim C, Landgraf F, Apel K (2007). EXECUTER1- and EXECUTER2-dependent transfer of stress-related signals from the plastid to the nucleus of *Arabidopsis thaliana*. *Proc. Natl. Acad. Sci. U. S. A.* 104:10270–5.
- Leister D., Romani I., Mittermayr L., Paieri F., Fenino E., Kleine T. 2014 “Identification of target genes and transcription factors implicated in translation dependent retrograde signaling in *Arabidopsis*” *Mol. plant.* DOI: 10.1093/mp/ssu066
- Liere K, Maliga P. (1999) In vitro characterization of the tobacco rpoB promoter reveals a core sequence motif conserved between phage-type plastid and plant mitochondrial promoters. *EMBO J* a;18:249–57
- Lichtenthaler H.K. (1987). Chlorophylls and carotenoids: Pigments of photosynthetic biomembranes. - *Methods in Enzymology*, 148: 350-382.
- Lo C, Wang N, Lam E (2005) Inducible double stranded RNA expression activates reversible transcript turnover and stable translational suppression of a target gene in transgenic tobacco. *FEBS Lett* 579: 1498–1502

6. References

Margulis L (1981) *Symbiosis in Cell Evolution*. New York, W. H. Freeman

Matthew J Terry 1,2* and Alison G. Smith (2013) A model for tetrapyrrole synthesis as the primary mechanism for plastid-to-nucleus signaling during chloroplast biogenesis. published: 13 February doi: 10.3389/fpls.2013.00014

Meskaukiene R, Würsch M., Laloi C, Vidi PA, Coll NS, Kessler F, Baruah A, Kim C, Apel K (2009) A mutation in the *Arabidopsis* *MTERF*-related plastid protein SOLDAT10 activates retrograde signaling and suppresses 1O₂-induced cell death. *Plant J* 60: 399–410

Miller G., V. Shulaev, and R. Mittler, (2008) “Reactive oxygen signaling and abiotic stress,” *Physiologia Plantarum*, vol. 133, no. 3, pp. 481–489

Miller G., K. Schlauch, R. Tam (2009)., “The plant NADPH oxidase RBOHD mediates rapid systemic signaling in response to diverse stimuli,” *Science Signaling*, vol. 2, no. 84, pp. 45–49,

Mokry M., Nijman, A. Van Dijken, R. Benjamins, R. Heidstra et al., 2011 Identification of factors required for meristem function in *Arabidopsis* using a novel next generation sequencing fast forward genetics approach. *BMC Genomics* 12: 256.

Mochizuki N., Brusslan, J.A., Larkin, R., Nagatani, A., and Chory, J. (2001). *Arabidopsis* genomes uncoupled 5 (GUN5) mutant reveals the involvement of Mg-chelatase H subunit in plastid-to-nucleus signal transduction. *Proc Natl Acad Sci USA* 98, 2053-2058

Mullineaux CW, Pascal AA, Horton P, Holzwarth AR (1993) Excitation energy quenching in aggregates of the LHC II chlorophyll-protein complex: a time-resolved fluorescence study. *Biochim Biophys Acta* 1141: 23–28

Oelmüller, R., and Mohr, H. (1986). Photooxidative destruction of chloroplasts and its consequences for expression of nuclear genes. *Planta* 167, 106–113.

Pesaresi P, Schneider A, Kleine T, Leister D (2007) Interorganellar communication. *Curr Opin Plant Biol* 10: 600-606.

6. References

Pesaresi P, Masiero S, Eubel H, Braun HP, Bhushan S, et al. (2006) Nuclear photosynthetic gene expression is synergistically modulated by rates of protein synthesis in chloroplasts and mitochondria. *Plant Cell* 18: 970-991.

Pesaresi P, Varotto C, Meurer J, Jahns P, Salamini F, et al. (2001) Knock-out of the plastid ribosomal protein L11 in *Arabidopsis*: effects on mRNA translation and photosynthesis. *Plant J* 27: 179-189.

Piippo, M., Allahverdiyeva, Y., Paakkarinen, V., Suoranta, U., Battchikova, N., and Aro, E.-M. (2006). Chloroplast-mediated regulation of nuclear genes in *Arabidopsis thaliana* in the absence of light stress. *Physiol. Genomics* 25, 142–152.

Pogson, B.J., Woo, N.S., Forster, B., and Small, I.D. (2008). Plastid signaling to the nucleus and beyond. *Trends in Plant Science* 13, 602-609.

Quesada V, Sarmiento-Mañús R, González-Bayón R, Hricová A, Pérez-Marcos R, Graciá-Martínez E, Medina-Ruiz L, Leyva-Díaz E, Ponce MR, Micol JL (2011) *Arabidopsis RUGOSA2* encodes an MTERF family member required for mitochondrion, chloroplast and leaf development. *Plant J* 68: 738–753

Ramel F, Birtic S, Ginies C, Soubigou-Taconnat L, Triantaphylidès C, Havaux M. 2012b. Carotenoid oxidation products are stress signals that mediate gene responses to singlet oxygen in plants. *Proceedings of the National Academy of Sciences, USA* 109, 5535–5540.

Roberti, M., Polosa, P. L., Bruni, F., Manzari, C., Deceglie, S., Gadaleta, M. N., et al. (2009). The MTERF family proteins: mitochondrial transcription regulators and beyond. *Biochim. Biophys. Acta* 1787, 303–311.

Romani I., Nikolay M., Arianna M., Luca T., Svetlana M., Kristina K., Hannes R., Christian Schmitz-Linneweber, Gerhard W., Dario L., and Tatjana K.* (2015) MTERF6, a Member of the *Arabidopsis* Mitochondrial Transcription Termination Factor Family, Is Required for

6. References

Maturation of Chloroplast tRNA^{Ala}(GAU) Plant Physiology Preview
a.DOI:10.1104/pp.15.00964

Romani, I., Tadini, L., Rossi, F., Masiero, S., Pribil, M., Jahns, P., Kater, M., Leister, D., and Pesaresi, P. (2012). Versatile roles of *Arabidopsis* plastid ribosomal proteins in plant growth and development. *Plant J.* 72, 922–934

Saini G, Meskauskiene R, Pijacka W, Roszak P, Sjögren LLE, Clarke AK, Straus M, Apel K. 'happy on norflurazon' (hon) mutations implicate perturbation of plastid homeostasis with activating stress acclimatization and changing nuclear gene

Salomé PA, Oliva M, Weigel D, Krämer U (2013). Circadian clock adjustment to plant iron status depends on chloroplast and phytochrome function. *EMBO. J.* 32:511-23.

Sauret-Güeto, P, Botella-Pavía, Ú Flores-Pérez, JF Martínez-García,(2006) Plastid cues posttranscriptionally regulate the accumulation of key enzymes of the methylerythritol phosphate pathway in *Arabidopsis* *Plant physiology* 141 (1), 75-84

Schmitz-Linneweber C, Ruwe H, (2012) Short non-coding RNA fragments accumulating in chloroplasts: footprints of RNA binding proteins? *Nucleic Acids Res.* 2012 Apr;40(7):3106-16. doi: 10.1093/nar/gkr1138. Epub 2011 Dec 1.

Schönfeld, C., Wobbe, L., Borgstadt, R., Kienast, A., Nixon, P. J., and Kruse, O. (2004). The nucleus-encoded protein MOC1 is essential for mitochondrial light acclimation in *Chlamydomonas reinhardtii*. *J. Biol. Chem.* 279, 50366–50374

Shiina T, Tsunoyama Y, Nakahira Y, Khan MS (2005) Plastid RNA polymerases, promoters, and transcription regulators in higher plants. *Int Rev Cytol* 244: 1–68

Strand A, Asami T., Alonso, J., Ecker, J.R., and Chory, J. (2003). Chloroplast to nucleus communication triggered by accumulation of Mg-protoporphyrin IX. *Nature* 421, 79-83.

6. References

- Susek, Ausubel, F.M., and Chory, J. (1993). Signal-transduction mutants of *Arabidopsis* uncouple nuclear *Cab* and *Rbcs* gene expression from chloroplast development. *Cell* 74, 787-799
- Sun L., Zhang H., Li, D., Huang, L., Hong, Y., Ding, X.S., Nelson, R.S., Zhou, X. and Song, F. (2013) Functions of rice NAC transcriptional factors, ONAC122 and ONAC131, in defense responses against *Magnaporthe grisea*. *Plant Mol. Biol.* 81, 41–56
- Sullivan JA, Gray JC (1999) Plastid translation is required for the expression of nuclear photosynthesis genes in the dark and in roots of the pea *lip1* mutant. *Plant Cell* 11: 901-910
- S. Bhattacharjee (2010) “Sites of generation and physicochemical basis of formation of reactive oxygen species in plant cell,” in *Reactive Oxygen Species and Antioxidants in Higher Plants*, S. Dutta Gupta, Ed., pp. 1–30, CRC Press, New York, NY, USA,
- Terzioglu M, Ruzzenente B, Harmel J, Mourier A, Jemt E, López MD, Kukat C, Stewart JB, Wibom R, Meharg C, et al (2013) MTERF1 binds mtDNA to prevent transcriptional interference at the light-strand promoter but is dispensable for rRNA gene transcription regulation. *Cell Metab* 17: 618–626
- Tiller N, Bock R (2014) The translational apparatus of plastids and its role in plant development. *Mol Plant* 7: 1105–1120
- Triantaphylidès, C., Krischke, M., Hoeberichts, F. A., Ksas, B., Gresser, G., Havaux, M., et al. (2008). Singlet oxygen is the major reactive oxygen species involved in photooxidative damage to plants. *Plant Physiol.* 148, 960–968. doi: 10.1104/pp.108.125690
- Varotto C, Pesaresi P. Meurer J, Oelmüller R, Steiner-Lange S, Salamini F, Leister D (2000). Disruption of the *Arabidopsis* photosystem I gene *psaE1* affects photosynthesis and impairs growth. *Plant. J.* 22:115-24.

6. References

- Varshney, U., Lee, C.P., and RajBhandary, U.L. 1991. Direct analysis of amino-acylation levels of tRNAs in vivo. *J. Biol. Chem.* 266: 24712–247
- Vass I, Cser K(2009) Janus-faced charge recombinations in photosystem II photoinhibition. *Trends Plant Sci* 14: 200–205
- Wagner, D., Przybyla, D., Op den Camp, R., Kim, C., Landgraf, F., Lee, K.P., Wu" rsch, M., Laloi, C., Nater, M., Hideg, E., and Apel, K. (2004). The genetic basis of singlet oxygen-induced stress responses of *Arabidopsis thaliana*. *Science* 306, 1183–1185.
- Walter M, Kilian J, Kudla J (2002) PNPase activity determines the efficiency of mRNA 3'-end processing, the degradation of tRNA and the extent of polyadenylation in chloroplasts. *EMBO J* 21: 6905–6914
- Watkins, K.P., Kroeger, T.S., Cooke, A.M., Williams-Carrier, R.E., Friso, G., Belcher, S.E., van Wijk, K.J., and Barkan, A. (2007). A ribonuclease III domain protein functions in group II intron splicing in maize chloroplasts. *Plant Cell* 19: 2606–2623
- Woodson, J. D. & Chory, J., (2008) Coordination of gene expression between organellar and nuclear genomes. *Nature Reviews Genetics* 9: 383–395
- Woodson JD, Pérez-Ruiz JM, Chory J (2011). Heme synthesis by plastid ferrochelatase I regulates nuclear gene expression in plants. *Curr. Biol.* 21:897–903.
- Xiao Y, Savchenko T, Baidoo EE, Chehab WE, Hayden DM, Tolstikov V, Corwin JA, Kliebenstein DJ, Keasling JD, Dehesh K (2012). Retrograde signaling by the plastidial metabolite MEcPP regulates expression of nuclear stress-response genes. *Cell.* 149:1525-35.
- Yamamoto, T., Lin, H.X., Sasaki, T., and Yano, M. (2000). Identification of heading date quantitative trait locus Hd6 and characterization of its epistatic interactions with Hd2 in rice using advanced backcross progeny. *Genetics* 154, 885–891.

6. References

Yu H, Chen X, Hong YY, Wang Y, Xu P, Ke SD, Liu HY, Zhu JK, Oliver DJ, Xiang CB (2008) Activated expression of an *Arabidopsis* HD-START protein confers drought tolerance with improved root system and reduced stomatal density. *Plant Cell* 20: 1134–1151

Zhang ZW, Yuan S, Feng H, Xu F, Cheng J, Zhang DW, Hong H, Lin HH (2011). Transient accumulation of Mg-protoporphyrinIX regulates expression of *PhANGs*: new evidence for the signaling role of tetrapyrroles in mature *Arabidopsis* plants. *J. Plant. Physiol.* 168:714–21.

7. Acknowledgment

Acknowledgment

I would like to thank Prof. Dr. Dario Leister for giving me the opportunity and the funding to accomplish my Ph.D. in his research group.

Special thanks to :

Catherine Colas des Francs-Small and Ian Small for providing the clb19-3 seeds;
David B. Stern for providing the rnr1-3 seeds;

Thank to Eric Lam for donating the pMW4 and pMW4G vectors useful for our EtOh inducible lines

Elisabeth Gerick for technical assistance.

Arianna morosetti and Lukas Mittermayr for the previous work done during their PhD program and the support that they gave me in my first days of PhD program

Thanks to Tatjana Klein for all the ideas proposed in my PhD program and the motivation that I got in these 3 years .

I would like to thank Dr. Paolo Pesaresi for the support in my new life in germany and for the cooperation for the first paper that we publish together

Luca Tadini for realizing the in vivo pulse labeling of thylakoid membrane protein (figure 5) and psychological support. and the help to realize the papers that we published together

I thank Nikolay Manavski for the technical and psychological support that he gave during the realization of our last paper.

Special thanks to my best friend Myriam, my coffee break fellow

7. Acknowledgment

And to my friend Giusy that was always here for me to listen my complaining and check my thesis.

Deep thank to the special guy that now is in my life was able make me relax and loved during this time and make possible to reach my goal with the thesis. Thank ALEX

Thank to my family that are always here for me, and to my mom that always believed in me.

Thank to everybody that cooperated to make my life in Germany a success.

Curriculum Vitae

PERSONAL DETAILS

Name: Isidora Romani

Date of birth: 03/06/1987

Place of birth: Ponte San Pietro (BG), Italy

Citizenship: Italian

EDUCATION

01.2012 – 04.2015

PhD student in LMU fakultät für
biologie München: Supervision Dario
Leister and Tatjana Kleine

Topic of the thesis : retrograde
signaling between chloroplast and
nucleo

12.2009 – 12.2011

Università degli Studi di Milano
master degree in Molecular Biology
of cell.

Final grade(110/110)

Topic thesis: Plant development and
acclimation: the versatile role of
plastids

10.2007 – 12.2009

Università degli Studi di Milano

Bachelor Degree

Training at MADS group laboratory

8. Curriculum Vitae

(120h)

Bachelor Degree in biological Sciences. grade Final grade 100/110

Topic thesis:

Functional analysis of Gun1 protein and its possible involvement in the communication organelles-nucleus in *Arabidopsis thaliana*

09.2001 – 07.2006

High school Liceo Primo Levi in San Donato Milanese, Italien
Grad (82/100)

PAPERS PUBLISHED

Journal: The Plant Journal 2012
DOI: 10.1111/tpj.12000

Titel: "Versatile roles of arabidopsis plastid ribosomal proteins in plant growth and development"

Autoren: **Isidora Romani**, Luca Tadini, Fabio Rossi, Simona Masiero, Mathias Pribil, Peter Jahns, Martin Kater, Dario Leister, Paolo Pesaresi

Original Research, Front. Plant Sci. - Plant Physiology, Abgabe am : 24 Sept 2012,
DOI: 10.3389/fpls.2012.00282

Titel: "Thylakoid redox signals are integrated into organellar-gene-expression-dependent..."

Autoren: Luca Tadini, **Isidora Romani**, Mathias Pribil, Peter Jahns, Dario Leister*, Pesaresi

8. Curriculum Vitae

Molecular Plant 05/2014

DOI:10.1093/mp/ssu066

Titel: "Identification of target genes and transcription factors implicated in translation-dependent retrograde signaling in Arabidopsis"

Autoren: Dario Leister, **Isidora Romani**, Lukas Mittermayr, Francesca Paieri, Elena Fenino, Tatjana Kleine

Plant Physiology

DOI:10.1104/pp.15.00964

Titel: "MTERF6, a Member of the Arabidopsis Mitochondrial Transcription Termination Factor Family, Is Required for Maturation of Chloroplast tRNA^{Ala}(GAU)"

Autoren: **Romani Isidora**, Nikolay Manavski¹, Arianna Morosetti, Luca Tadini, Svetlana Maier, Kristina Kühn, Hannes Ruwe, Christian Schmitz-Linneweber, Gerhard Wanner, Dario Leister, and Tatjana Kleine* (2015)

Declaration

Declaration / Eidesstattliche Erklärung

Ich versichere hiermit an Eides statt, dass die vorgelegte Dissertation von mir selbständig und ohne unerlaubte Hilfe angefertigt ist.

München 2016

Romani Isidora